

Stress and Vibration Analysis of a MDOF Excavator Bucket

By
Md Shahriar Islam
Student No. 131601

Supervised By
Prof. Dr. Md. Zahid Hossain

A thesis submitted to the Department of Mechanical and Chemical
Engineering (MCE) in partial fulfillment of the requirement for the
degree of Master of Science in Mechanical Engineering

بِسْمِ اللَّهِ الرَّحْمَنِ الرَّحِيمِ



Department of Mechanical and Chemical Engineering (MCE)

Islamic University of Technology (IUT)

October, 2015

Certificate of Approval

The thesis titled “Stress and vibration analysis of a MDOF excavator bucket” submitted by Md Shahriar Islam bearing student number 131601 of Academic Year 2013-2014 has been found as satisfactory and accepted as partial fulfillment of the requirement for the degree of Master of Science in Mechanical Engineering on 30 October, 2015.

Board of Examiners

.....
Prof. Dr. Md. Zahid Hossain

Professor
Department of Mechanical and Chemical Engineering
Islamic University of Technology (IUT)
Board Bazar, Gazipur
Dhaka, Bangladesh

Chairman
(Supervisor)

.....
Prof. Dr. A.K.M. Sadrul Islam

Head,
Department of Mechanical and Chemical Engineering
Islamic University of Technology (IUT)
Board Bazar, Gazipur
Dhaka, Bangladesh

Member
(Ex-officio)

.....
Prof. Dr. Md. Nurul Absar Chowdhury

Professor
Department of Mechanical and Chemical Engineering
Islamic University of Technology (IUT)
Board Bazar, Gazipur
Dhaka, Bangladesh

Member

.....
Prof. Dr. Md. Abdus Salam Akanda

Professor
Department of Mechanical Engineering
Bangladesh University of Engineering and Technology (BUET)
Dhaka, Bangladesh

Member
(External)

Candidate's Declaration

It is hereby declared that this thesis or any part of it has not been submitted elsewhere for the award of any degree or diploma.

Signature of the Candidate

Md Shahriar Islam

Department of Mechanical and Chemical Engineering (MCE)

Islamic University of Technology (IUT)

Board Bazar, Gazipur

Dhaka, Bangladesh

Signature of the Supervisor

Prof. Dr. Md. Zahid Hossain

Professor

Department of Mechanical and Chemical Engineering (MCE)

Islamic University of Technology (IUT)

Board Bazar, Gazipur

Dhaka, Bangladesh

Dedication

This thesis is dedicated to my parents and adorable wife.

Acknowledgement

The author expresses gratefulness to almighty Allah for his blessings, which enabled him to complete this thesis successfully.

The author expresses gratitude to his supervisor Prof. Dr. Md. Zahid Hossain, Department of Mechanical and Chemical Engineering (MCE), Islamic University of Technology (IUT), for his continuous guidance, helpful suggestions and supervision at all stages of this thesis work. Deepest gratitude to Mr. Rakibul Hassan, Assistant Engineer, Applied Mechanics Lab, Department of Mechanical and Chemical Engineering (MCE), Islamic University of Technology (IUT), for his help throughout this work.

The author expresses his acknowledgement to Islamic University of Technology (IUT) authority, all the faculty and staff members of the Department of Mechanical and Chemical Engineering (MCE).

The author is indebted to his parents for providing the financial and mental support in pursuing this degree and research work. Without their supports, none of these works would be possible. The author expresses his thanks to his wife for her continuous support and encouragement, which helped for the best use of time.

In spite of his best effort to complete this work, the author seeks excuses if there is any mistake found in this report.

Author

Abstract

Multi degrees of freedom (MDOF) excavator is a very popular machine in today's mining industry and are also popularly used in roads and building constructions or demolition and for material handling. All these uses involve exposure of the bucket to high amount of linear and non-linear reaction forces which might sometimes cross the limit of endurable stress of the bucket, also because of the continuation of reaction forces noise and vibration is observed in the bucket which propagates to the whole excavator body.

There have been very limited research works done till now on the engineering analysis of excavator or excavator bucket. Most of the works concentrated on the different attachments' modified or optimized design, and almost no work has been done on the vibration analysis of the bucket particularly. The vibration due to input digging force and reaction force damage the bucket and its cutting teeth with the time being, so it is a common practice to change the bucket with a new one or replace the teeth which are no longer usable. Some companies use reinforced steel with the bucket as attachments to increase its strength and resist wear when mining. This research work is focused on different techniques of using rubber and other materials with the bucket as attachments to reduce vibration so that it can last longer and work under less disturbances.

In this thesis work three dimensional (3D) MDOF (Multi Degrees of Freedom) bucket is modelled with the help of SOLIDWORKS software and analyzed in ANSYS 14 software. In ANSYS Software three different analysis platform is used on the 3D model namely Modal, Harmonic and Static Structure analysis. Firstly, the Modal analysis is done to understand the mode shapes and natural frequencies of the bucket. Secondly, Harmonic analysis is done to understand the vibration amplitudes in different natural frequencies. And lastly Static Structure analysis is performed to understand the equivalent von-mises stresses developed in the bucket. The simulation or numerical analysis has been performed on a standard bucket then several cases were developed. The use of rubber materials with the bucket as attachments to reduce vibration and to observe change in the mode shapes and natural frequencies is a major highlight of this thesis work. Also use of other materials and their effect is observed in this thesis work. Different techniques were studied to use rubber strips which will not increase the total weight of the bucket but will reduce vibration and stress developed in the system. The thesis also includes how the different

aspects of using attachments such as how much thickness it should be or what are the effects of thickness of attachments.

The numerical simulation is validated with published journal paper for the stress developed in the bucket and results found are in well agreement with the results of the paper. An experiment is also performed on a bucket model made locally with local materials and using common mechanical tools such as bending, rolling, scissor and welding. The experimental model is fixed on a fixture then vibration output was measured under different loads. Then rubber sheet and rubber strips also attached with this experimental model and experimentation was done. Similar model was developed in the SOLIDWORKS software and analyzed accordingly in ANSYS and validated with the experimentation. The experiment was only performed on the harmonic analysis of the bucket with and without rubber and the results found from the experiments are in similar pattern with the simulation results.

Table of Contents

Certificate of Approval
Candidate’s declaration
Dedication
Acknowledgement
Abstract
Table of Contents
List of Tables
List of Figures

Chapter 1: Introduction

1.1. Excavator.....2
 1.1.1. Excavator attachments and configuration.....3
 1.1.2 Excavator Bucket.....4
1.2 Vibration.....6
1.3. Von Mises Stress7
1.4. The importance of vibration analysis and reduction.....09
1.5. Research Objective.....10
1.6. Possible outcomes.....10
1.7. Outline of methodology.....11

Chapter 2: Literature Review

2.1. Introduction.....14
2.2. Utility of FEA and optimization for backhoe attachment15

2.3. Optimization of backhoe attachment.....	17
2.5. Summary of the literature review.....	19

Chapter 3: Problem specification and numerical Simulation

3.1. Introduction.....	21
3.2. Modeling of the Bucket	21
3.3. Numerical Analysis Procedure.....	22
3.4. Boundary Conditions and Input Force.....	23
3.5. Meshing.....	24
3.6. Definition of Cases.....	25

Chapter 4: Result of Numerical Simulation and Discussion

4.0. Introduction.....	31
4.1. Modal Analysis	31
4.1.1. Mode Shapes and Natural Frequencies for Case 1.....	31
4.1.2. Mode Shapes and Natural Frequencies for Case 2.....	35
4.1.3. Mode Shapes and Natural Frequencies for Case 3.....	38
4.1.4. Mode Shapes and Natural Frequencies for Case 4.....	39
4.1.5. Mode Shapes and Natural Frequencies for Case 5.....	42
4.1.6. Mode Shapes and Natural Frequencies for Case 6.....	44
4.2. Harmonic Analysis.....	46
4.2.2. Harmonic Response of Case 2.....	46
4.2.3. Harmonic Response of Case 3.....	53
4.2.4. Harmonic Response of Case 4.....	59
4.2.5. Harmonic Response of Case 5.....	66
4.2.6. Harmonic Response of Case 6.....	73
4.3. Static Structure Analysis	79

4.3.1. Von Mises Stress and Total Deformation for Case 1.....	79
4.3.2. Von Mises Stress and Total Deformation for Case 2.....	81
4.3.3. Von Mises Stress and Total Deformation for Case 3.....	82
4.3.4. Von Mises Stress and Total Deformation for Case 4.....	85
4.3.5. Von Mises Stress and Total Deformation for Case 5.....	88
4.3.6. Von Mises Stress and Total Deformation for Case 6.....	90
Chapter 5: Experimental Results and Validation	
5.1. Introduction.....	93
5.2. Experimental Set-up.....	93
5.3. Experiment and Simulation Case.....	97
5.4. Experimental Procedure.....	98
5.5. Experiment and Simulation Results.....	100
Chapter 6: Conclusion and Recommendation	
6.1. Conclusion.....	105
6.2. Recommendations.....	105
REFERENCE	

List of Tables

Chapter 4: Result of Numerical analysis and Discussion	Page Number
Table 4.1.1. Natural Frequency (Hz) at Case 1	32
Table 4.1.2. Natural Frequency (Hz) at Case 2	35
Table 4.1.3. Natural Frequency (Hz) at Case 3	39
Table 4.1.4. Natural Frequency (Hz) at Case 4	40
Table 4.1.5. Natural Frequency (Hz) at Case 5	43
Table 4.1.6. Natural Frequency (Hz) at Case 6	45
Table 4.3.1. Von-mises stress and Total Deformation at case 1	79
Table 4.3.2. Von-mises stress and Total Deformation comparison at case 2	81
Table 4.3.3. Von-mises stress and Total Deformation comparison at case 3	82
Table 4.3.4. Von-mises stress and Total Deformation comparison at case 4	85
Table 4.3.5. Von-mises stress and Total Deformation comparison at case 5	88
Table 4.3.6. Von-mises stress and Total Deformation comparison at case 6	90

List of Figures

Chapter 1: Introduction		Page No.
Fig.1.1.	A Typical Excavator.	2
Fig. 1.2.	Different Types of Excavator. [19]	3
Fig. 1.1.2.	Excavator Bucket Terminology. [by CWS Industries]	5
Fig. 1.3.1.	A simple tension test and a real life loading condition.	7
Fig.1.3.2.	Representation of a pure distortion case.	8

Chapter 3: Problem Specification and Numerical Simulation		
Fig. 3.1.	Bucket Model Specifications.	21
Fig. 3.2.	Bucket Model General Terminology.	22
Fig. 3.4.	Boundary conditions and input forces on the bucket.	23
Fig. 3.5.	Bucket model after meshing.	24
Fig. 3.6.1	Bare Bucket model.	25
Fig. 3.6.2.	Bucket models with different attachments.	26
Fig. 3.6.3.	Bucket models with different arrangement of rubber strips.	27
Fig. 3.6.4.	Bucket models with different arrangements of rubber.	28
Fig. 3.6.5.	Bucket models with different thickness of rubber strips.	29
Chapter 4: Result of Numerical analysis and Discussion		
Fig. 4.1.1 (a)	1 st mode shape at case 1.	32
Fig. 4.1.1 (b)	2 nd mode shape at case 1.	33
Fig. 4.1.1 (c)	3 rd mode shape at case 1.	33
Fig. 4.1.1 (d)	4 th mode shape at case 1.	34
Fig. 4.1.1 (e)	5 th mode shape at case 1.	34
Fig. 4.1.2.1.	1 st mode shapes for case 2.	36
Fig. 4.1.2.2.	2 nd mode shapes for case 2.	36
Fig. 4.1.2.3.	3 rd mode shapes for case 2.	37
Fig. 4.1.2.4.	4 th mode shapes for case 2.	37
Fig. 4.1.2.5.	5 th mode shapes for case 2.	38
Fig. 4.1.4.4.	4 th mode shapes for case 4.	41
Fig. 4.1.4.5.	5 th mode shapes for case 4.	42
Fig. 4.1.5.4	4 th mode shapes for case 5.	43
Fig. 4.1.5.5.	5 th mode shapes for case 5.	44

Fig. 4.2.2.1.a	Amplitudes along X-Direction at 1 st mode for case 2 compared with case 1.	48
Fig. 4.2.2.1.b	Amplitudes along Y-Direction at 1 st mode for case 2 compared with case 1.	48
Fig. 4.2.2.1.c	Amplitudes along Z-Direction at 1 st mode for case 2 compared with case 1.	48
Fig. 4.2.2.2.a	Amplitudes along X-Direction at 2 nd mode for case 2 compared with case 1.	49
Fig. 4.2.2.2.b	Amplitudes along Y-Direction at 2 nd mode for case 2 compared with case 1.	49
Fig. 4.2.2.2.c	Amplitudes along Z-Direction at 2 nd mode for case 2 compared with case 1.	49
Fig. 4.2.2.3.a	Amplitudes along X-Direction at 3 rd mode for case 2 compared with case 1.	50
Fig. 4.2.2.3.b	Amplitudes along Y-Direction at 3 rd mode for case 2 compared with case 1.	50
Fig. 4.2.2.3.c	Amplitudes along Z-Direction at 3 rd mode for case 2 compared with case 1.	50
Fig. 4.2.2.4.a	Amplitudes along X-Direction at 4 th mode for case 2 compared with case 1.	51
Fig. 4.2.2.4.b	Amplitudes along Y-Direction at 4 th mode for case 2 compared with case 1.	51
Fig. 4.2.2.4.c	Amplitudes along Z-Direction at 4 th mode for case 2 compared with case 1.	51
Fig. 4.2.2.5.a	Amplitudes along X-Direction at 5 th mode for case 2 compared with case 1.	52
Fig. 4.2.2.5.b	Amplitudes along Y-Direction at 5 th mode for case 2 compared with case 1.	52
Fig. 4.2.2.5.c	Amplitudes along Z-Direction at 5 th mode for case 2 compared with case 1.	52
Fig. 4.2.3.1.a.	Amplitudes along X-Direction at 1 st mode for case 3 compared with case 1.	54
Fig. 4.2.3.1.b	Amplitudes along Y-Direction at 1 st mode for case 3 compared with case 1.	54
Fig. 4.2.3.1.c.	Amplitudes along Z-Direction at 1 st mode for case 3 compared with case 1.	54
Fig. 4.2.3.2.a.	Amplitudes along X-Direction at 2 nd mode for case 3 compared with case 1.	55
Fig. 4.2.3.2.b	Amplitudes along Y-Direction at 2 nd mode for case 3 compared with case 1.	55
Fig. 4.2.3.2.c.	Amplitudes along Z-Direction at 2 nd mode for case 3 compared with case 1.	55
Fig. 4.2.3.3.a.	Amplitudes along X-Direction at 3 rd mode for case 3 compared with case 1.	56
Fig. 4.2.3.3.b	Amplitudes along Y-Direction at 3 rd mode for case 3 compared with case 1.	56
Fig. 4.2.3.3.c.	Amplitudes along Z-Direction at 3 rd mode for case 3 compared with case 1.	56
Fig. 4.2.3.4.a.	Amplitudes along X-Direction at 4 th mode for case 3 compared with case 1.	57

Fig. 4.2.3.4.b	Amplitudes along Y-Direction at 4 th mode for case 3 compared with case 1.	57
Fig. 4.2.3.4.c	Amplitudes along Z-Direction at 4 th mode for case 3 compared with case 1.	57
Fig. 4.2.3.5.a.	Amplitudes along X-Direction at 5 th mode for case 3 compared with case 1.	58
Fig. 4.2.3.5.b	Amplitudes along Y-Direction at 5 th mode for case 3 compared with case 1.	58
Fig. 4.2.3.5.c.	Amplitudes along Z-Direction at 5 th mode for case 3 compared with case 1.	58
Fig. 4.2.4.1.a.	Amplitudes along X-Direction at 1 st mode for case 4 compared with case 1.	61
Fig. 4.2.4.1.b	Amplitudes along Y-Direction at 1 st mode for case 4 compared with case 1.	61
Fig. 4.2.4.1.c.	Amplitudes along Z-Direction at 1 st mode for case 4 compared with case 1.	61
Fig. 4.2.4.2.a.	Amplitudes along X-Direction at 2 nd mode for case 4 compared with case 1.	62
Fig. 4.2.4.2.b	Amplitudes along Y-Direction at 2 nd mode for case 4 compared with case 1.	62
Fig. 4.2.4.2.c.	Amplitudes along Z-Direction at 2 nd mode for case 4 compared with case 1.	62
Fig. 4.2.4.3.a.	Amplitudes along X-Direction at 3 rd mode for case 4 compared with case 1.	63
Fig. 4.2.4.3.b	Amplitudes along Y-Direction at 3 rd mode for case 4 compared with case 1.	63
Fig. 4.2.4.3.c.	Amplitudes along Z-Direction at 3 rd mode for case 4 compared with case 1.	63
Fig. 4.2.4.4.a.	Amplitudes along X-Direction at 4 th mode for case 4 compared with case 1.	64
Fig. 4.2.4.4.c.	Amplitudes along Y-Direction at 4 th mode for case 4 compared with case 1.	64
Fig. 4.2.4.5.a.	Amplitudes along X-Direction at 5 th mode for case 4 compared with case 1.	65
Fig. 4.2.4.5.b	Amplitudes along X-Direction at 5 th mode for case 4 compared with case 1.	65
Fig. 4.2.4.5.c.	Amplitudes along X-Direction at 5 th mode for case 4 compared with case 1.	65
Fig. 4.2.5.1.a	Amplitudes along X-Direction at 1 st mode for case 5.	68
Fig. 4.2.5.1.b	Amplitudes along Y-Direction at 1 st mode for case 5.	68
Fig. 4.2.5.1.c	Amplitudes along Z-Direction at 1 st mode for case 5.	68
Fig. 4.2.5.2.a	Amplitudes along X-Direction at 2 nd mode for case 5.	69
Fig. 4.2.5.2.b	Amplitudes along Y-Direction at 2 nd mode for case 5.	69
Fig. 4.2.5.2.c	Amplitudes along Z-Direction at 2 nd mode for case 5.	69

Fig. 4.2.5.3.a	Amplitudes along X-Direction at 3 rd mode for case 5.	70
Fig. 4.2.5.3.b	Amplitudes along Y-Direction at 3 rd mode for case 5.	70
Fig. 4.2.5.3.c	Amplitudes along Z-Direction at 3 rd mode for case 5.	70
Fig. 4.2.5.4.a	Amplitudes along X-Direction at 4 th mode for case 5.	71
Fig. 4.2.5.4.c	Amplitudes along Z-Direction at 4 th mode for case 5.	71
Fig. 4.2.5.5.a	Amplitudes along X-Direction at 5 th mode for case 5.	72
Fig. 4.2.5.5.b	Amplitudes along Y-Direction at 5 th mode for case 5.	72
Fig. 4.2.5.5.c	Amplitudes along Z-Direction at 5 th mode for case 5.	72
Fig. 4.2.6.1.a	Amplitudes along X-Direction at 1 st mode for case 6.	74
Fig. 4.2.6.1.b	Amplitudes along Y-Direction at 1 st mode for case 6.	74
Fig. 4.2.6.1.c	Amplitudes along Z-Direction at 1 st mode for case 6.	74
Fig. 4.2.6.2.a	Amplitudes along X-Direction at 2 nd mode for case 6.	75
Fig. 4.2.6.2.b	Amplitudes along Y-Direction at 2 nd mode for case 6.	75
Fig. 4.2.6.2.c	Amplitudes along Z-Direction at 2 nd mode for case 6.	75
Fig. 4.2.6.3.a	Amplitudes along X-Direction at 3 rd mode for case 6.	76
Fig. 4.2.6.3.b	Amplitudes along Y-Direction at 3 rd mode for case 6.	76
Fig. 4.2.6.3.c	Amplitudes along Z-Direction at 3 rd mode for case 6.	76
Fig. 4.2.6.4.a	Amplitudes along X-Direction at 4 th mode for case 6.	77
Fig. 4.2.6.4.c	Amplitudes along Z-Direction at 4 th mode for case 6.	77
Fig. 4.2.6.5.a	Amplitudes along X-Direction at 5 th mode for case 6.	78
Fig. 4.2.6.5.b	Amplitudes along Y-Direction at 5 th mode for case 6.	78
Fig. 4.2.6.5.c	Amplitudes along Z-Direction at 5 th mode for case 6.	78
Fig. 4.3.1.1.	Von-mises stress for the bare bucket at case 1.	80
Fig. 4.3.1.2.	total deformation for the bare bucket at case 1.	80
Fig. 4.3.2.1.	Von-mises stress for case 2.	82

Fig. 4.3.2.2.	Total deformation for Case 2.	82
Fig. 4.3.3.1.	Von-mises stress for case 3.	83
Fig. 4.3.3.2.	Total deformation for Case 3.	84
Fig. 4.3.4.1.	Von-mises stress for case 4.	86
Fig. 4.3.4.2.	Total deformation for Case 4.	87
Fig. 4.3.5.1.	Von-mises stress for case 5.	89
Fig. 4.3.5.2.	Total deformation for Case 5.	89
Fig. 4.3.6.1.	Von-mises stress for case 6.	91
Fig. 4.3.6.2.	Total deformation for Case 6.	91
Chapter 5: Experimental Results and Validation		
Fig. 5.2.1 (a)	Bucket Model and Fixture for Experiment	93
Fig. 5.2.1 (b)	Experimental Bucket model specifications.	94
Fig. 5.2.2.	Shaker K2007E01	95
Fig. 5.2.3.	Force Sensor	95
Fig. 5.2.4.	Signal Conditioner	95
Fig. 5.2.5.	Cable	95
Fig. 5.2.6.	Function Generator	95
Fig. 5.2.7.	Oscilloscope	96
Fig. 5.3.	The Cases of Experiment and Simulation.	98
Fig. 5.4.	Experimental Arrangement to perform vibration analysis of bucket.	99
Fig. 5.7.1.	Experimental Results Comparison at 2 nd mode.	102
Fig. 5.7.2.	Experimental Results Comparison at 3 rd mode.	102
Fig. 5.7.3.	Simulation Results Comparison at 2 nd mode.	103
Fig. 5.7.4.	Simulation Results Comparison at 3 rd mode.	103

APPENDIX		
Fig A.1.1	Von Mises stress developed in the bucket. [16]	109
Fig A.1.2.	Total deformation developed in the bucket. [16]	109
Fig A.2.1.	Von Mises stress developed in the bucket.	110
Fig A.2.2.	Total deformation developed in the bucket.	110
Fig. 4.1.3.1	1 st mode shapes for case 3.	111
Fig. 4.1.3.2.	2 nd mode shapes for case 3.	112
Fig. 4.1.3.3.	3 rd mode shapes for case 3.	113
Fig. 4.1.3.4	4 th mode shapes for case 3.	114
Fig. 4.1.3.5	5 th mode shapes for case 3.	115
Fig. 4.1.4.1.	1 st mode shapes for case 4.	116
Fig. 4.1.4.2.	2 nd mode shapes for case 4.	117
Fig. 4.1.4.3.	3 rd mode shapes for case 4.	118
Fig. 4.1.5.1	1 st mode shapes for case 5.	119
Fig. 4.1.5.2	2 nd mode shapes for case 5.	119
Fig. 4.1.5.3	3 rd mode shapes for case 5.	120
Fig. 4.1.6.1.	1 st mode shapes for case 6.	121
Fig. 4.1.6.2	2 nd mode shapes for case 6.	121
Fig. 4.1.6.3	3 rd mode shapes for case 6.	122
Fig. 4.1.6.4	4 th mode shapes for case 6.	122
Fig. 4.1.6.5	5 th mode shapes for case 6.	123

Chapter 1

Introduction

1.1 Excavator:

Excavators are heavy construction equipment consisting of a boom, arm or stick, bucket and cab on a rotating platform known as the "house". The house sits atop an undercarriage with tracks or wheels. They are a natural progression from the steam shovels and often called power shovels. All movement and functions of a hydraulic excavator are accomplished through the use of hydraulic fluid, with hydraulic cylinders and hydraulic motors. Excavators are also called **diggers, JCBs, mechanical shovels, or 360-degree excavators** (sometimes abbreviated simply to **360**). Tracked excavators are sometimes called "trackhoes" by analogy to the backhoe. In the UK, wheeled excavators are sometimes known as "rubber ducks."

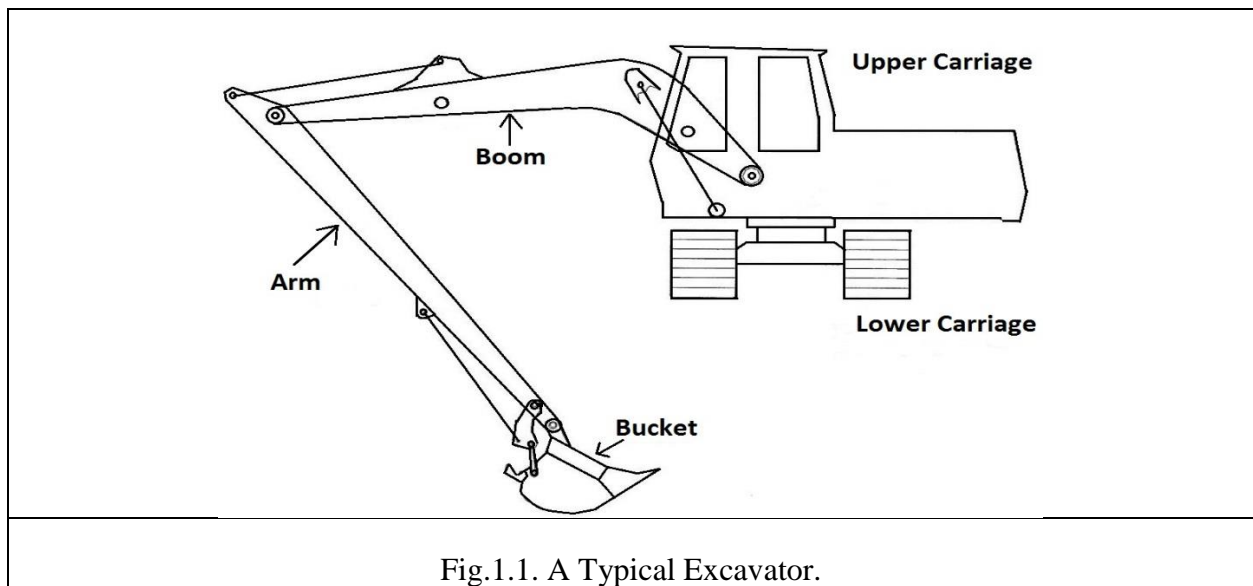


Fig.1.1. A Typical Excavator.

Excavators are used in many ways:

- Digging of trenches, holes, foundations
- Material handling
- Brush cutting with hydraulic attachments
- Forestry work and Forestry mulching
- Demolition
- General grading/landscaping
- Mining, especially, but not only open-pit mining
- River dredging
- Driving piles, in conjunction with a pile driver

- Drilling shafts for footings and rock blasting, by use of an auger or hydraulic drill attachment



CAT 5230 in coal mining operation



A L&T Komatsu Excavator seen in India



A New Holland E215 in Hamburg, Germany.

Fig. 1.2. Different Types of Excavator. [22]

Modern, hydraulic excavators come in a wide variety of sizes. The smaller ones are called mini or compact excavators. For example, Caterpillar's smallest mini-excavator weighs 2,060 pounds (930 kg) and has 13 hp; their largest model is the largest excavator available (a record previously held by the Orenstein & Koppel RH400) the CAT 6090, it weighs in excess of 2,160,510 pounds (979,990 kg), has 4500 hp and has a bucket size of around 52.0 m³ depending on bucket fitted.

1.1.1 Excavator attachments and configuration

Hydraulic excavator capabilities have expanded far beyond excavation tasks with buckets. With the advent of hydraulic-powered attachments such as a breaker, a grapple or an auger, the excavator is frequently used in many applications other than excavation. Many excavators feature a quick coupler for simplified attachment mounting, increasing the machine's utilization on the jobsite. Excavators are usually employed together with loaders and bulldozers. Most wheeled, compact and some medium-sized (11 to 18-tonne) excavators have a backfill (or dozer) blade. This is a horizontal bulldozer-like blade attached to the undercarriage and is used for levelling and pushing removed material back into a hole.

The two main sections of an excavator are the undercarriage and the house. The undercarriage includes the blade (if fitted), tracks, track frame, and final drives, which have a hydraulic motor and gearing providing the drive to the individual tracks, and the house includes the operator cab, counterweight, engine, fuel and hydraulic oil tanks. The house attaches to the undercarriage

by way of a center pin. High pressure oil is supplied to the tracks' hydraulic motors through a hydraulic swivel at the axis of the pin, allowing the machine to slew 360° unhindered.

The main boom attaches to the house, and can be one of several different configurations:

- Most are mono booms: these have no movement apart from straight up and down.
- Some others have a knuckle boom which can also move left and right in line with the machine.
- Another option is a hinge at the base of the boom allowing it to hydraulically pivot up to 180° independent to the house; however, this is generally available only to compact excavators.
- There are also triple-articulated booms (TAB).

Attached to the end of the boom is the stick (or dipper arm). The stick provides the digging force needed to pull the bucket through the ground. The stick length is optional depending whether reach (longer stick) or break-out power (shorter stick) is required.

On the end of the stick is usually a bucket. A wide, large capacity (mud) bucket with a straight cutting edge is used for cleanup and levelling or where the material to be dug is soft, and teeth are not required. A general purpose (GP) bucket is generally smaller, stronger, and has hardened side cutters and teeth used to break through hard ground and rocks. Buckets have numerous shapes and sizes for various applications. There are also many other attachments which are available to be attached to the excavator for boring, ripping, crushing, cutting, lifting, etc.

1.1.2 Excavator Bucket:

Excavator buckets are made of solid steel and generally present teeth protruding from the cutting edge, to disrupt hard material and avoid wear-and-tear of the bucket. Subsets of the excavator bucket are: the ditching bucket and trenching bucket. A ditching bucket is a wider bucket with no teeth, 5–6 feet (1.5–1.8 m) used for excavating larger excavations and grading stone. A trenching excavator bucket is normally 6 to 24 in (150 to 610 mm) wide and with protruding teeth.

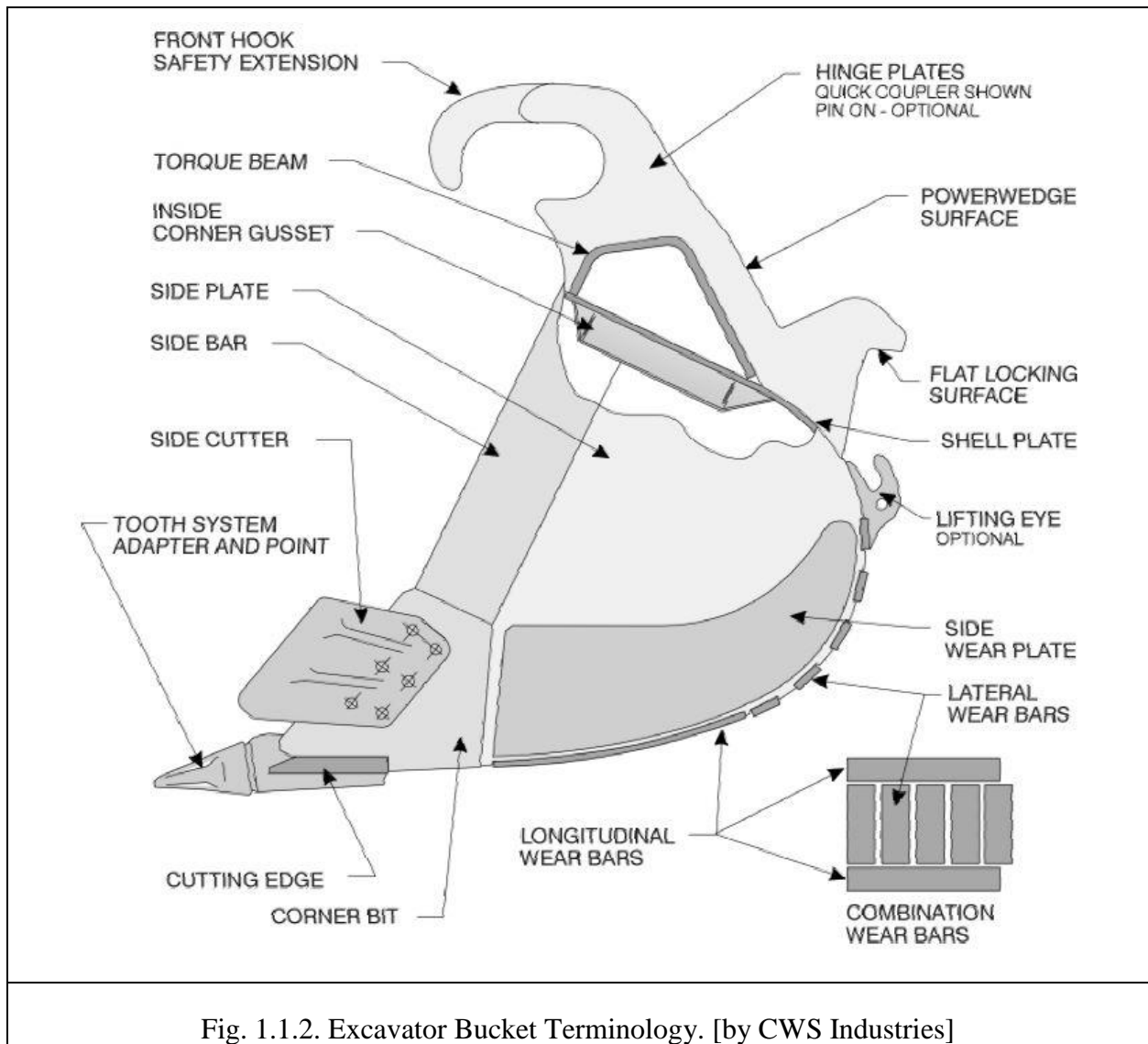


Fig. 1.1.2. Excavator Bucket Terminology. [by CWS Industries]

This is an advanced excavator bucket by CWS Industries which have additional side cutter to cut an advanced design of tooth. Also it is reinforced with side wear plate and lateral wear bars to resist wear. The coupling mechanism at the hook and hinge plate is also an advanced one to withstand high load at the bucket. This type of advanced bucket is of high cost so will not be available to all consumers. However was the key idea of using reinforcement with the standard and usual bucket in this thesis.

1.2 Vibration

Modal analysis:

Modal analysis is the study of the dynamic properties of structures under vibrational excitation.

Modal analysis is the field of measuring and analyzing the dynamic response of structures and fluids when excited by an external force. Examples would include measuring the vibration of a car's body when it is attached to an electromagnetic shaker, or the Modal analysis is the study of the dynamic properties of structures under vibrational excitation.

The goal of modal analysis in structural mechanics is to determine the natural mode shapes and frequencies of an object or structure during free vibration. It is common to use the finite element method (FEM) to perform this analysis because, like other calculations using the FEM, the object being analyzed can have arbitrary shape and the results of the calculations are acceptable. The types of equations which arise from modal analysis are those seen in Eigen systems. The physical interpretation of the eigenvalues and eigenvectors which come from solving the system are that they represent the frequencies and corresponding mode shapes. Sometimes, the only desired modes are the lowest frequencies because they can be the most prominent modes at which the object will vibrate, dominating all the higher frequency modes.

Harmonic analysis:

Any sustained cyclic load will produce a sustained cyclic response (a harmonic response) in a structural system. Harmonic response analysis gives the ability to predict the sustained dynamic behavior of structures, thus enabling to verify whether or not the designs will successfully overcome resonance, fatigue, and other harmful effects of forced vibrations.

Harmonic response analysis is a technique used to determine the steady-state response of a linear structure under loads that vary sinusoidally (harmonically) with time. The idea is to calculate the structure's response at several frequencies and obtain a graph of some response quantity (usually displacements) versus frequency. "Peak" responses are then identified on the graph and stresses reviewed at those peak frequencies.

This analysis technique calculates only the steady-state, forced vibrations of a structure. The transient vibrations, which occur at the beginning of the excitation, are not accounted for in a harmonic response analysis.

1.3. Von Mises Stress:

Von Mises stress is widely used by designers to check whether their design will withstand a given load condition.

Use of Von Mises stress: Von Mises stress is considered to be a safe haven for design engineers. Using this information an engineer can say his design will fail, if the maximum value of Von Mises stress induced in the material is more than strength of the material. It works well for most cases, especially when the material is ductile in nature.

When does a material fail? : One of the easiest way to check when a material fails is a *simple tension test*. Here the material is pulled from both ends. When the material reaches the yield point (for ductile material) the material can be considered as failed. The simple tension test is a unidirectional test, this is shown in the first part of Fig.1.3.1.

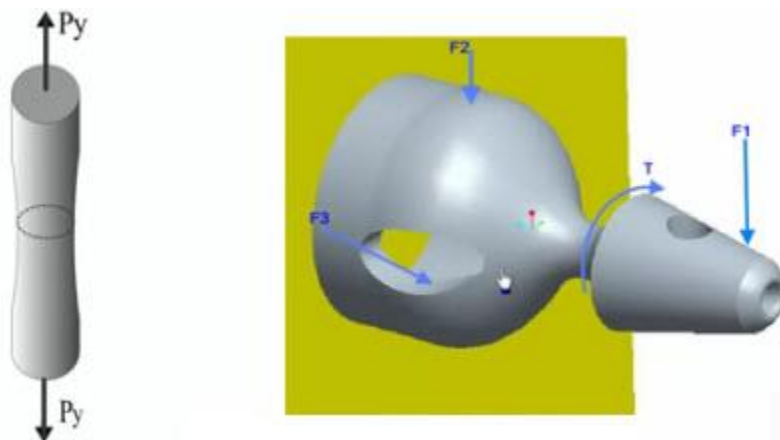


Fig. 1.3.1. A simple tension test and a real life loading condition.

Now consider the situation in second part of Fig.1.3.1, an actual engineering problem with a complex loading condition. Can we say here also, that the material fails when the maximum normal stress value induced in the material is more than the yield point value. If we use such an assumption, we would be using a failure theory called 'normal stress theory'. Many years of

engineering experience has shown that normal stress theory doesn't work in most of the cases. The most preferred failure theory used in industry is 'Von Mises stress' based.

Distortion energy theory: The concept of Von Mises stress arises from the *distortion energy failure theory*. Distortion energy failure theory is comparison between 2 kinds of energies, 1) Distortion energy in the actual case 2) Distortion energy in a simple tension case at the time of failure. According to this theory, failure occurs when the distortion energy in actual case is more than the distortion energy in a *simple tension case* at the time of failure.

Distortion energy: It is the energy required for shape deformation of a material. During pure distortion, the shape of the material changes, but volume does not change. This is illustrated in Fig.1.3.2.

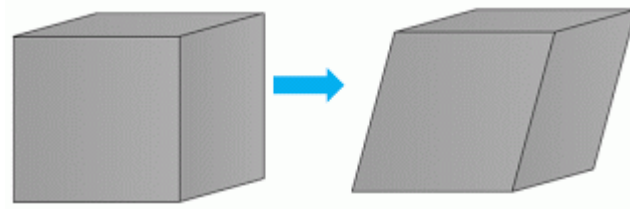


Fig.1.3.2. Representation of a pure distortion case.

Distortion energy required per unit volume, u_d for a general 3 dimensional case is given in terms of principal stress values as:

$$u_d = \frac{1 + \nu}{3E} \left[\frac{(\sigma_1 - \sigma_2)^2 + (\sigma_2 - \sigma_3)^2 + (\sigma_3 - \sigma_1)^2}{2} \right]$$

Distortion energy for *simple tension case* at the time of failure is given as:

$$u_{d,sim} = \frac{1 + \nu}{3E} \sigma_y^2$$

Expression for Von Mises stress: The above 2 quantities can be connected using *distortion energy failure theory*, so the condition of failure will be as follows.

$$\left[\frac{(\sigma_1 - \sigma_2)^2 + (\sigma_2 - \sigma_3)^2 + (\sigma_3 - \sigma_1)^2}{2} \right]^{1/2} \geq \sigma_y$$

The left hand side of the above equation is denoted as Von Mises stress.

$$\left[\frac{(\sigma_1 - \sigma_2)^2 + (\sigma_2 - \sigma_3)^2 + (\sigma_3 - \sigma_1)^2}{2} \right]^{1/2} = \sigma_v$$

So as a failure criterion, the engineer can check whether Von Mises stress induced in the material exceeds yield strength (for ductile material) of the material. So the failure condition can be simplified as

$$\sigma_v \geq \sigma_y$$

1.4. The importance of vibration analysis and it's reduction:

The measurement of natural frequencies is a major concern as it will tell us if a system's natural frequencies will be same as the operating frequencies which can tell if resonance will occur or not. It is a major aspect to avoid resonance as it will destroy the system. The vibration amplitude measurement is important because there will always be vibration in any system which has moving parts and exposed to any force. These vibration amplitude is required to reduce because the operator involved with the system will be exposed to vibration that can harm him physically and mentally in the long run. Also because of the vibration noise occurs which harms people nearby after certain level.

1.5. Research Objective

- a) The thesis is focused on vibration analysis and stress developed in an excavator bucket due to reaction force from the soil or rock that it can cut or mine. Firstly, modal analysis is done to understand the natural frequencies and mode shapes, secondly harmonic analysis is done to understand vibration amplitudes and lastly stress analysis is done to find out Von mises stress developed at the different regions of the bucket.
- b) Design modification is done for further reduction of stress and vibration using different damping materials. The use of rubber is focused most as rubber is the popular damping material used and also a cheaper one. Then the results were analysed and compared.
- c) Finally design optimization of an effective excavator bucket with reinforcements is given which will be a cheaper one after modification but less exposed to vibrations.

1.6. Possible outcome

- a) A clear understanding of the Mode shapes and natural frequencies of the standard excavator bucket.
- b) An effective model of excavator bucket with less stress developed or keeping the stress constant but less vibration developed.
- c) A much less vibrating model because of optimization in damping for most of the natural frequencies.
- d) Less weight obtained for employing structural concept. Where traditional reinforcements use high density steel increasing the weight of the bucket but the modification in this thesis will literally keep the bucket weight same as low density rubber is used.
- e) Increase in the strength of the bucket because of reinforcements of different materials in the bucket.

1.7. Outline of Methodology:

- a) Modelling of an excavator bucket using Solidworks software. The modelling was done using a standard specification provided online by Hand Engineering Ltd., Drumone, Oldcastle, Co. Meath, Ireland. The modelling procedure in the software involve using 2D drawing, shell and extrude options and all other necessary features. The model involves a constant thickness almost everywhere for the ease of design and analysis. The bush is also attached with the bucket hanger which is modelled likewise where the fixed support is given as boundary condition.
- b) The model needs to be converted into proper file to take to the analysis platform and analyse afterwards which is done by the software itself. The import of the model is then done in the ANSYS analysis platform.
- c) ANSYS Workbench is used as project platform where different analysis methods are available to use. The Modal, Harmonic and Static Structure analysis tools is opened in the workbench project.
- d) The input of the engineering data is an important step to be done at the beginning of the analysis where material properties have been put in the system for specific part of the model drawn and imported in the system.
- e) Use of Different techniques (using rubber and other materials with bucket) to reduce stress, vibration and weight is a major highlight of the thesis which is done in the modelling and engineering data section.
- f) Proper meshing is performed to analyse the model. A method of automated meshing is done at the beginning then individual meshing and sizing was performed for getting solution.
- g) The boundary conditions have been put on the meshed region of interest and also reaction and input forces have been defined using direct tool from the software at the different meshing region of interest.
- h) The solution is performed and results have been extracted from the software for further analysis and comparisons.
- i) An experiment have also been performed on a small bucket model which was manufactured locally. The experiment of harmonic analysis was done and the results of amplitudes and input forces have been taken for consideration at first three natural frequencies.

- j) Comparison of the results of the experiment with the simulation results is done as the similar experimental model is drawn in the Solidworks software then simulation was performed in that model.
- k) The natural frequencies, mode shapes and von mises stress were found out of the standard excavator bucket and later compared with the modifications in each section.
- l) A conclusion and recommendation is given for the different modification of the bucket in each section of the result comparison.

Chapter 2

Literature Review

2.1 Introduction:

Considerable attentions were focused on designing of the excavator equipment, where basically the attachments which are boom, arm and bucket were designed [1]. The designs involved also included modifications in sizes and actually the basic thesis to understand excavator attachments.

Today hydraulic excavators are widely used in construction, mining, excavation, and forestry applications. The terrain condition, soil parameters, and the soil-tool interaction forces exerted during excavation operation are required to find out because these forces are important for better design of the tool, backhoe parts and for trajectory planning [2]. There are many variations in hydraulic excavators. They may be either crawler or rubber-tire-carrier-mounted, and there are many different operating attachments such as boom, arm and bucket. With the options in types, attachments, and sizes of machines, there are differences in appropriate applications and therefore variations in economic advantages of using excavator. Due to severe working conditions, excavator parts are subject to corrosive effects and high loads [3]. The excavator mechanism/attachment works under unpredictable working conditions that is why poor strength properties of the excavator parts like boom, arm and bucket limit the life expectancy of the excavator. Therefore, excavator parts must be strong enough to cope with caustic working conditions of the excavator [4]. Normally the excavator is working under cyclic motion during excavation process. Due to this repetitive nature of work, cyclic stresses are developed in the parts of backhoe attachment. The various cyclic loads depend on the working conditions. It is necessary to perform field measurement to take these loads into account in design. Loads and strains of the excavator attachments have been measured and investigated for three excavator models to determine the design loads of attachments comparing stresses [5]. High level of stresses can cause the damage of critical parts of excavators and it will adversely affected on productivity of machine.

Now a days weight is major concern while designing the machine components. So for reducing the overall cost as well as for smoothing the performance of machine, optimization is needed.

2.2. Utility of FEA and optimization for attachment

Finite Element Analysis (FEA) is a very effective technique in strength calculations of the structures working under known load and boundary conditions. We can determine the critical loading conditions of the excavator by performing static force analysis of the mechanism involved for different piston displacements. Preparation of the CAD model can be done either using a commercial FEA program or using a separate commercial program, which is specialized for CAD. Structural optimization for strength is a popular subject in modern engineering design. It has been widely used to obtain an optimum strength/material mass ratio for structures under specified load conditions [4]. The FEA and optimization is versatile tool for designing the backhoe attachment in hydraulic excavator.

Finite element analysis is an important part of the overall design process, serving to verify or validate a design prior to its manufacture. Because finite element analysis is a simulation tool, the actual design is idealized, with the quality of the idealization dependent on the skill and experience of the analyst. Naresh N. Oza, had carried out the FEA and optimization of Earth moving attachment as backhoe in 2006 [6]. They have done the EFA of the boom, arm and bucket by following the standard practice of analysis and carry out the solution for stress and deflection analysis, finally the results are compared with the results obtained from the MathCAD. Optimization for weight is also carried by them and reduces the weight of arm from 180 Kg to 154 Kg and stresses reduced from 386 MPa to 263 MPa. The weight of the bucket is reduced from 165 Kg to 156 Kg, and the developed stresses are within the limit [6].

The computational modeling techniques and computer programs developed for the structural design analysis of a micro excavator digging arm mechanism under static or quasi-static loading conditions are outlined by MA Bromfield and WT Evans in 1988 [7]. The computer programs allow the design engineer to analyze the forces and stresses at numerous locations on the digging arm, which can assume various geometric configurations. The computer theory was used to develop an integrated CAD software package to allow the design engineer to carry out structural analysis and design optimization calculations on the Powerfab 360WT microexcavator. Product development times and costs have been reduced as a result of using the CAD software. The results showed good correlation between theoretical and experimental stresses, considering

the many simplifications that were made in the modelling technique [7]. Ram Vadhe and Vrajesh Dave, in 1993 have developed a multi-body model of an excavator and to simulate the prototype testing conditions. Multi-body simulation involves the simulation of rigid body system under the application of cylinder forces and/or motions. The link to be designed is considered as a flexible body. Two cycles of digging and dumping operations are simulated to determine the reaction forces generated at each joint and stresses generated on the flexible body. The generated load case can be used for detailed FE analysis. The stress results of particular gauge locations are also compared with experimental data. They have concluded that the desktop prototype testing helps the designer to find out the worst operating condition, severe conditions and locate the trajectory of operation [8].

Tadeusz Smolnicki, Damian Derlukiewicz, and Mariusz Stańco, in 2008, have represented an application of the finite element method and accurate representation of the rigidity of support elements, mounting bolts, and phenomena occurring in the raceway–rolling element–raceway assembly of a caterpillar excavator, allowed for identification of the load distribution onto the individual rolling elements of the bearing. The results were compared with the classical compound model (iterative solution), however not taking into account deformation of the support elements under load. It was concluded that there is a significant discrepancy in not only the load distribution but also in the maximum load values. For the upper track the differences reach 70%, and for the lower track 25%. The evaluated bearing, selected according to the guidelines of one of the largest manufacturers of slewing bearings, for an existing single-bucket excavator, is subject to very high loads [9].

Luigi Solazzi, in 2010, have carried out study on the boom and the arm of an excavator in order to replace the material, which they are usually made of, with another material. In particular, the study wants to substitute the steel alloy for an aluminum alloy. This change lightens the components of the arm, allows to increase the load capacity of the bucket and so it is possible to increase the excavator productivity per hour. It has been assumed that the material used to make the arm is the steel alloy S355 JO EN 10025.

The evaluation of the new geometry of the arm with the different material has been studied in order to obtain at least the same safety factor and deformability of the original geometry (steel

alloy) and for the new geometry (aluminium alloy). On the basis of the relationships state above between the geometry of the steel alloy panel and the geometry of the aluminium alloy panel, for each component of the arm has been developed a new cross-section. They achieve that the total weight of the arm is reduced of about 50% and the capacity of the bucket increase of about 30%. Also increase the capacity of the bucket from 1 cubic m to 1.35 cubic m and so to increase the productivity per hour of the excavator [10].

2.3. Optimization of excavator attachment

J. Mottl has described ‘Voting Method’ for optimization of the weight of an excavator in 1992. He has carried out optimization for all parts of the excavator such as the chassis, cabin, jib, etc. with consideration as non-linear programming problem [11].

Mehmet Yener, in 2005, Parameterization of boom geometry is done to add some flexibility to interface called OPTIBOOM. Optimization of boom carried out for HMK 220LC model excavator [4].

In general there are 3 types of structural optimization techniques: sizing, geometrical and topology optimization. Out of these three techniques, topology optimization may give better results by changing the initial topology. Starting from an initial design, more than 100 alternative designs were created and compared with each other in terms of boom mass and maximum von Mises stresses. 21 shape parameters have been changed to obtain new boom geometries and the best design has been found at 90th design alternative. Maximum von Mises stress value at the 90th boom is 146 MPa while it is 186 MPa in the initial boom shape. Maximum von Mises stress has been reduced by 21.5 %. Mass of the 90th model is 1454 Kg and mass of the initial boom is 1403 kg. thus, mass of the boom increases only by 3.6 % [4].

Yefei Li, Xianghong Xu and Qinying Qiu, in 2006, have described a Grid-enabled analysis with self-developed codes provides easy access to computational and database capabilities to enhance the engineering system based on FEM results. The aim is to obtain better lighter and cheaper designs by using Finite Element Method. They have explained a strategy of combining a design of expert system platform and at genetic algorithm (GA). Optimization is carried out using genetic algorithm followed by a local search on the best point found using the Lagrange interval

search method from self-developed codes. The results then used to build CAD model for validating the stress and displace distribution of the whole parts of working equipment using the ANSYS model. A parametric geometry model suitable for FEM analysis is first generated using CAD software Pro/Engineer. The subsequent mesh is generated with minimum reference to the geometry information, as only the top-level entities in the CAD model are referenced in the meshing. There are two typically mesh tools used, either direct access provided to CAD parts and assemblies in their native mode, or third-party standard exchange data formats used. They have utilized interface between them which produce ANF file format as exchange geometry. Generation is processed in ANSYS batch mode. Volume mesh is then generated by applying parameters on adaptive meshing. The structure FEA solver ANSYS is then used to solve the problem, the model used in this work is an assembly static analysis. The problem is both complex and has a high computational cost. The goal is to reduce the weight and manufacture cost of hydraulic excavator, FEM is adopted here to analysis the whole structure's stress and displacement distribution [12].

Evolutionary structural optimization method is used for removing inefficient material from the structure by using the predefined criteria. Optimum solutions of boom of HMK360 LC excavator is carried out. Initial design of the boom was 5% heavier than the final design and maximum stress was 10% higher than the Von Mises design stress criterion. Maximum stress was limited by predetermined global maximum stress value and weight is decreased 4.6% of the initial design. Actually obtained result is not the best one but it is one of the good results which is satisfying design criteria and aimed mass [13].

Jakub Gottvald (2012) evaluated measuring of vibrations on a Bucket Wheel Excavator (BWE) during mining process [14]. They have studied the dynamic behavior of buckets wheel during working under mines. The main aim of this study was on vibration caused and its effect on the arm assembly of the excavator. Natural frequencies and shapes are very significant characteristic of dynamical behavior of structures. Their determination is mostly the first step in solving of various dynamical problems. Knowledge of natural frequencies and shapes gives us the possibility to assume how the structure will be sensitive to dynamical loads. Calculations of dynamical characteristics are very significant part in designing of structures in which various loadings are of utmost priority (Jakub Gottvald, 2011 and Jakub Gottvald, 2012) [15].

Bhaveshkumar P. PATEL and Jagdish M. PRAJAPATI [16] in their paper focused on structural weight optimization of backhoe excavator attachment using FEA approach by trial and error method. Shape optimization also performed for weight optimization and results are compared with trial and error method which shows identical results. The FEA of the optimized model also performed and their results are verified by applying classical theory [16].

In their paper Anil Jadhav, Vinayak Kulkarni, Abhijit Kulkarni, Prof. Ravi. K [17] depicted importing and meshing of CAD model of bucket and lower arm of excavator and its finite element analysis for strength and deformation evaluation. Also this paper covers the kinematic analysis of whole assembly for understanding the behavior of the various joints which are used for connecting the parts of excavator [17].

From the technical paper of KOMATSU the concept of using reinforced laminated steel damper at different places of the bucket provide an attenuation of about 5db noise. However detail investigation is still under process for this concept [18].

2.4. Summary of the literature review and scope of present work:

Considerable amount of vibration analysis is done by Gottvald for BWE (Bucket Wheel Excavator) which is for multiple bucket attached with wheel, but not for the single bucket. Some works were done on the design optimization of bucket, mostly by Jagdish M. PRAJAPATI [16] [19] [20] but not on the harmonic analysis of the bucket. These works are based on stress analysis which include load and design optimization. Optimization also performed in the size and material section for the attachments. Some paper [17] contains free vibration analysis for a bucket which did not consider material optimization or damping of the vibration and only discussed the natural frequencies of the attachments (boom, arm and bucket). This thesis will be focused on both vibration and strength analysis of the bucket with different reinforced materials as damping materials. Different techniques of using damping materials will also be used to upgrade excavator bucket. The natural frequencies and mode shapes for these optimizations will also be discussed.

Chapter 3

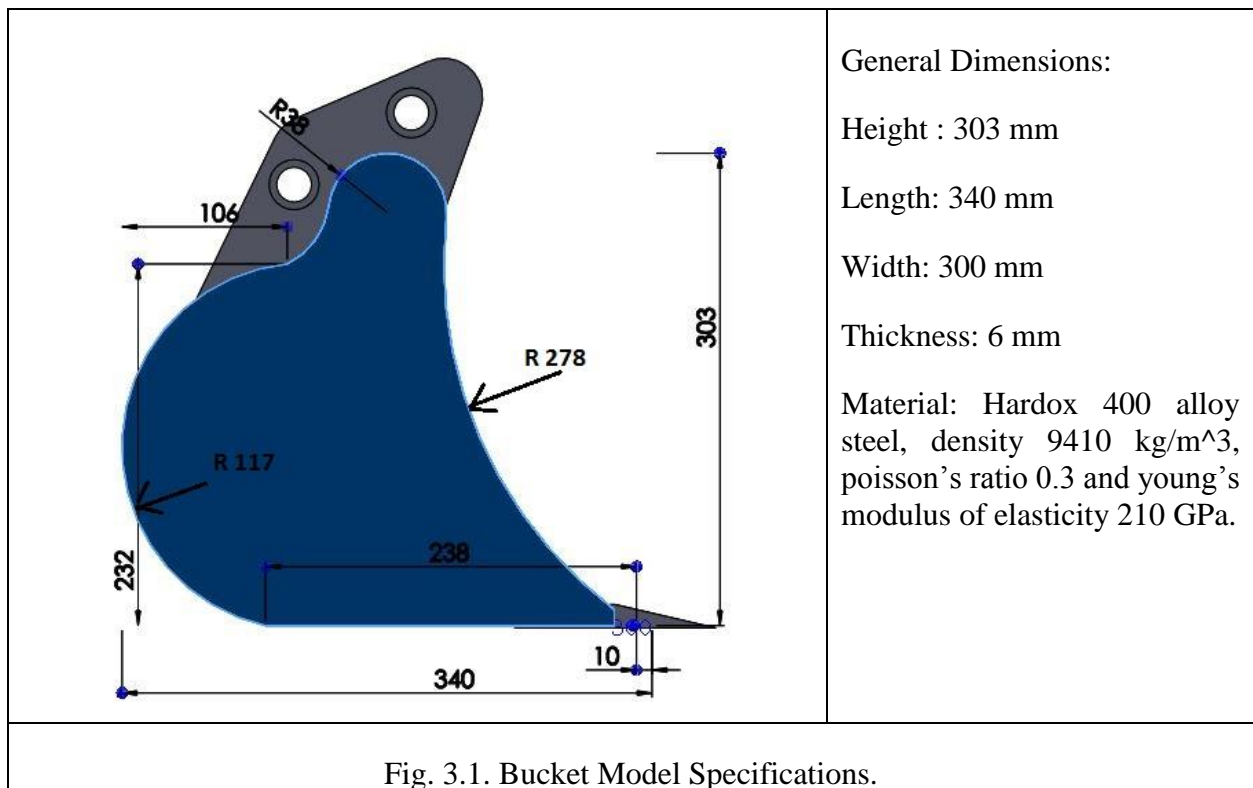
Problem Specification and Numerical Simulation

3.1. Introduction:

This chapter will discuss the excavator model's standard specification and modeling of the bucket. Later how the bucket was taken into a FEA platform and with boundary conditions the solution was performed. The modifications done on the bucket that are reinforcing of bucket with rubber and other materials are categorized into different cases for further explanation and discussion.

3.2. Modeling of the Bucket:

A standard 0.8 T Digging bucket of Hand Engineering Ltd., Drumone, Oldcastle, Co. Meath, Ireland, is used to model and perform numerical simulation. The bucket is drawn in SOLIDWORKS Software and later transformed into specific file to perform numerical analysis in ANSYS Software.



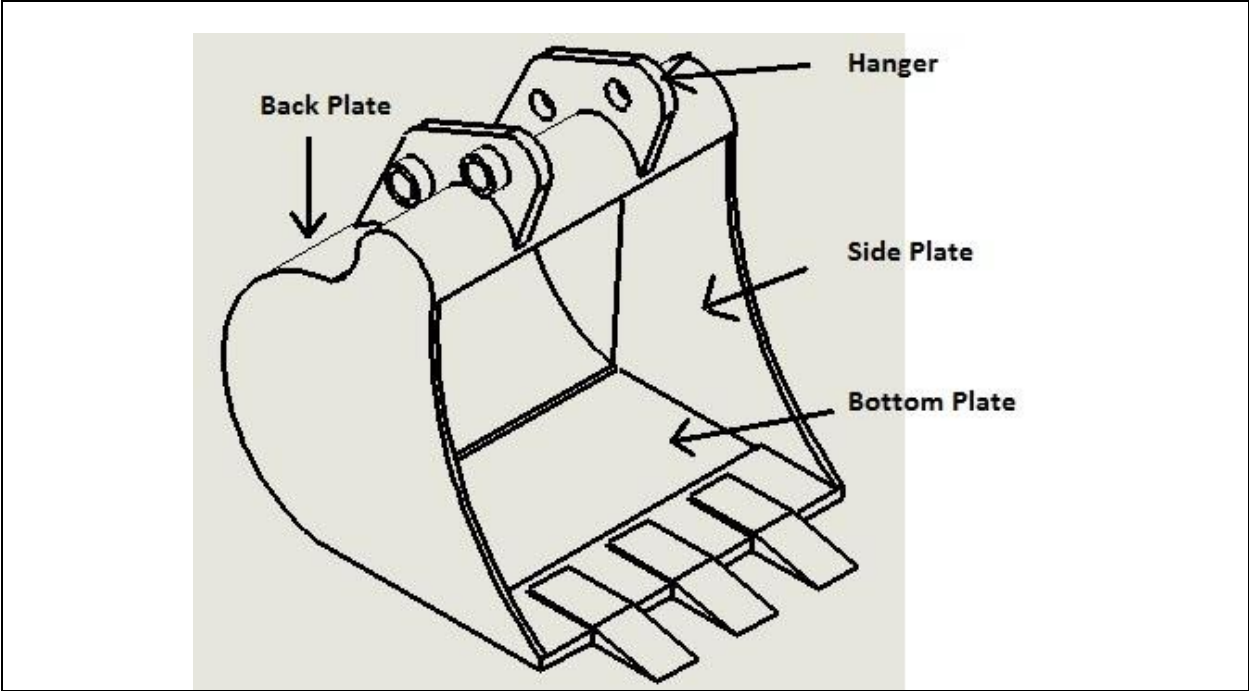


Fig. 3.2. Bucket Model General Terminology.

3.3. Numerical Analysis Procedure:

The numerical analysis involves following several procedures in the ANSYS Software. The flow chart of the procedure:

Create a New Project at the ANSYS Workbench		
Open 3 Analysis System		
Modal	Harmonic Response	Static Structure
Open Engineering Data to input all the material properties		
Import Geometry		
Open Model from each analysis system		
Specify Geometry with specific material		
Mesh		
Analysis Setting specifies analysis specifications		
Define Boundary Conditions		

Define Input Force in the System
Solve
Collect Specific Data Set from Solution Tree

3.4. Boundary Conditions and Input Force:

The boundary conditions and input forces on the bucket for different analysis have been taken from a published research papers [16] where the digging force is taken on the three teeth maximum 2542 N distributed at an angle 38.23 degree with the surface of the bottom plate or X-direction and the force given by the cylinder on the bucket is constant 11380 N perpendicular on the surface of the bottom plate or parallel to Y-direction. The boundary condition taken here in form that the bucket mounting lug bush is fixed from inside at A and B, so the cylindrical surface A and B from inside is considered fixed.

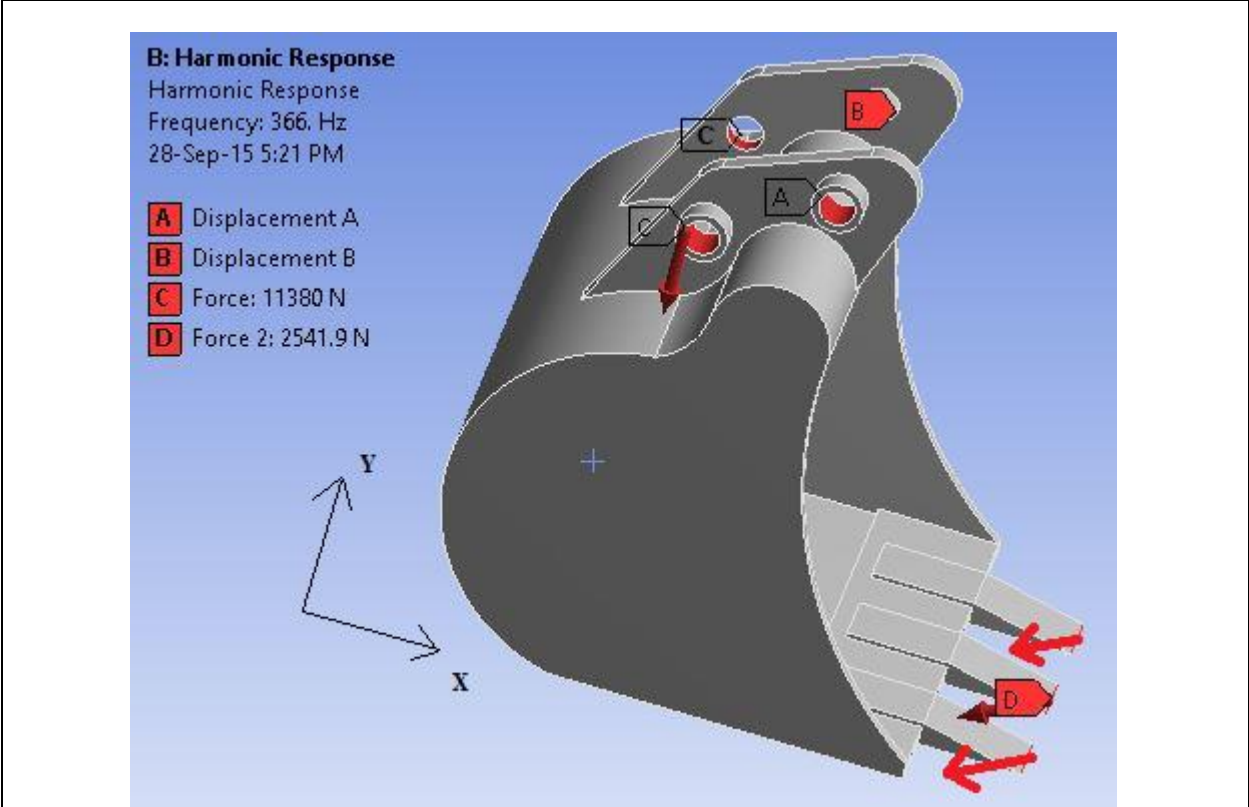


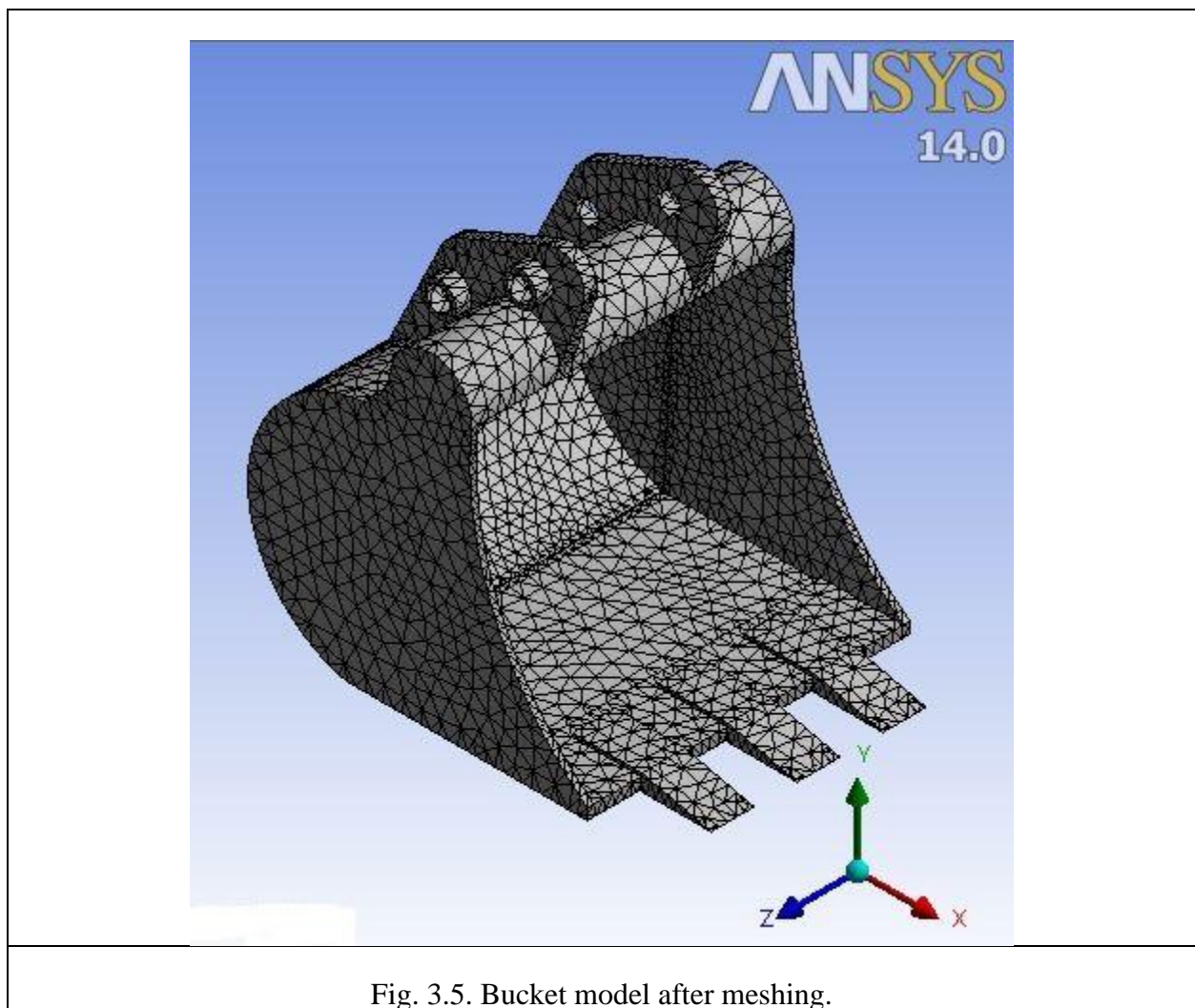
Fig. 3.4. Boundary conditions and input forces on the bucket.

The modal analysis is done only giving these boundary conditions. Then for the Harmonic analysis the boundary conditions were kept as usual and the forces given where maximum force at the three

teeth 2542 N and Cylinder force constant 11380N at the C. Lastly for stress analysis the boundary conditions were kept same and the forces given as constant 2542N and 11380N.

3.5. Meshing:

Proper meshing is performed to analyse the model. A method of automated meshing is done at the beginning then individual meshing and sizing was performed for getting simulation results. A total of 17762 elements and 35085 nodes were produced after meshing. A minimum edge length of 1mm is used in the meshing.



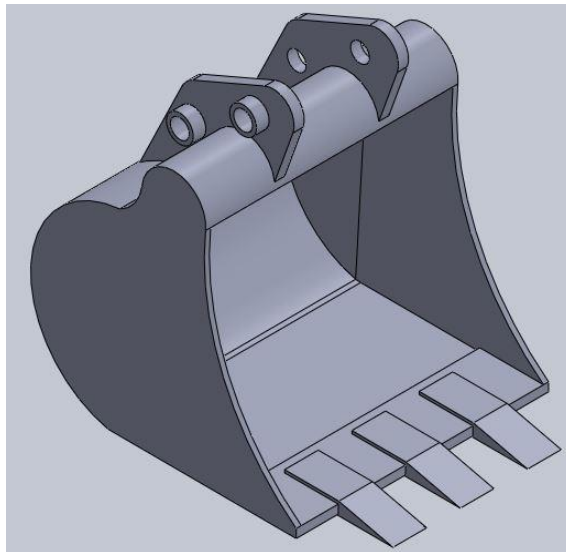
3.6. Definition of Cases:

Several techniques have been studied in this thesis to reduce vibration and stress of the excavator bucket. For this, the techniques have been categorized in different cases for the ease of analysis and conclusion. The cases are:

3.6.1. Case 1

a. Bucket.

The 1st case is taken as a bare bucket which is a standard bucket drawn in SOLIDWORKS Software with no attachments with it. This bucket will be analyzed for modal, harmonic and stress analysis and later will be compared with other techniques/cases that will be applied and analyzed to see the changes of vibration and stress output.



(a)

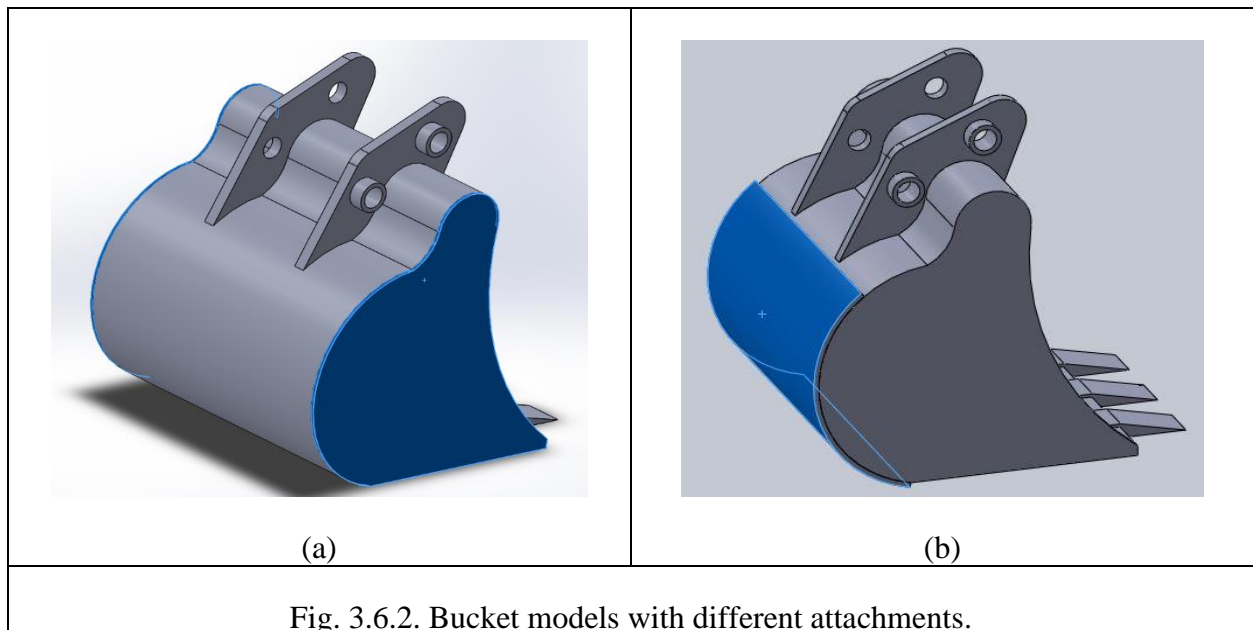
Fig. 3.6.1. Bare Bucket model.

The material properties of the bucket taken are density 9410 kg/m^3 , Poisson's ratio 0.3 and young's modulus of elasticity 210 GPa. [16]

3.6.2. Case 2

- (a) Bucket with 2 whole side rubber sheets.
- (b) Bucket with 1 whole rubber sheet at the back

The case 2 includes two different investigations of excavator with rubber where 5 mm thickness rubber sheet have been used as showed in the figures. Fig. (a) is bucket with 5 mm thickness rubber sheets on the both side plates of the bucket. And Fig. (b) is bucket with 5 mm thickness rubber sheet at the back plate of the bucket.



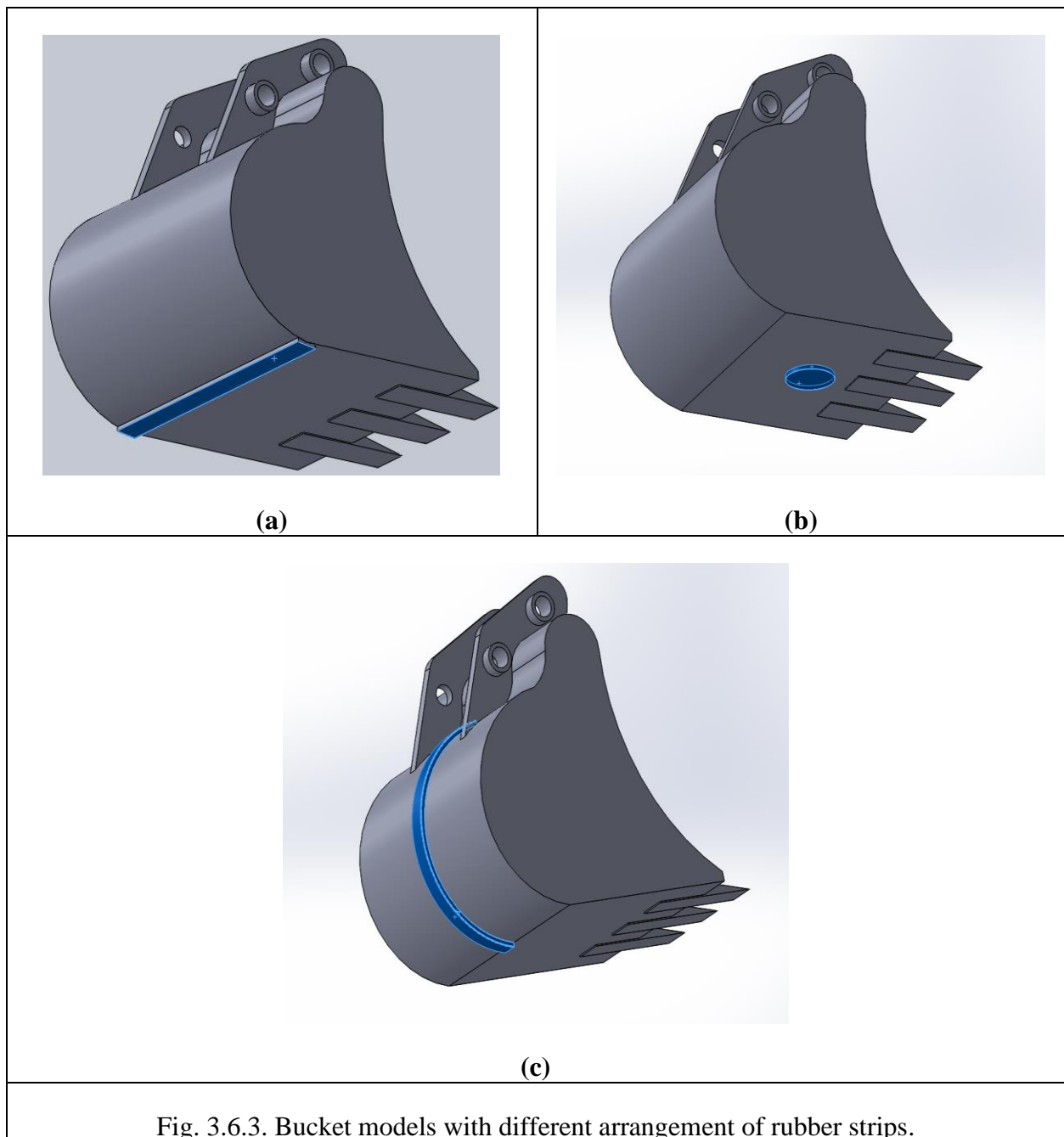
The modelling of the case 2 involves 1st modelling of part file in the SOLIDWORKS Software then using mating option the rubber sheets are attached with bucket in assembly section. The material properties taken for the rubber are density 4100 kg/m³, Poisson's ratio 0.41 and young's modulus of elasticity 8 MPa. [21]

3.6.3. Case 3

(a) Bucket with 1 rubber strip, (b) Bucket with 1 round rubber,

(c) Bucket with 1 back strip

5 mm thickness rubber strips have been used here for investigation.

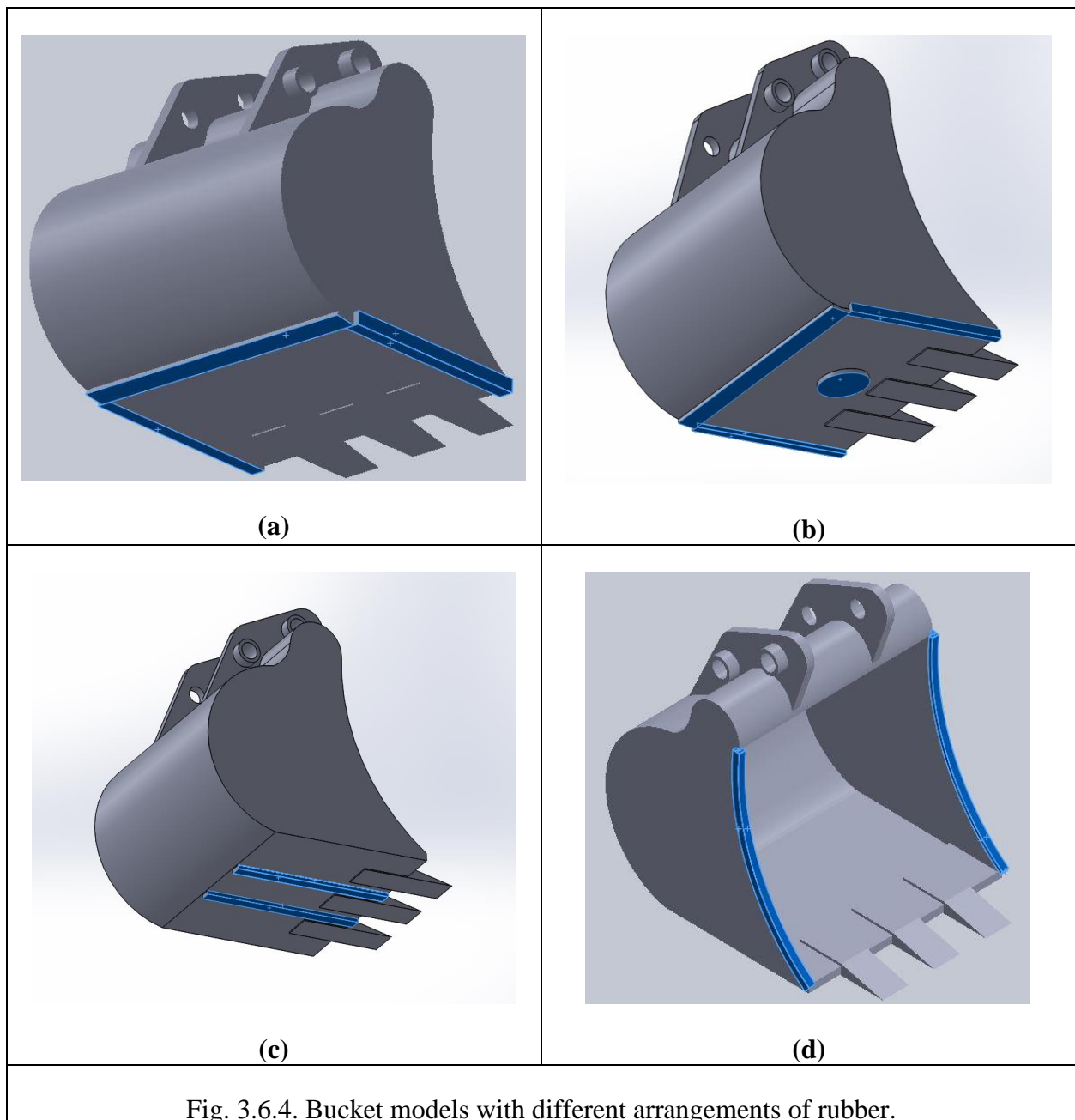


3.6.4. Case 4

(a) Bucket with 3 rubber strips, (b) Bucket with 4 rubber,

(c) Bucket with 2 bottom rubber strips, (d) Bucket with 2 side rubber strips.

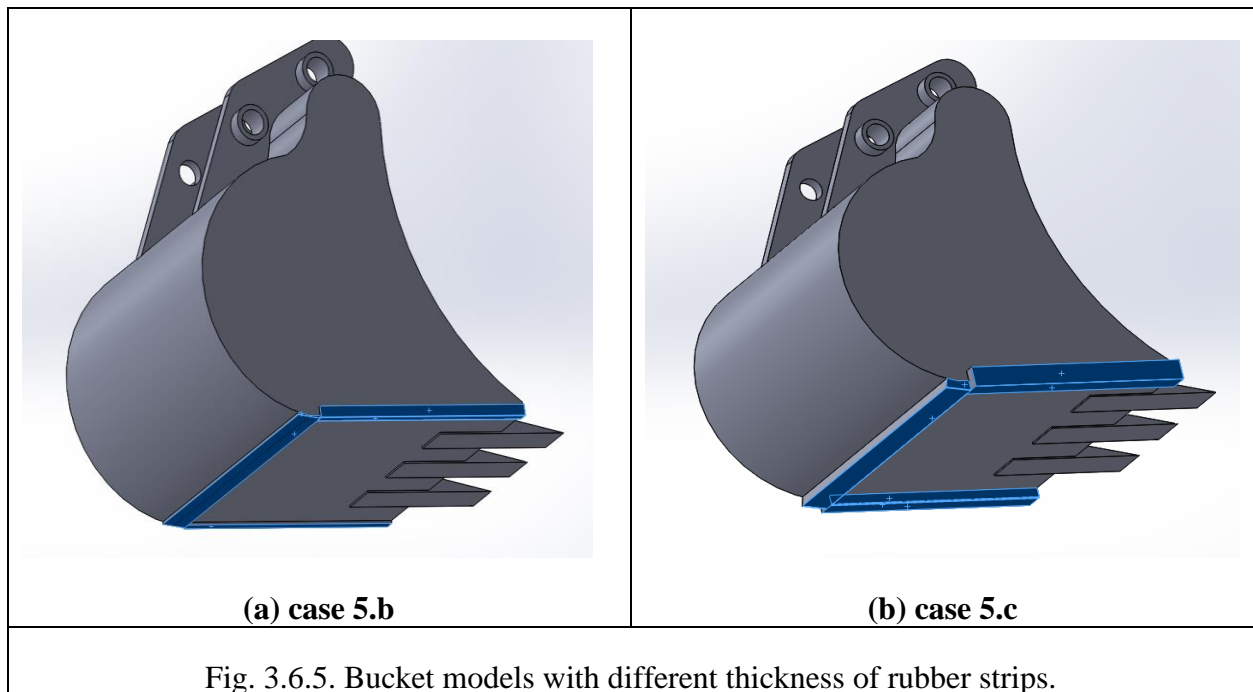
All the modifications use 5 mm thickness rubber.



3.6.5. Case 5

- (a) Bucket with 3 rubber strips of 5 mm thickness.
- (b) Bucket with 3 rubber strips half thickness (2.5 mm thickness).
- (c) Bucket with 3 rubber strips Double thickness (10 mm thickness).

At this case 5 mm thickness rubber have been used for case 5 (a). The half thickness means to use rubber strip of 2.5 mm thickness case 5 (b). And the double thickness means to use rubber strips of 10 mm thickness case 5 (c).



3.6.6. Case 6

- a. Bucket with 3 rubber strips
- b. Bucket with 3 aluminium strips
- c. Bucket with 3 steel strips

At this case the technique is to use aluminum and steel strips of 5 mm thickness in place of rubber strips of 5 mm thickness.

Chapter 4

Results of Numerical Simulation and Discussion

4. Introduction

The numerical simulation was performed on the bucket without any rubber attachments and then with different attachments. Then for each attachments or arrangements of rubber which are categorized into different cases results were compared and a conclusion was drawn for all the modifications. Firstly, modal analysis was performed on the bucket, secondly harmonic analysis and lastly stress analysis was performed. For all the analysis comparative discussion with conclusion was drawn in each section and also at the conclusion chapter an overall conclusion and recommendations were made based on the results of these numerical simulations.

4.1 Modal Analysis:

Modal analysis results show us the mode shapes and natural frequencies of different modes of the system. The mode shapes can show and predict the vulnerable places of vibration for a particular natural frequency. That is why it is important to learn about the mode shape of the bucket for different natural frequencies. In this section we have found mode shapes and natural frequencies of the bare bucket and bucket with different attachments up to 5th mode. The mode shapes were discussed with the actual figure found from the numerical simulation tool. The change of the mode shapes can be observed more vividly if animations directly seen from the software. To understand from the figure we need to concentrate on the color grading in the bucket for different deformations. Red color means highest deformations in the area and dark blue color means no deformations at the area. The deformation range can be of different for different attachments of rubber with bucket. The natural frequencies are listed for different cases and compared accordingly.

4.1.1. Mode Shapes and Natural Frequencies for Case 1

The mode shapes of different natural frequencies are different and the range in deformations and their concentration on different areas on the bucket changes shown in Fig. 4.1.1. (a), (b), (c), (d) and (e). At the 1st and 2nd modes most of the deformations occur at all three teeth and mostly in Y-direction. The second mode shows a lot of vibration or deformation in the bottom plate and back plate of the bucket than 1st mode as the light red color suggests and also highest vibration at all the teeth like 1st mode. At the 3rd mode interestingly high deformation is in the

middle tooth than other teeth and very less deformation at other places. The 4th and 5th modes suggest maximum vibration at the side plates but not at the bottom and back plate and very less vibration at all teeth.

The natural frequencies of case 1 are listed in the table and later with other cases they are compared.

Table 4.1.1. Natural Frequency (Hz) at Case 1

	Modes of Natural Frequency (Hz)				
	1 st	2 nd	3 rd	4 th	5 th
a. Bucket (case 1)	55.6	96.865	253.54	373.09	471.51

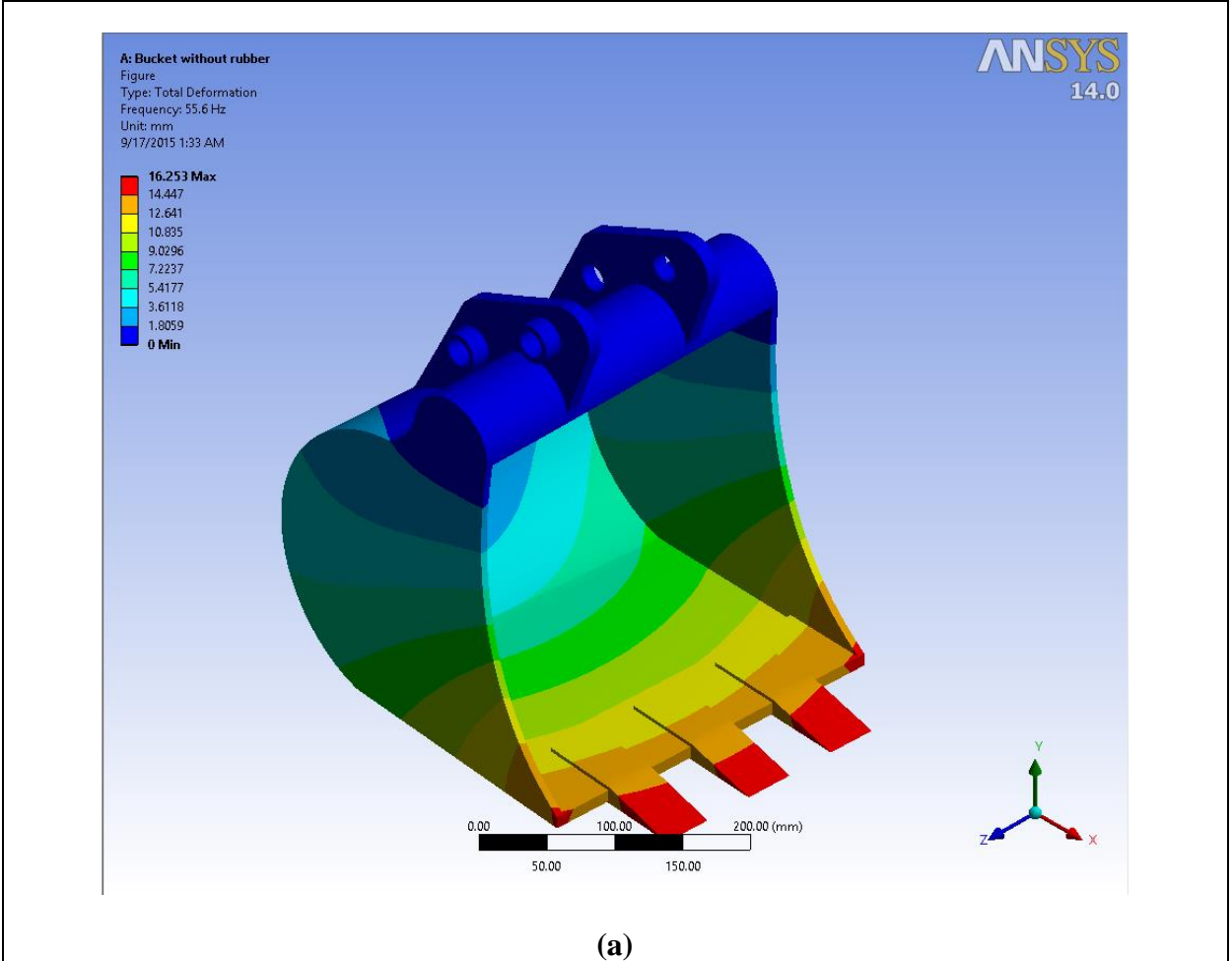
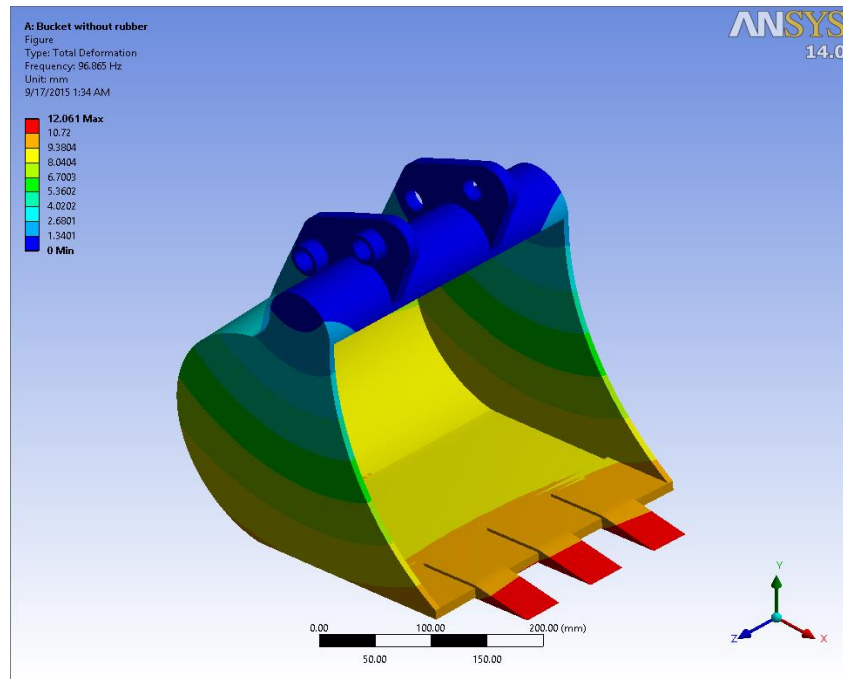
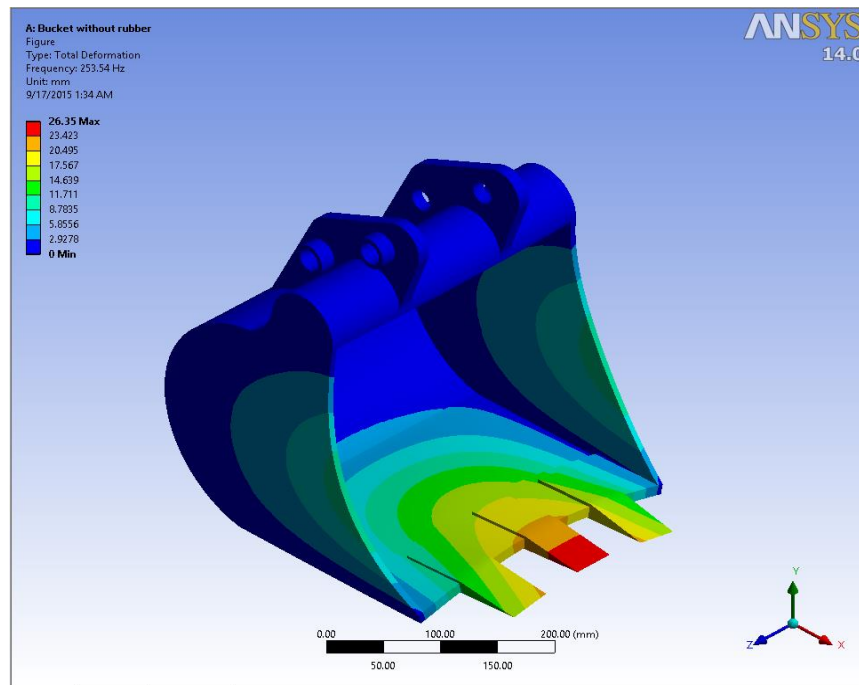


Figure 4.1.1.(a) 1st mode shape at case 1.



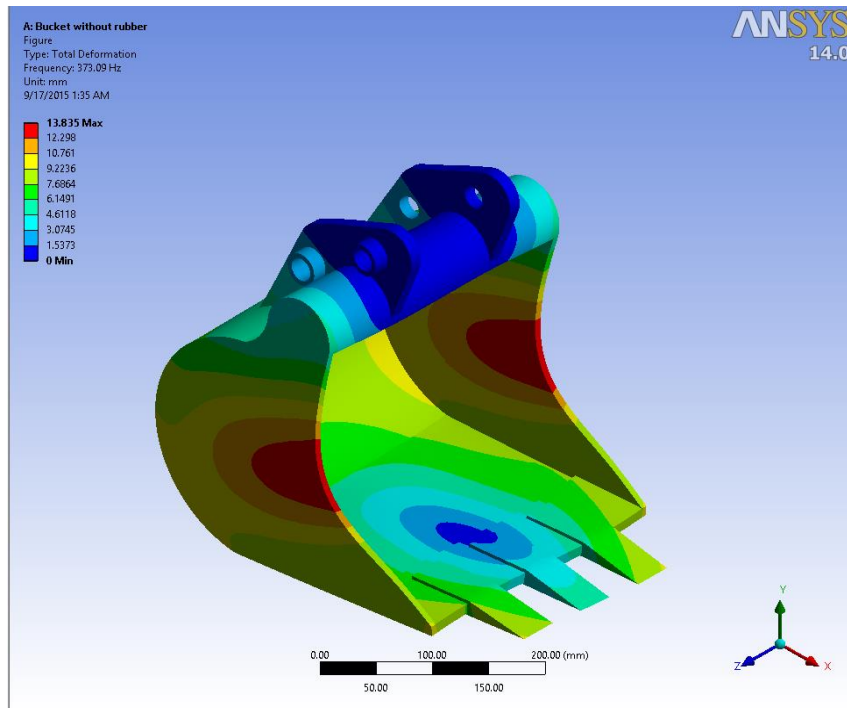
(b)

Figure 4.1.1.(b) 2nd mode shape at case 1.



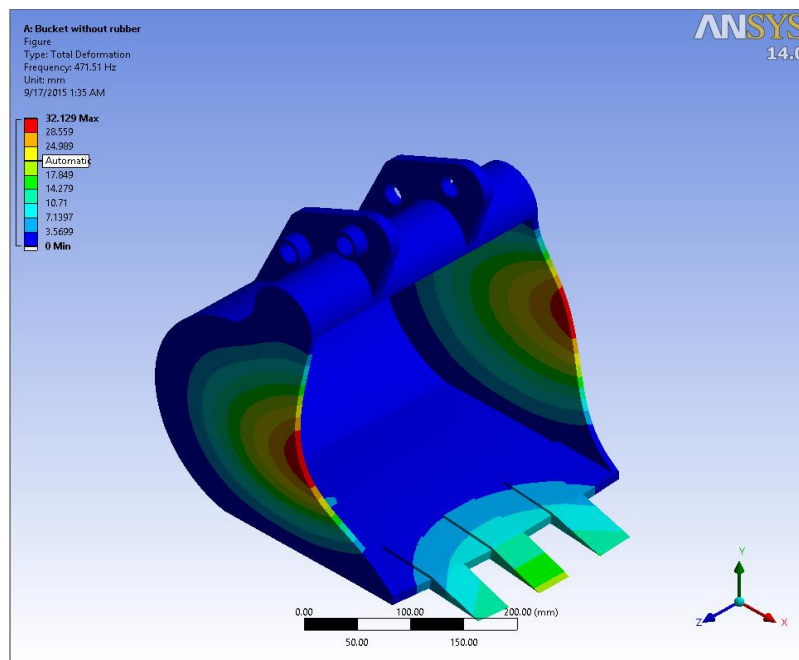
(c)

Figure 4.1.1.(c) 3rd mode shape at case 1.



(d)

Figure 4.1.1.(d) 4th mode shape at case 1.



(e)

Figure 4.1.1.(e) 5th mode shape at case 1.

4.1.2. Mode Shapes and Natural Frequencies for Case 2

The mode shapes at case 2 for different attachments of rubber are observed in these figures from Fig. 4.1.2.1 to Fig. 4.1.2.5 and found for most modes the mode shapes are similar to the mode shape of the bare bucket (case 1) except 4th mode shape. For the modifications of whole back rubber sheet (case 2.b) the deformation area increases at the side plates of the bucket seen in Figure 4.1.2.4.b. The reason for such phenomenon can be explained as we have used rubber sheet at the back of the bucket so the back side has become stiffer than side plates, which is why side plates are vulnerable to vibration with high amplitudes.

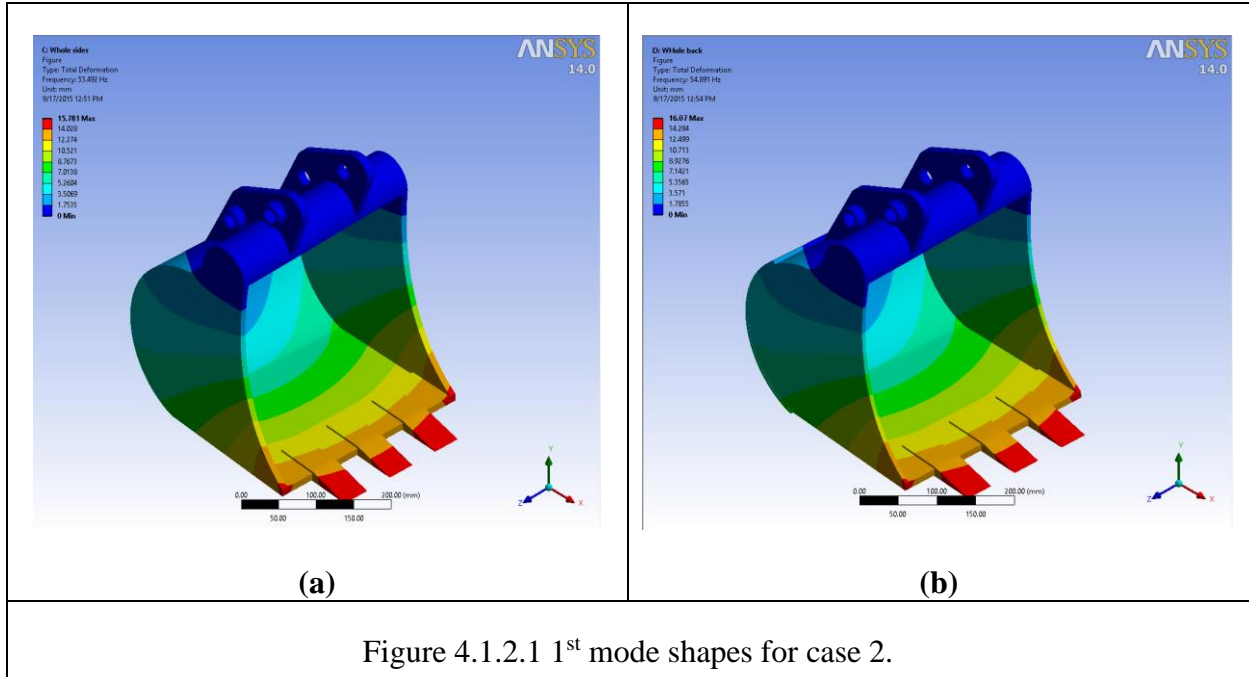
Table 4.1.2. Natural Frequency (Hz) at Case 2

	Modes of Natural Frequency (Hz)				
	1 st	2 nd	3 rd	4 th	5 th
a. Bucket (Case 1)	55.6	96.865	253.54	373.09	471.51
b. Bucket with 2 whole sides rubber sheets (Case 2.a)	53.492	93.763	249.48	348.63	425.56
c. bucket with 1 whole rubber sheet at the back (Case 2.b)	54.891	91.86	252.17	351.49	469.1

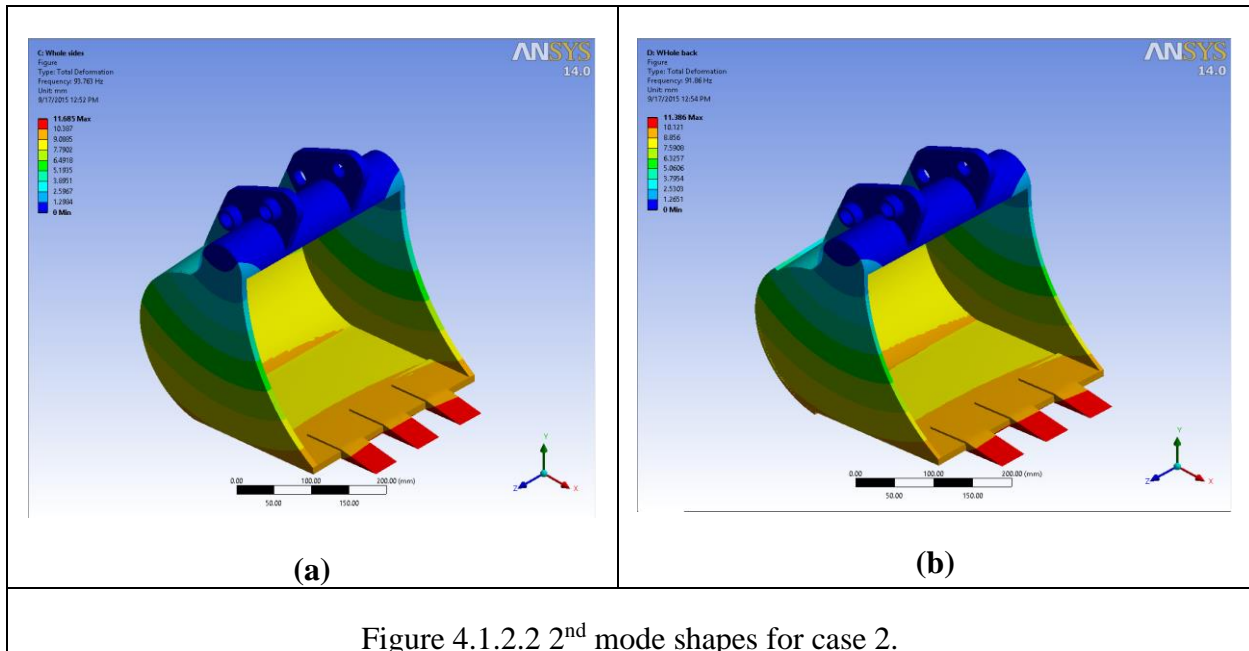
The natural frequencies for the case 2 compared with case 1 is shown in table 4.1.2. The 1st mode shows that for using 2 whole side rubber sheets natural frequency shifts to the left most or reduced from bare bucket's natural frequency. For the 2nd mode it is for the use of 1 whole rubber sheet at the back. The 3rd modes' natural frequency shift to the left also for both the attachments but shifts mostly for using 2 whole side rubber sheets. Again at the 4th mode use of 2 whole side rubber sheets shifts natural frequency to the left most or reduce highest. Similar shift is seen at the 5th mode. For all these modes the percentage of change in natural frequency is maximum 10%. The rubber sheets used in case 2 are of 5 mm thickness and less density 4100 kg/m³ which is why the amount of external material in the system is very less compared to the

mass of the bucket. That is why the stiffness to weight ratio doesn't change or deviate much from the actual system resulting very less deviation of natural frequency of the system.

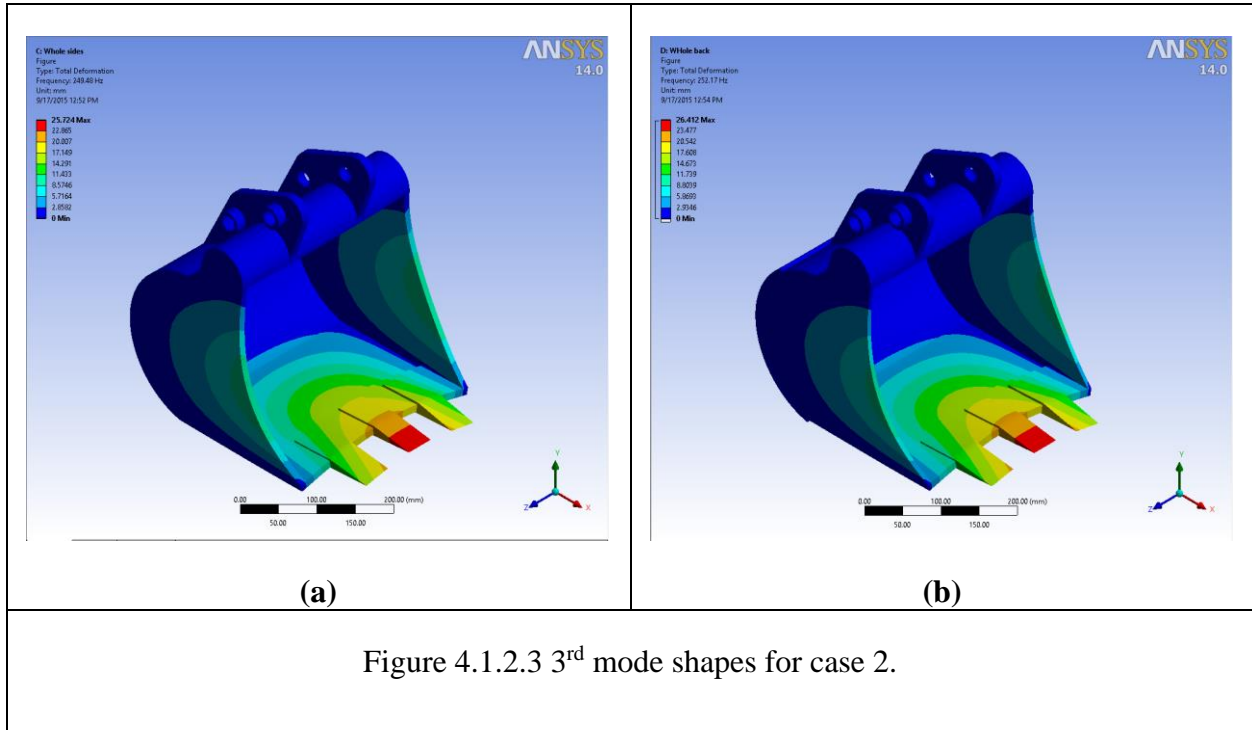
4.1.2.1. 1st Mode Shapes



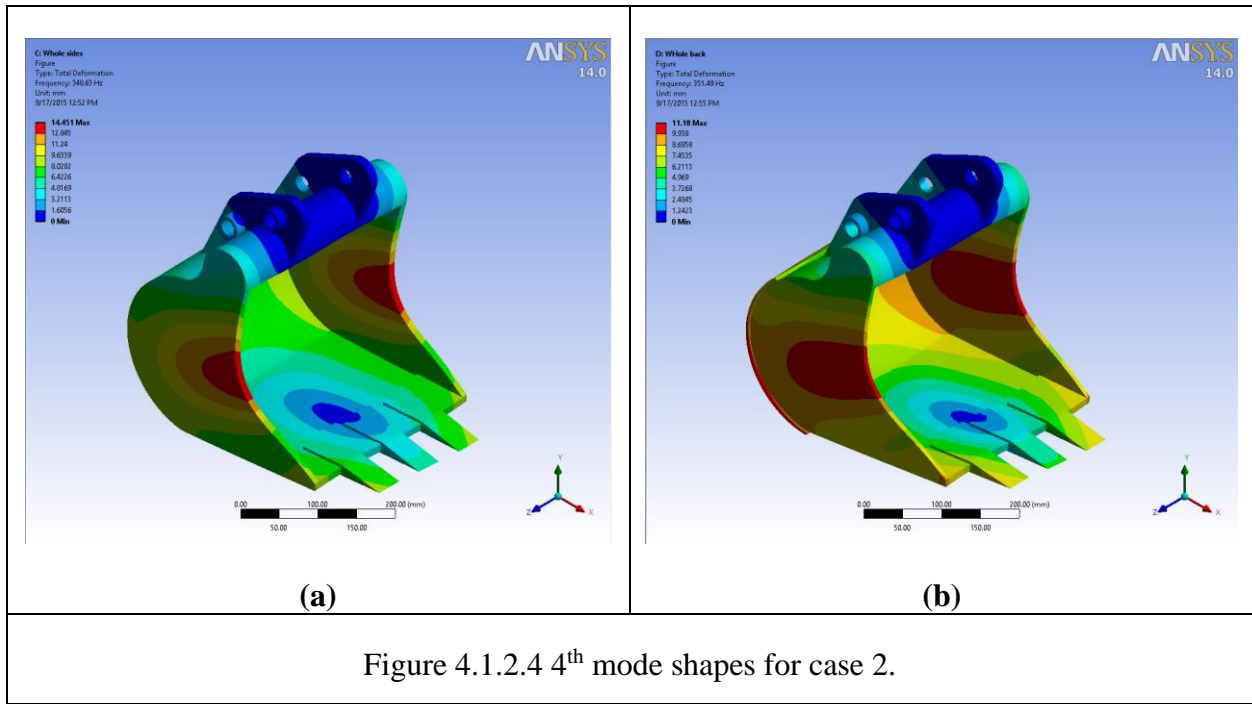
4.1.2.2. 2nd Mode Shapes



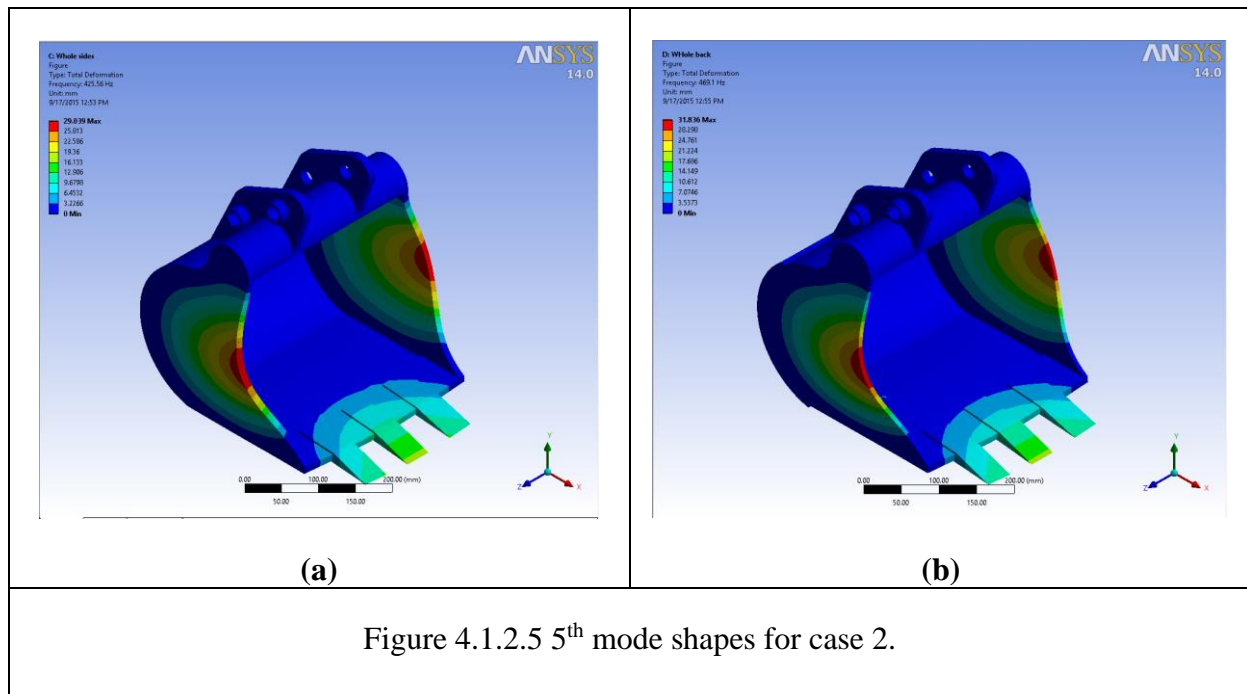
4.1.2.3. 3rd Mode Shapes



4.1.2.4. 4th Mode Shapes



4.1.2.5. 5th Mode Shapes



4.1.3. Mode Shapes and Natural Frequencies for Case 3

The mode shapes obtained from case 3 does not show much difference from the color grading figure (Fig. 4.1.3.1 to 4.1.3.5 of APPENDIX B) and also from the animation compared to mode shapes obtained from case 1. However the range in the deformation for different modifications are not same in all the modes.

The 1st mode shows that for using 1 rubbers strip natural frequency shifts to the left most than any other modification from bucket's natural frequency. Similar shift in natural frequency occurs for the 2nd mode. The 3rd modes' natural frequency shift to the left also for all the modifications but shifts mostly for using 1 round rubber. Again at the 4th mode use of 1 rubber strip shifts natural frequency to the left most. Similar observation is seen at the 5th mode also. For all these modes the percentage of change in natural frequency is maximum 0.8%.

Table 4.1.3. Natural Frequency (Hz) at Case 3

	Modes of Natural Frequency (Hz)				
	1st	2nd	3rd	4th	5th
a. Bucket (Case 1)	55.6	96.865	253.54	373.09	471.51
b. Bucket with 1 rubber strip (Case 3.a)	55.452	96.378	253.19	371.5	470.21
c. Bucket with 1 round rubber (Case 3.b)	55.471	96.619	252.07	372.99	471.67
d. Bucket with 1 back rubber strip (Case 3.c)	55.593	96.485	253.47	371.62	471.68

4.1.4. Mode Shapes and Natural Frequencies for Case 4

The mode shapes at case 4 for different attachments of rubber are observed in these figures and found for most modes the mode shapes are similar (shown in Fig. 4.1.4.1 to Fig. 4.1.4.3. of APPENDIX C) to the mode shapes of the bare bucket without attachments (case 1) except 4th mode and 5th mode shapes (shown in Fig. 4.1.4.4. and Fig. 4.1.4.5.) of bucket with two side rubber strips (case 4.d). At this case the deformation decreases at the side plates of the bucket seen in Figure 4.1.4.4.d and 4.1.4.5.d. It is obvious for these two mode shapes when side rubber strips are used as these strips increase the stiffness at the side plates which is why it actually damps the vibration at these regions if we compare with case 1.

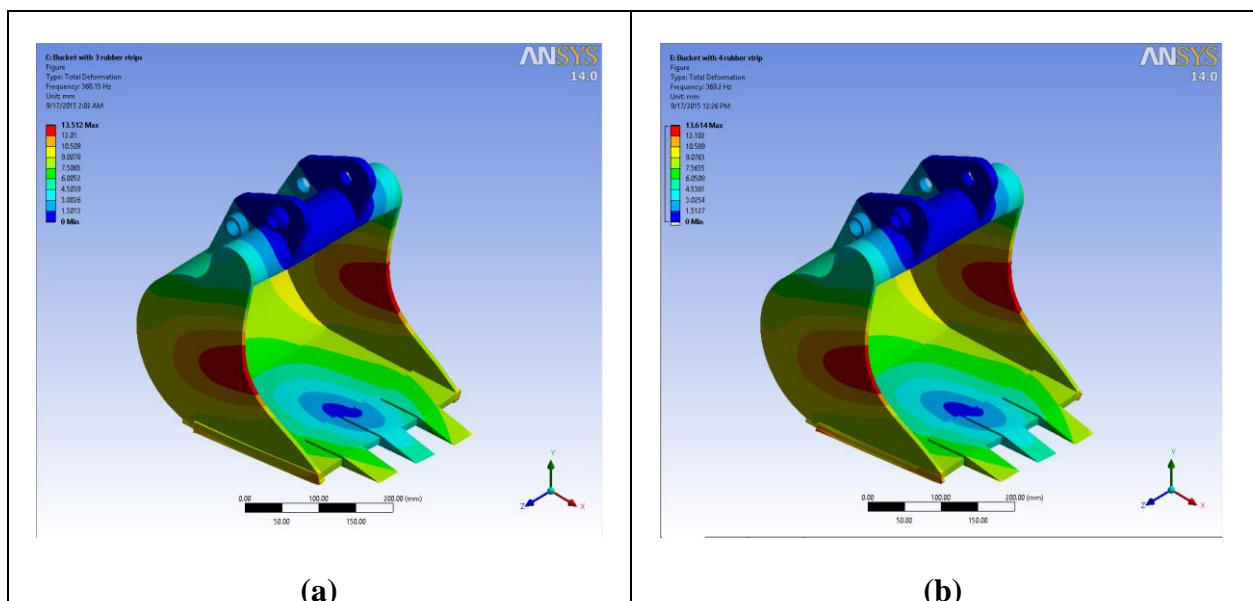
The 1st mode shows that for using 3 rubbers strips natural frequency shifts to the left most than any other modification from bucket’s natural frequency. Similar shift in natural frequency occurs for the 2nd mode also. The 3rd modes’ natural frequency shift to the left also for all the modifications but shifts mostly for using 2 bottom rubber strips, then using 2 side rubbers strips, and then for 3 rubber strips. Again at the 4th mode use of 3 rubber strips shifts natural frequency

to the left most. For the 5th mode most shift occurs when 2 side rubber strips used. For all these modes the percentage of change in natural frequency is maximum 5%.

Table 4.1.4. Natural Frequency (Hz) at Case 4

	Modes of Natural Frequency (Hz)				
	1 st	2 nd	3 rd	4 th	5 th
a. Bucket (Case 1)	55.6	96.865	253.54	373.09	471.51
b. Bucket with 3 rubber strips (Case 4.a)	54.579	95.426	252.83	368.15	467.83
c. Bucket with 4 rubber (Case 4.b)	54.736	95.552	251.25	369.2	467.98
d. Bucket with 2 bottom rubber strips (Case 4.c)	55.235	96.267	250.02	372.58	470.89
e. bucket with 2 side rubber strips (Case 4.d)	54.916	96.441	251.83	368.69	448.49

4.1.4.4. 4th Mode Shapes



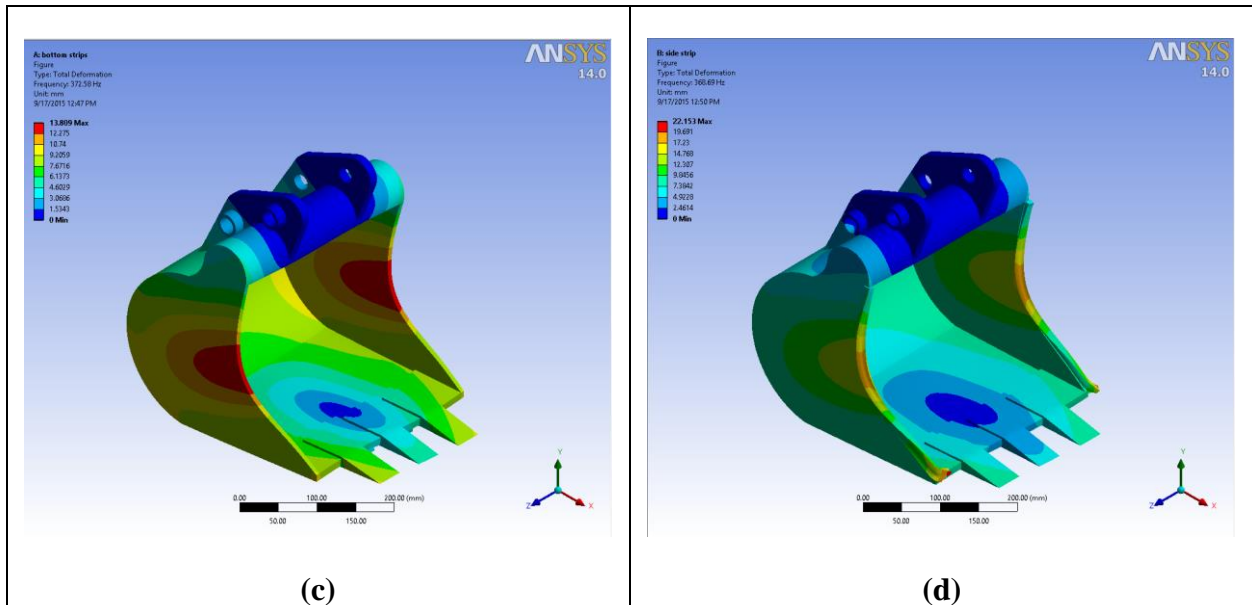
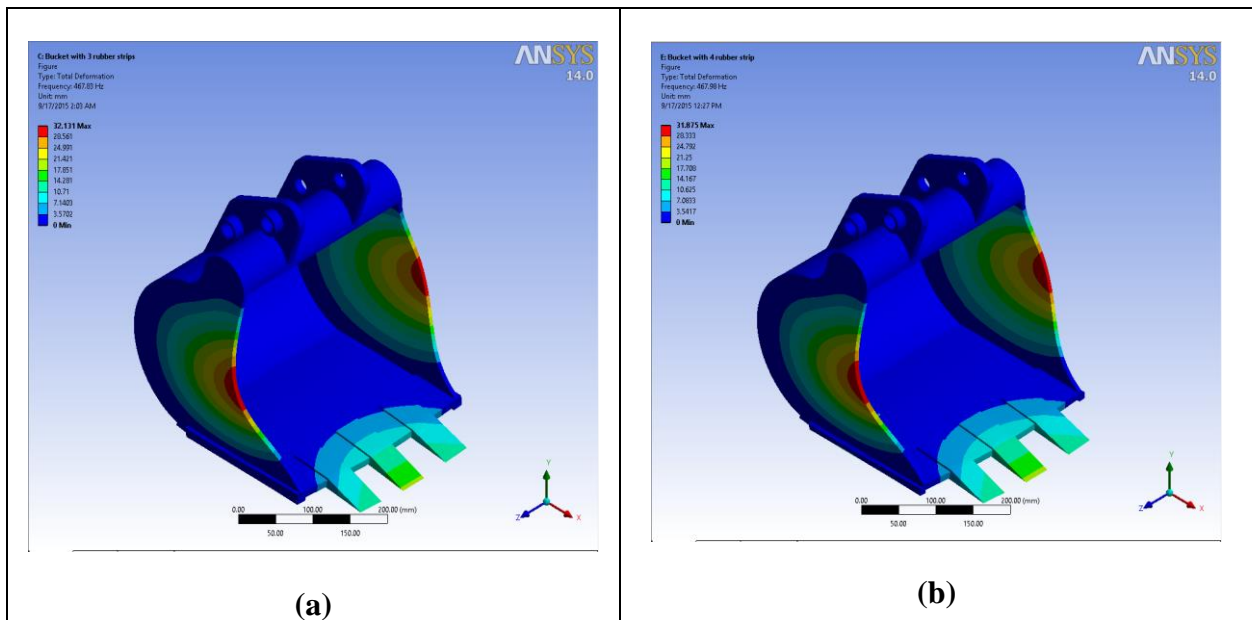
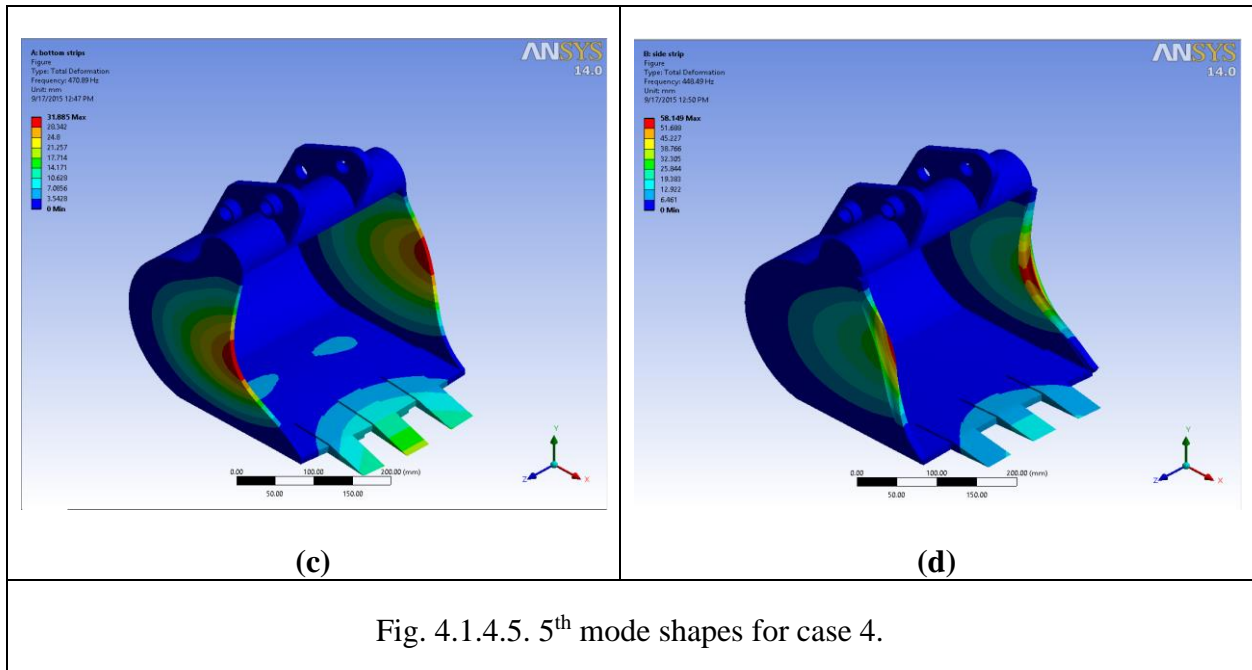


Fig. 4.1.4.4. 4th mode shapes for case 4.

4.1.4.5. 5th Mode Shapes





4.1.5. Mode Shapes and Natural Frequencies for Case 5

The mode shapes at case 5 for different attachments of rubber are observed in these figures and found for most modes the mode shapes are similar (shown in Fig.4.1.5.1. to Fig. 4.1.5.3. of APPENDIX D) to the mode shape of the bare bucket without any attachment (case 1) except 4th mode and 5th mode shapes of bucket with double thickness 3 rubber strips (case 5.(c)). At this modification the deformation is not seen any place in the bucket but only in the rubber that is used as seen in Fig. 4.1.5.4.b and 4.1.5.5.b.

The 1st mode shows that for using 3 rubber strips of double thickness, natural frequency shifts to the left most than any other modification from bucket's natural frequency. Similar shift of natural frequency is seen for the 2nd mode, 3rd mode, 4th mode and 5th modes. For all these modes the percentage of change in natural frequency is maximum 28%.

Table 4.1.5. Natural Frequency (Hz) at Case 5

	Modes of Natural Frequency (Hz)				
	1st	2nd	3rd	4th	5th
a. Bucket (case 1)	55.6	96.865	253.54	373.09	471.51
b. Bucket with 3 rubber strips (case 5.(a))	54.579	95.426	252.83	368.15	467.83
c. Bucket with 3 rubber strips half thickness (case 5.(b))	55.158	96.337	252.96	370.97	468.22
d. bucket with 3 rubber strips double thickness (case 5.(c))	53.34	93.416	252.24	333.36	336.72

4.1.5.4. 4th Mode Shapes

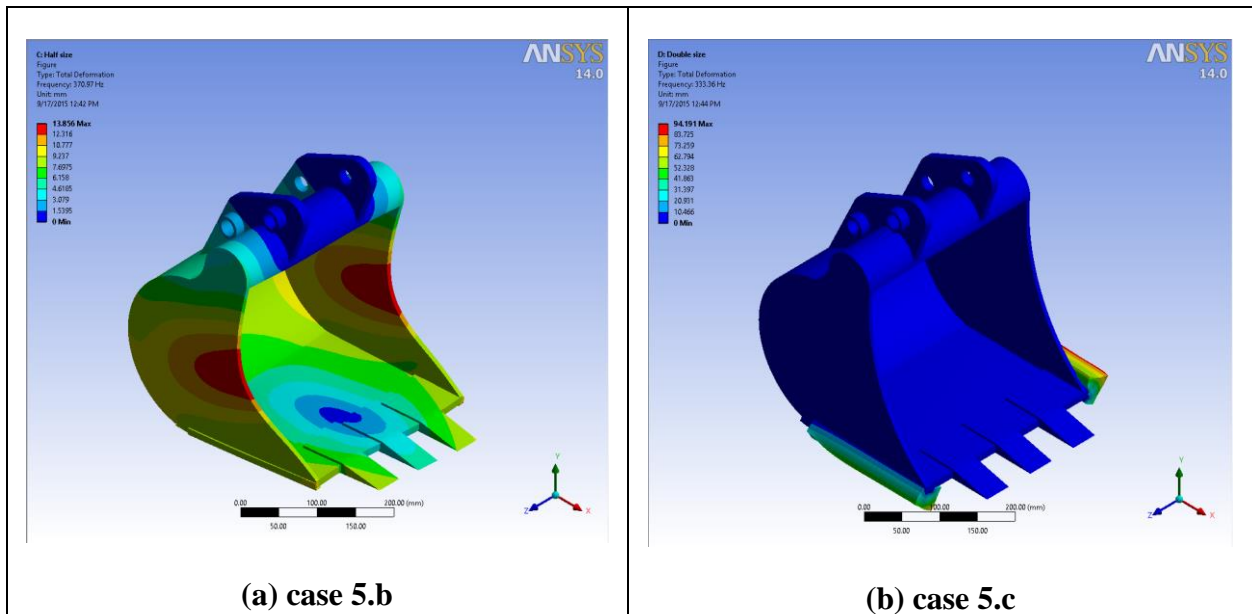


Fig. 4.1.5.4. 4th mode shapes for case 5.

4.1.5.5. 5th Mode Shapes

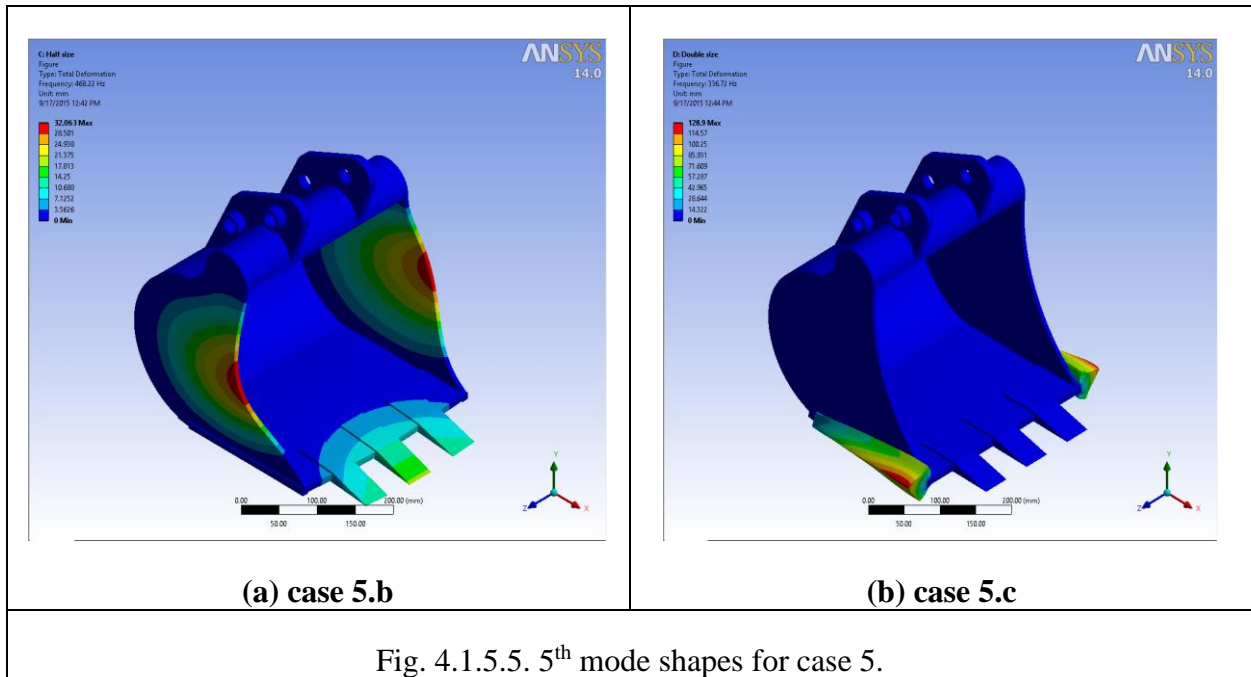


Fig. 4.1.5.5. 5th mode shapes for case 5.

4.1.6. Mode Shapes and Natural Frequencies for Case 6

The mode shapes are also similar for all these attachments of case 6 shown in Fig. 4.1.6.1 to Fig. 4.1.6.5. of APPENDIX E, though the range in the deformation varies for different attachments.

The 1st mode shows that for using 3 aluminum strips natural frequency shifts to the left most than any other modification from bucket's natural frequency. For the 2nd mode it is for the use of 3 rubber strips. The 3rd modes' natural frequency shift to the left only for the use of 3 rubber strips and for other two modification natural frequency shifts to the right. Similar shift is seen at the 5th mode. Again at the 4th mode use of 3 steel strips shifts natural frequency to the left most. For all these modes the percentage of change in natural frequency is maximum 10%.

Table 4.1.6. Natural Frequency (Hz) at Case 6

	Modes of Natural Frequency (Hz)				
	1st	2nd	3rd	4th	5th
a. Bucket (case 1)	55.6	96.865	253.54	373.09	471.51
b. Bucket with 3 rubber strips (case 6.a)	54.579	95.426	252.83	368.15	467.83
c. Bucket with 3 aluminum strips (case 6.b)	55.426	95.992	257.04	371.19	475.22
d. bucket with 3 steel strips (case 6.c)	54.612	93.775	261.83	365.82	482.34

The change in natural frequencies at case 6 from case1 are way different than any other attachments of any other cases. As we have used here different materials so the stiffness to weight ratio changes abruptly which is why sometimes we see the deviation in the natural frequency to the left or sometimes to the right than the natural frequencies of the bare bucket of case 1. The weight and stiffness of aluminum and steel is different than that of rubber. As we know that the natural frequency of any system depends on the mass matrix and stiffness matrix of the system so it is obvious the change in these two properties will change the natural frequencies of the system.

4.2. Harmonic Analysis:

Harmonic analysis is performed on the bare bucket of case 1 and then for different cases. The boundary conditions are same as modal analysis where fixed support is considered at the first two holes (A and B) of the hanger. The force from the hydraulic cylinder 11380 N was considered a constant force in the bucket at the second two pins of the hanger. The reaction force on the teeth are consider sinusoidal and amplitude is 2542 N. The boundary conditions and forces are taken from a published paper which analyzed similar excavator bucket for stress analysis [16]. The output result of amplitude vs frequency graph was drawn according to different cases and compared in each sections.

4.2.2. Harmonic Response of Case 2

The amplitudes shown in Fig. 4.2.2.1 (a) for all the rubber attachments reduce along X-axis of the 1st mode and the use of whole back rubber sheet reduces vibration amplitude most at this mode. Though along Y-axis of this mode seen in Fig. 4.2.2.1 (b) the amplitude for using all the attachments reduce but for the use of whole back rubber sheet literally gives no vibration. And also along Z-axis shown in Fig. 4.2.2.1 (c) the amplitude for all the attachments reduces. So, the use of whole back rubber sheet is the best choice at this 1st mode to reduce vibration.

The amplitudes observed at 2nd mode along all the axis from Fig. 4.2.2.2 (a), (b) and (c) show us that all the attachments reduce vibration. However the use of 2 whole side rubber will be wise choice at this 2nd mode than other attachment.

The amplitudes along X-axis of the 3rd mode reduce for all the attachments of rubber than the actual bucket of case 1 without rubber but not much seen in Fig. 4.2.2.3 (a). But for the vibration along Y-axis in Fig. 4.2.2.3 (b) of the mode the use of whole back rubber sheet increases vibration. And along Z-axis of Fig. 4.2.2.3 (c) the use of 2 whole side rubber sheet increases vibration amplitude while other reduce the vibration amplitude. So, we can say both the modifications are not wise choice to reduce vibration at the 3rd mode.

The vibration amplitude along X-axis of the 4th mode is literally absent for the use of 2 whole side rubber sheet but an increase in the amplitude is seen for the use of whole back rubber sheet Fig. 4.2.2.4 (a). Along Y-axis of this mode all the vibration amplitude increase Fig. 4.2.2.4 (b). Similarly at Z-axis Fig. 4.2.2.4 (c) the use of whole back rubber sheet give high amplitude of vibration. So, the use of 2 whole side rubber sheet at this 4th mode is good but still not much reliable to reduce overall vibration

Similar observation like 4th mode is seen in the 5th mode along all the directions Fig. 4.2.2.5 (a), (b) and (c). The use of 2 whole side rubber sheet show literally no vibration compared to the use of whole back rubber sheet. So, 2 whole side rubber sheets can be chosen to reduce vibration at this 5th mode.

From all the harmonic response it is seen that whole back rubber sheet can be used to reduce vibration at 1st mode but not for 2nd, 4th or 5th mode. And the use of 2 whole side rubber sheets is good for 2nd, 4th and 5th mode but not for other modes. So, both the attachments do not give much modifications which is why other cases are need to be studied. However as we know that the vibration amplitudes depend on the operating frequencies so these attachments still can be used to reduce vibration for certain conditions.

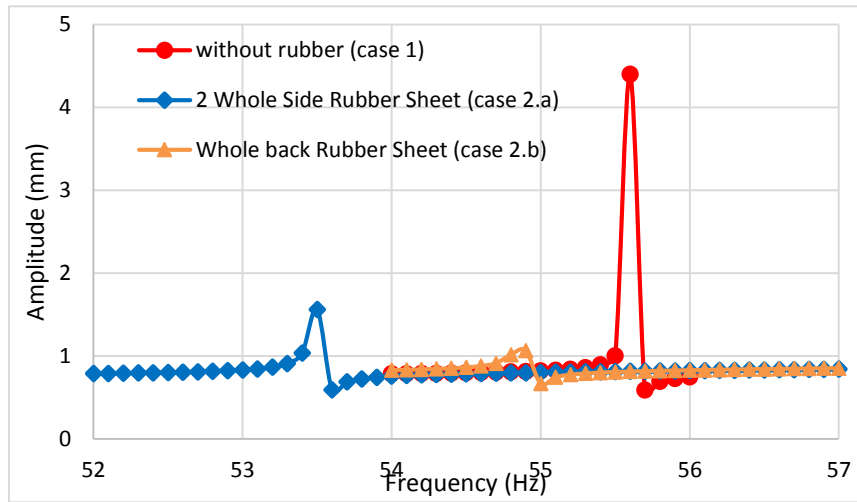


Fig. 4.2.2.1 (a) Amplitudes along X-Direction at 1st mode for case 2 compared with case 1.

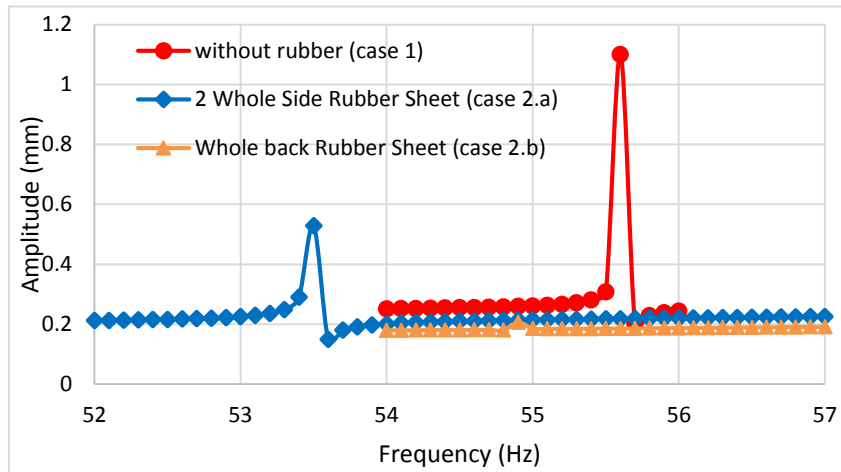


Fig. 4.2.2.1 (b) Amplitudes along Y-Direction at 1st mode for case 2 compared with case 1.

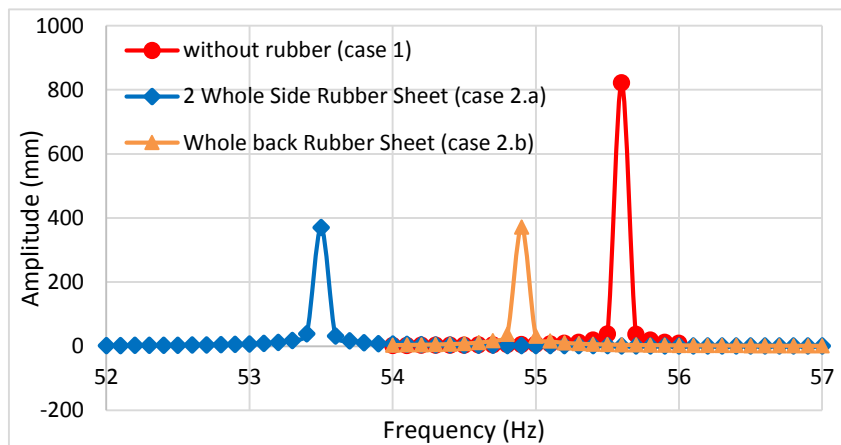


Fig. 4.2.2.1 (c) Amplitudes along Z-Direction at 1st mode for case 2 compared with case 1.

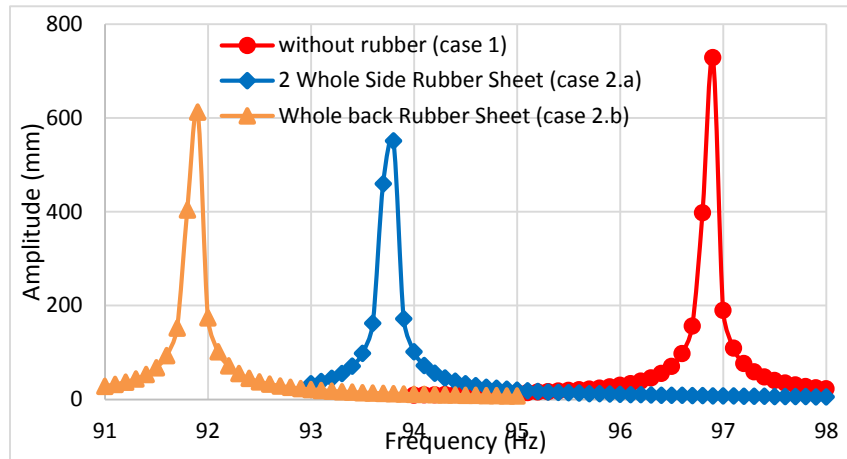


Fig. 4.2.2.2 (a) Amplitudes along X-Direction at 2nd mode for case 2 compared with case 1.

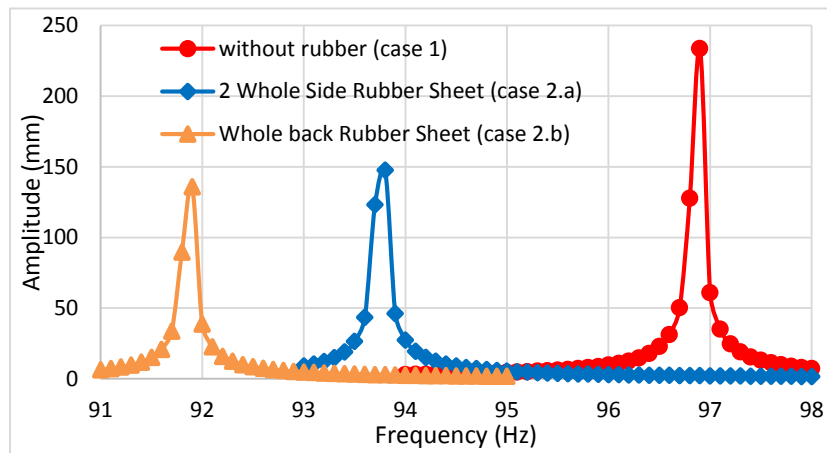


Fig. 4.2.2.2 (b) Amplitudes along Y-Direction at 2nd mode for case 2 compared with case 1.

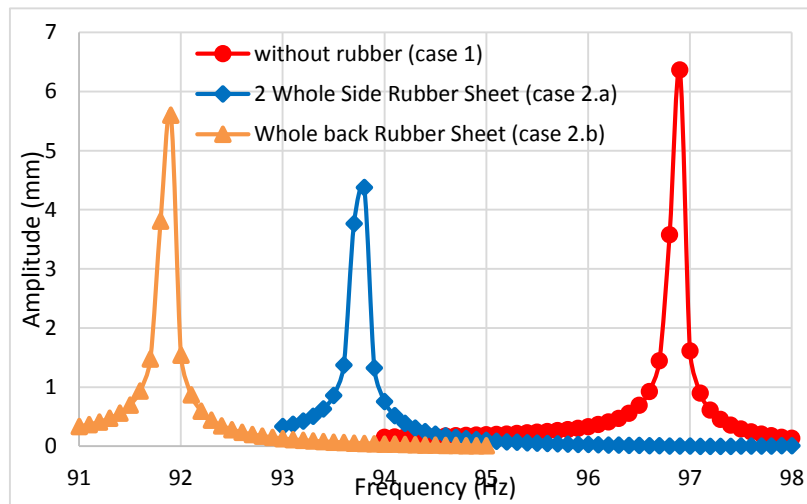


Fig. 4.2.2.2 (c) Amplitudes along Z-Direction at 2nd mode for case 2 compared with case 1.

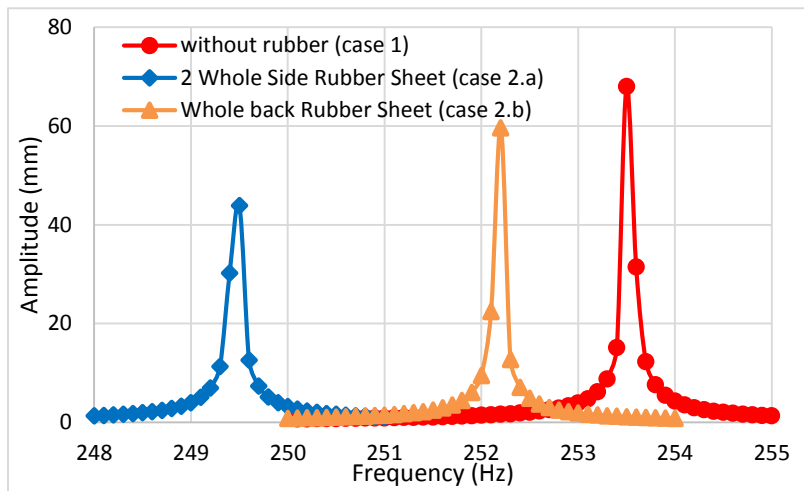


Fig. 4.2.2.3 (a) Amplitudes along X-Direction at 3rd mode for case 2 compared with case 1.

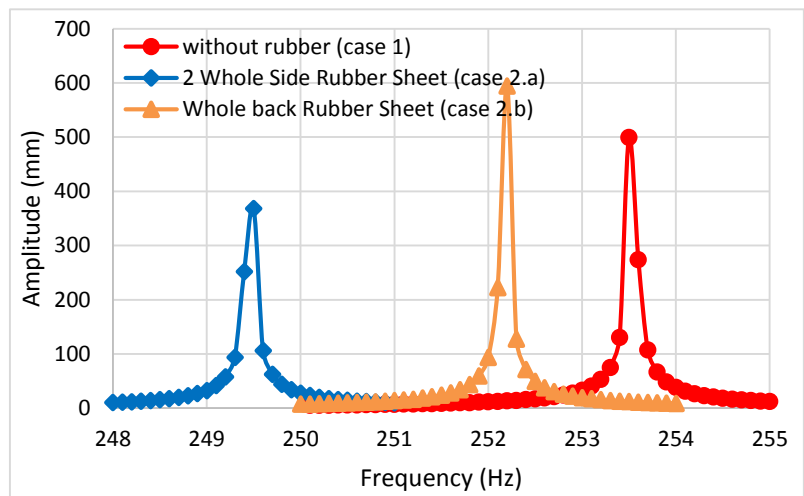


Fig. 4.2.2.3 (b) Amplitudes along Y-Direction at 3rd mode for case 2 compared with case 1.

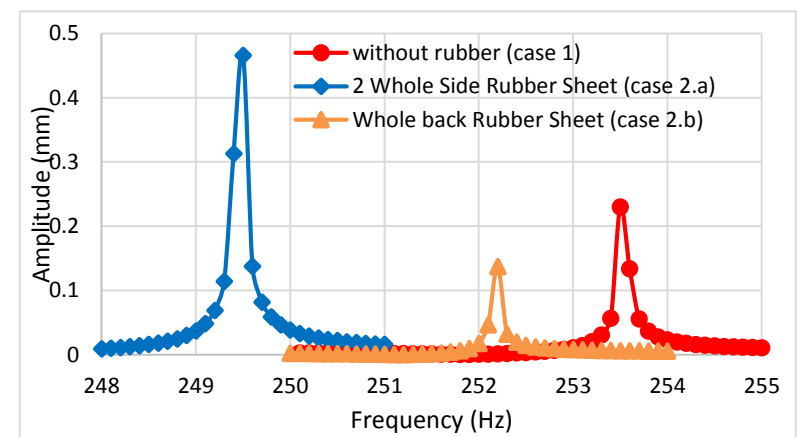


Fig. 4.2.2.3 (c) Amplitudes along Z-Direction at 3rd mode for case 2 compared with case 1.

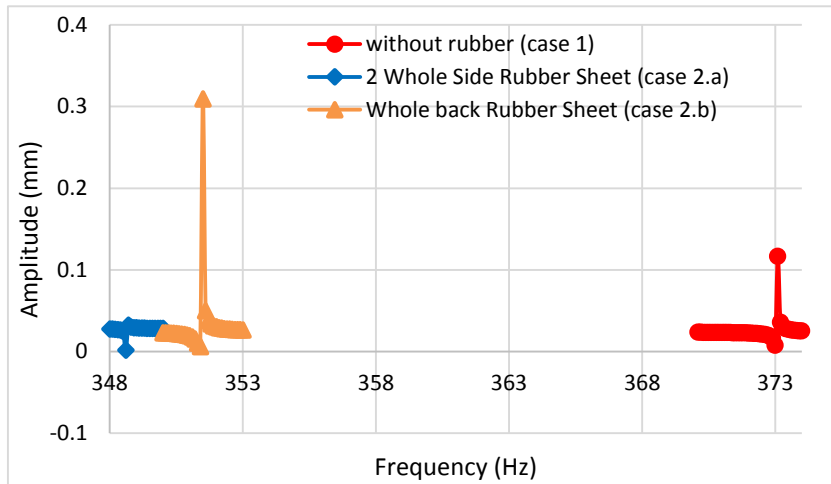


Fig. 4.2.2.4 (a) Amplitudes along X-Direction at 4th mode for case 2 compared with case 1.

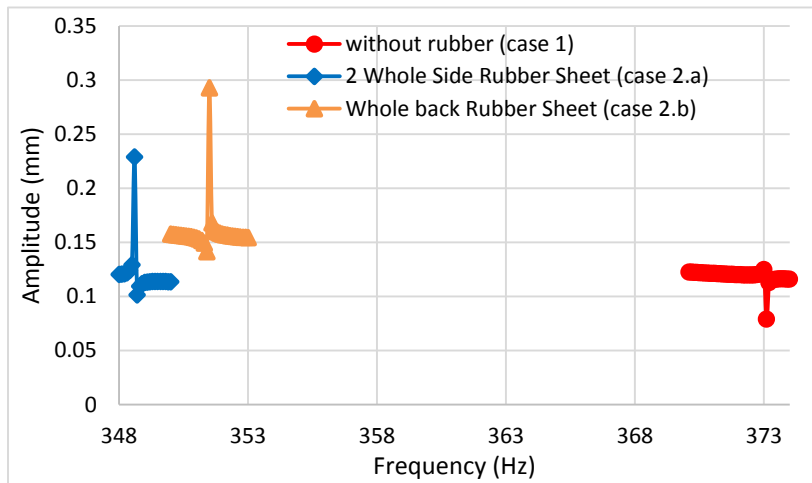


Fig. 4.2.2.4 (b) Amplitudes along Y-Direction at 4th mode for case 2 compared with case 1.

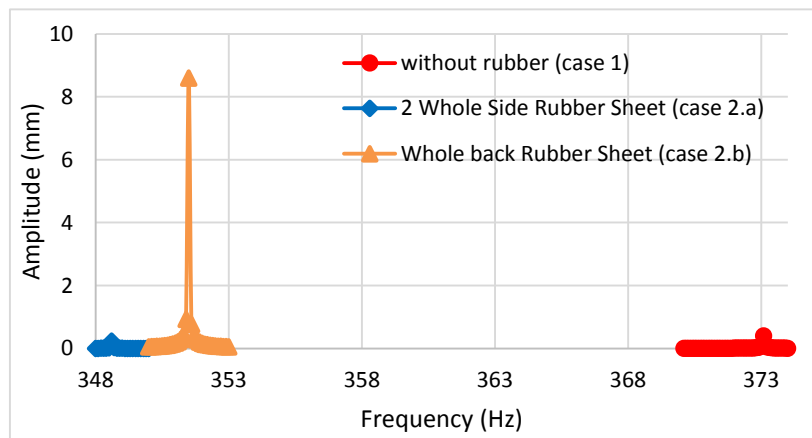


Fig. 4.2.2.4 (c) Amplitudes along Z-Direction at 4th mode for case 2 compared with case 1.

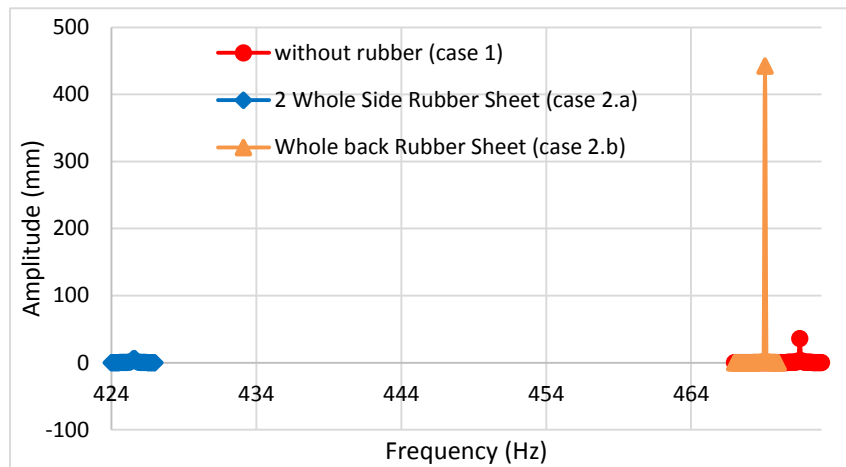


Fig. 4.2.2.5 (a) Amplitudes along X-Direction at 5th mode for case 2 compared with case 1.

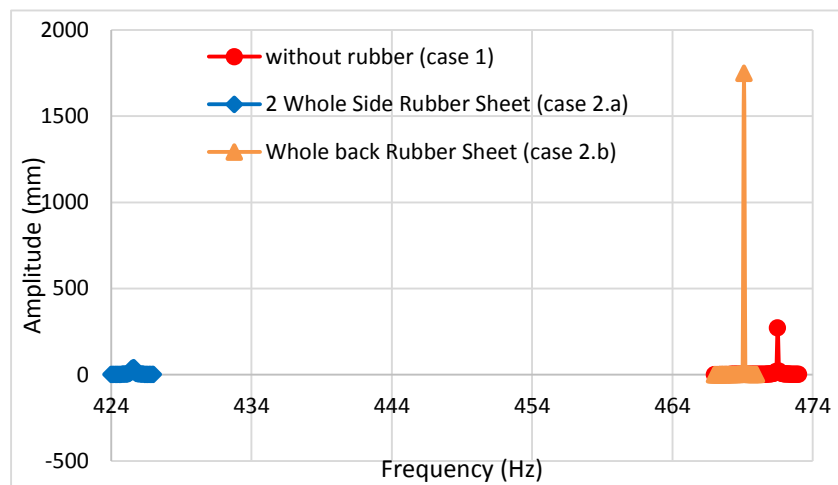


Fig. 4.2.2.5 (b) Amplitudes along Y-Direction at 5th mode for case 2 compared with case 1.

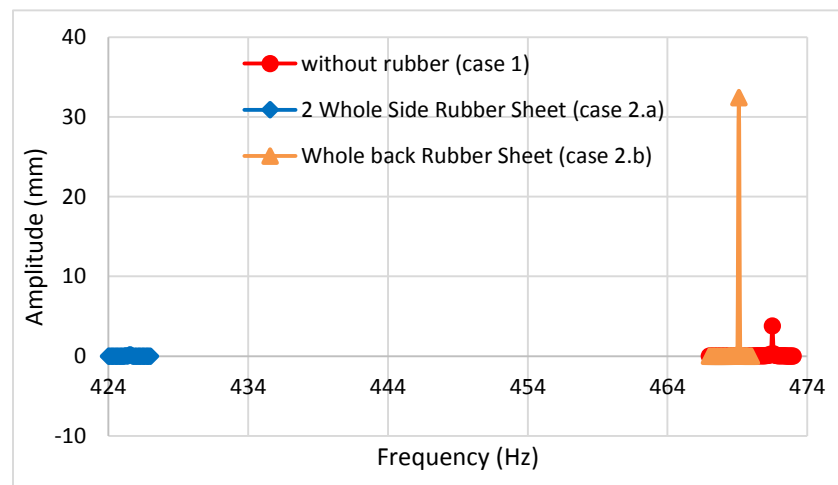


Fig. 4.2.2.5 (c) Amplitudes along Z-Direction at 5th mode for case 2 compared with case 1.

4.2.3. Harmonic Response of Case 3

The harmonic analysis of bucket with different rubber attachments in case 3 is observed here in these three figures for the 1st mode at different directions Fig. 4.2.3.1 (a), (b) and (c). The amplitude of vibration is easily observed here and for all these attachments the amplitude decreases. However, incorporation of 1 rubber strip gives less vibration and is seen preferable than any other attachments for all the directions. For this attachment of using 1 rubber strip literally gives no vibration at this 1st mode comparatively with other attachments. It is better choice over other attachments.

At this 2nd mode the amplitude increases in all three attachments of with 1 rubber strip, with 1 round rubber and with 1 back rubber strip than the bucket's (case 1) vibration in all directions Fig. 4.2.3.2 (a), (b) and (c). None of the attachments should be chosen to reduce vibration at this 2nd mode.

The 3rd mode's amplitudes along X-axis show us that the use of attachments do not reduce vibration amplitudes Fig. 4.2.3.3 (a). A similar observation is found at this mode along Y-axis Fig. 4.2.3.3 (b). But for the vibration along Z-axis the use of 1 rubber strip reduce vibration amplitude Fig. 4.2.3.3 (c), other attachments increase the vibration. So, again none of the attachments here can be selected to reduce vibration amplitude at this mode.

The amplitudes at the 4th mode along X-axis for 1 rubber strip and 1 round rubber are way bigger than the amplitude for bucket without any rubber, and other attachments actually decrease vibration amplitude Fig. 4.2.3.4 (a). Similarly none of the observation reduce vibration along Y-axis of this mode and also along Z-axis Fig. 4.2.3.4 (b) and Fig. 4.2.3.4 (c). So, none of the modification is better at this mode.

The vibration amplitude along X-axis for all the modifications is less than the amplitude for bucket without any rubber at this 5th mode Fig. 4.2.3.5 (a). However, the amplitude because of bucket with 1 round rubber is most reduced at this mode. Similar observation is found for the vibration along Y-axis and also along Z-axis Fig. 4.2.3.5 (b) and Fig. 4.2.3.5 (c). So, it is concluded that use of 1 round rubber is best choice for this 5th mode of vibration.

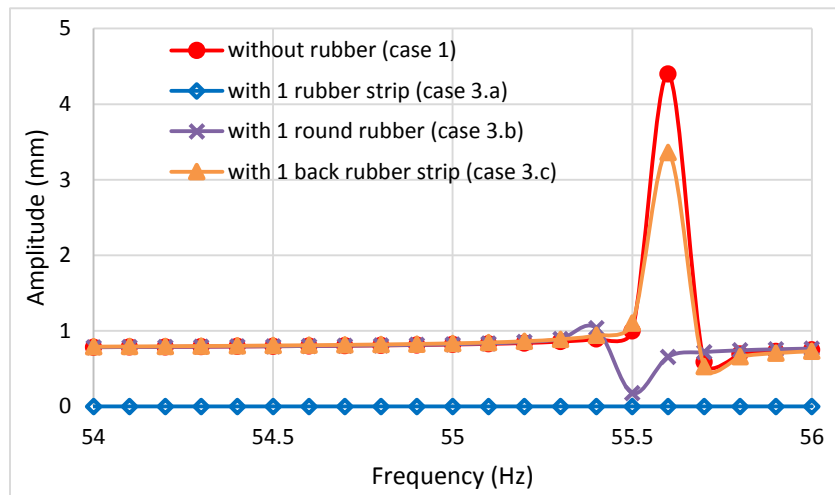


Fig. 4.2.3.1 (a) Amplitudes along X-Direction at 1st mode for case 3 compared with case 1.

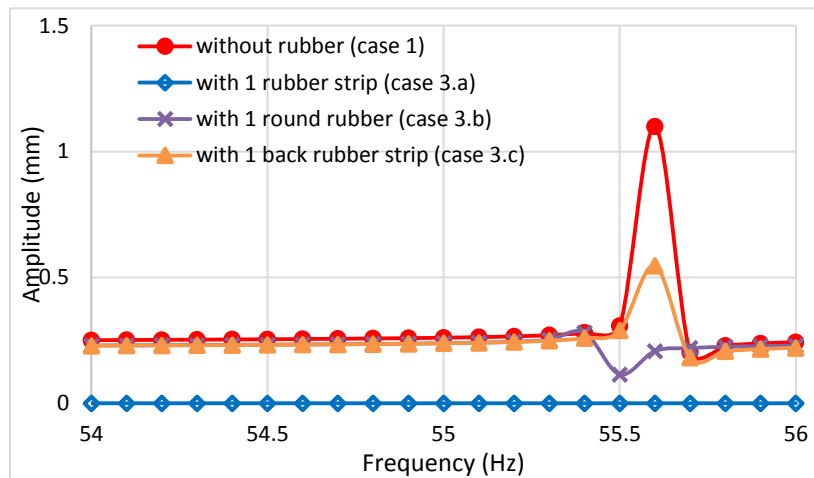


Fig. 4.2.3.1 (b) Amplitudes along Y-Direction at 1st mode for case 3 compared with case 1.

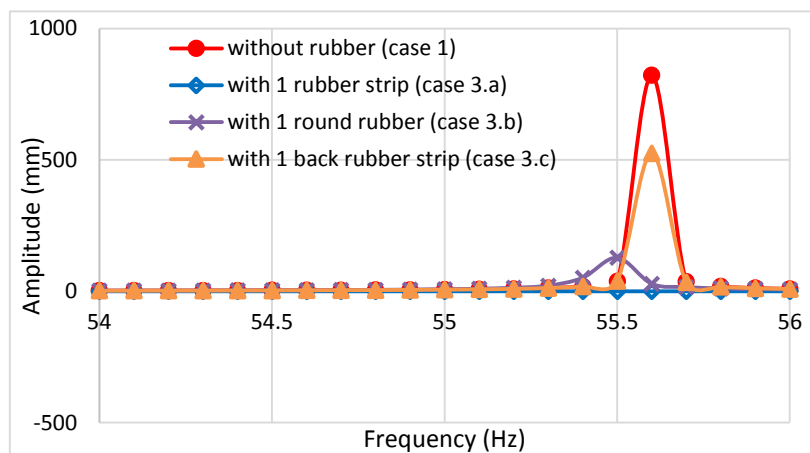


Fig. 4.2.3.1 (c) Amplitudes along Z-Direction at 1st mode for case 3 compared with case 1.

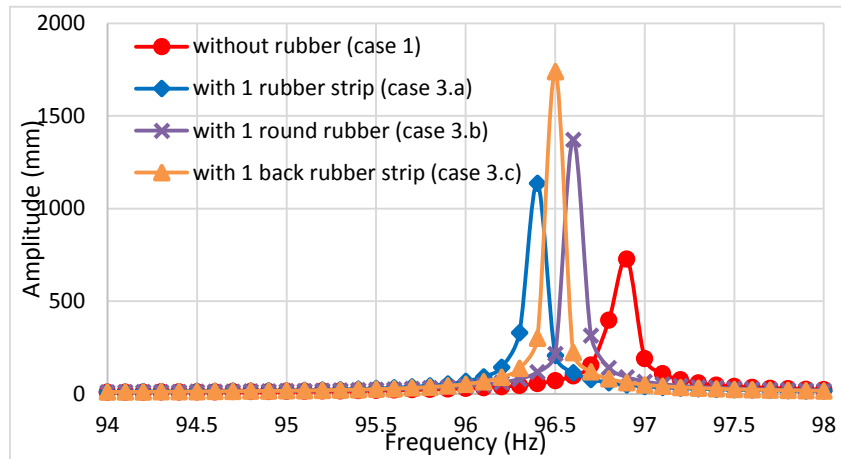


Fig. 4.2.3.2 (a) Amplitudes along X-Direction at 2nd mode for case 3 compared with case 1.

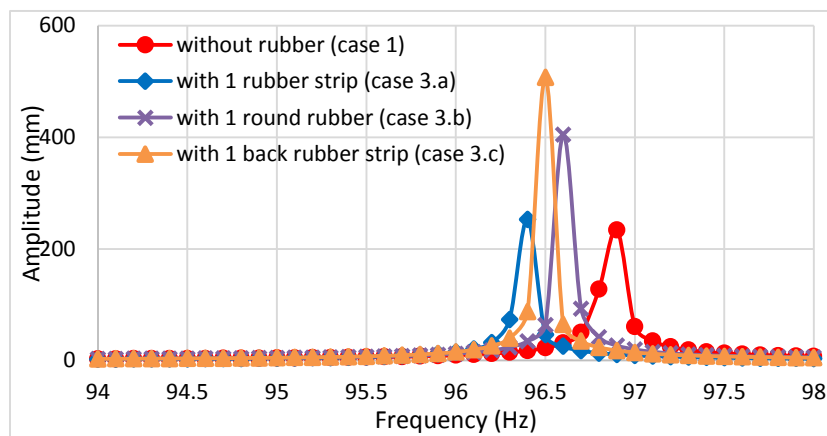


Fig. 4.2.3.2 (b) Amplitudes along Y-Direction at 2nd mode for case 3 compared with case 1.

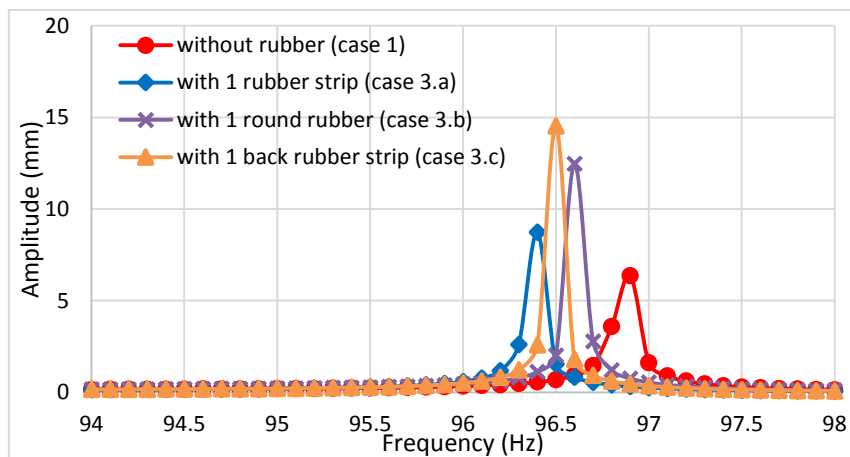


Fig. 4.2.3.2 (c) Amplitudes along Z-Direction at 2nd mode for case 3 compared with case 1.

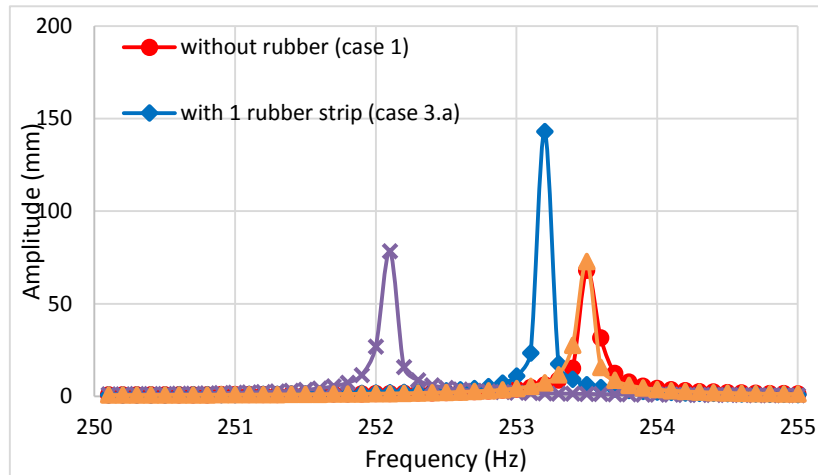


Fig. 4.2.3.3 (a) Amplitudes along X-Direction at 3rd mode for case 3 compared with case 1.

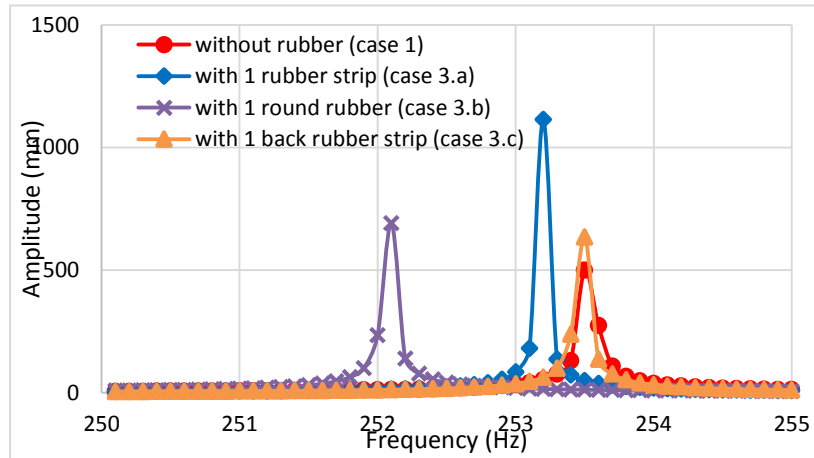


Fig. 4.2.3.3 (b) Amplitudes along Y-Direction at 3rd mode for case 3 compared with case 1.

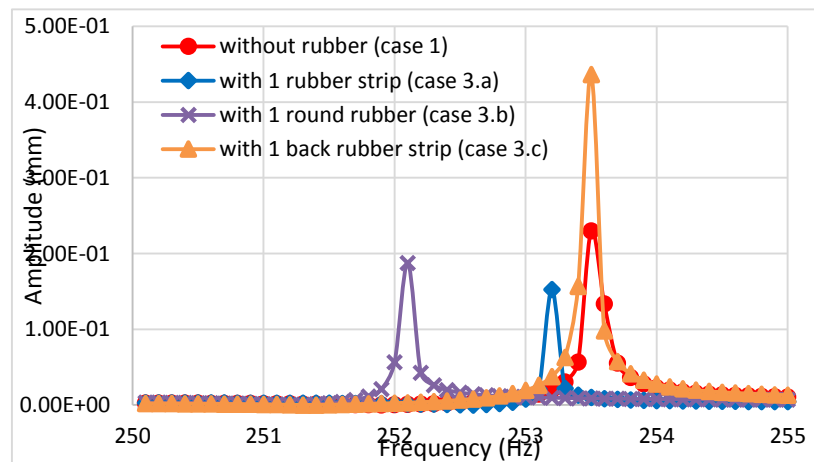


Fig. 4.2.3.3 (c) Amplitudes along Z-Direction at 3rd mode for case 3 compared with case 1.

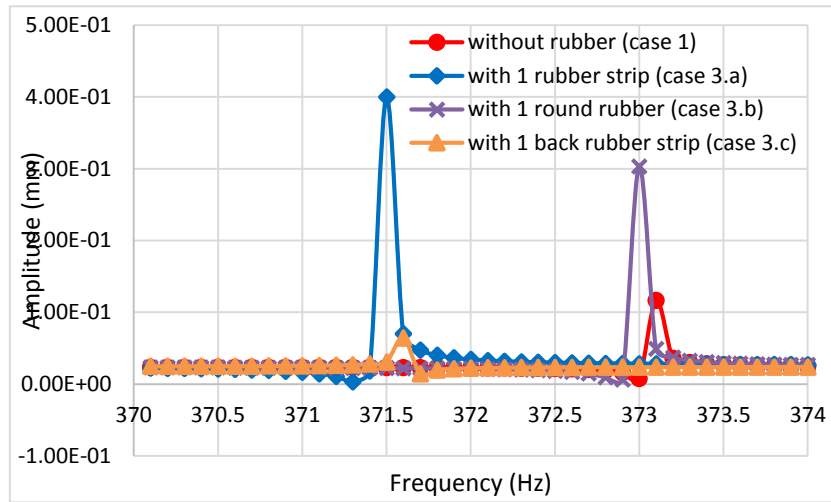


Fig. 4.2.3.4 (a) Amplitudes along X-Direction at 4th mode for case 3 compared with case 1.

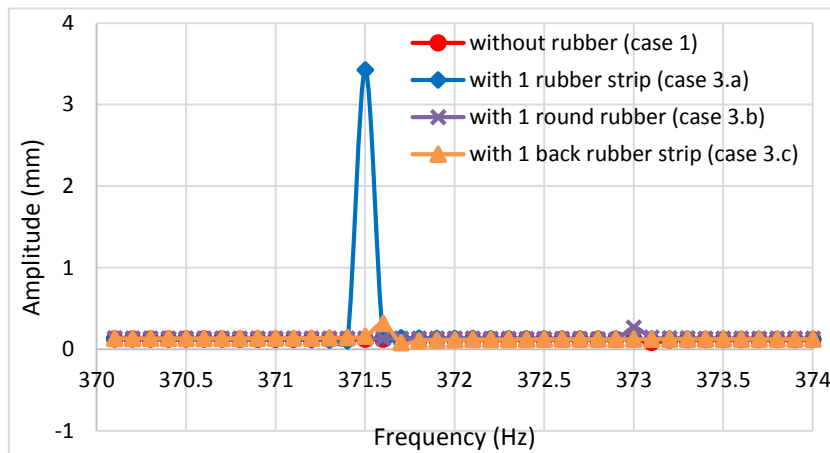


Fig. 4.2.3.4 (b) Amplitudes along Y-Direction at 4th mode for case 3 compared with case 1.

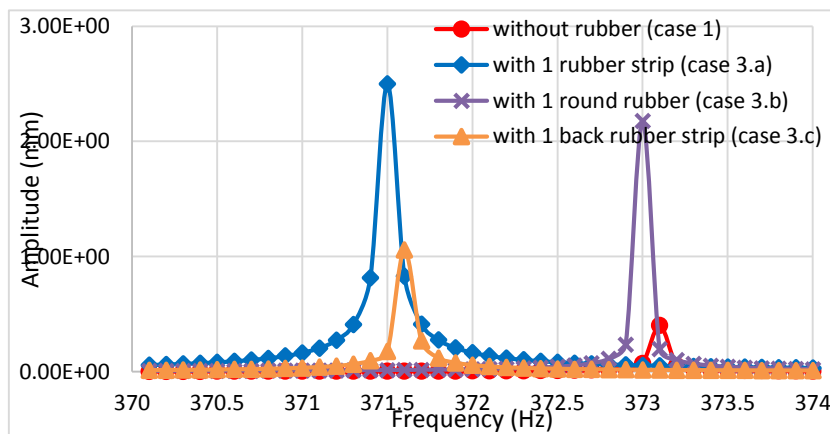


Fig. 4.2.3.4 (c) Amplitudes along Z-Direction at 4th mode for case 3 compared with case 1.

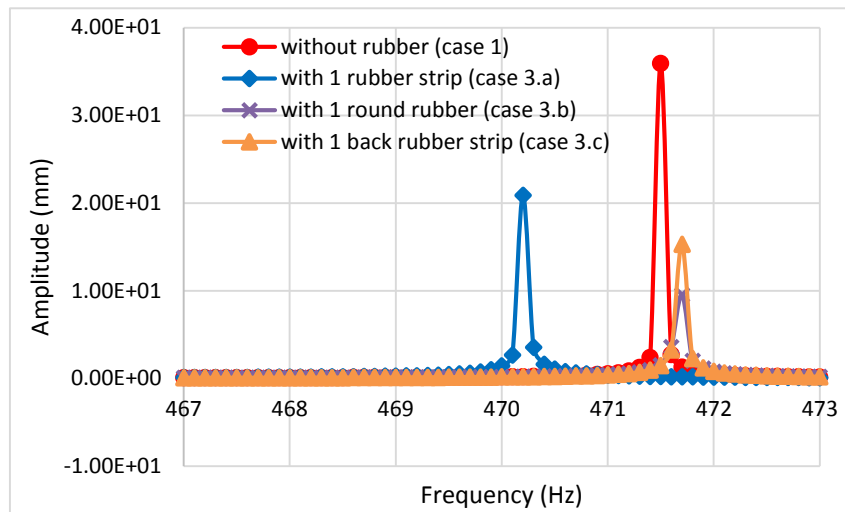


Fig. 4.2.3.5 (a) Amplitudes along X-Direction at 5th mode for case 3 compared with case 1.

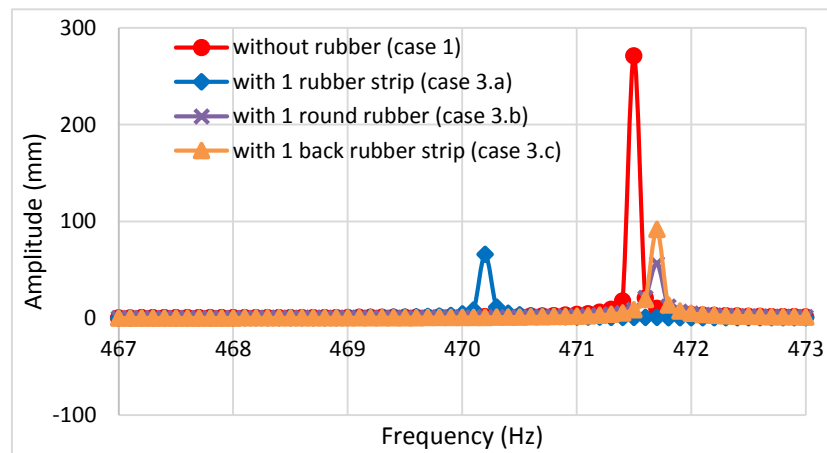


Fig. 4.2.3.5 (b) Amplitudes along Y-Direction at 5th mode for case 3 compared with case 1.

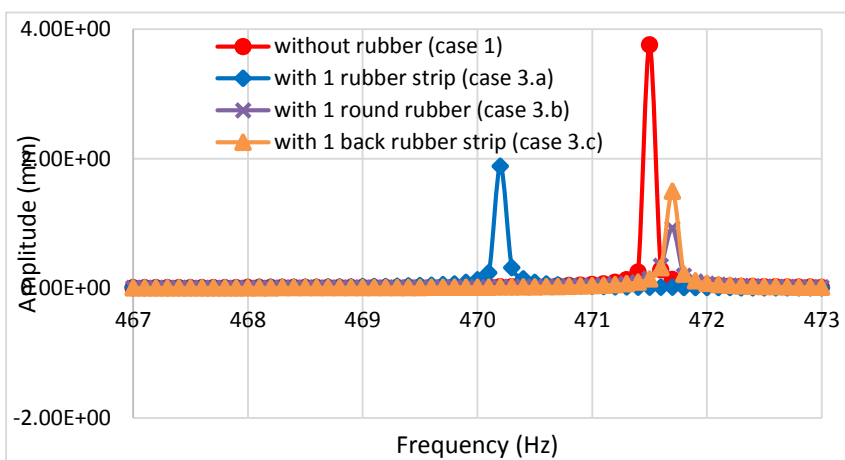


Fig. 4.2.3.5 (c) Amplitudes along Z-Direction at 5th mode for case 3 compared with case 1.

4.2.4. Harmonic Response of Case 4

The amplitudes along X-axis at 1st mode for all the attachments reduce for case 4 shown in Fig. 4.2.4.1 (a). Most reduction is found when 3 rubber strips used in the bucket, then the use of 2 side strips, then the use of 4 rubber and lastly the use of 2 bottom strips. Similarly at the Y-direction most amplitude reduction occurs for 3 rubber strips Fig. 4.2.4.1 (b). And along Z-axis most reduced amplitude is for the use of 2 bottom strips then the use of 4 rubber Fig. 4.2.4.1 (c). So, it can be said that the use of 3 rubber strips is comparatively better than any other attachments to reduce the vibration amplitude at this 1st mode.

The 2nd mode along X axis show us the amplitude of vibration increases when 3 rubber strips is used with the bucket along with the use of 2 bottom strips Fig. 4.2.4.2 (a). The use of 2 side strips reduces vibration and also 4 rubber. But along Y axis all of them reduces vibration while use of 3 rubber strips and 4 rubber reduces most Fig. 4.2.4.2 (b). And similar reduction in vibration amplitude is seen along Z-axis of this mode Fig. 4.2.4.2 (c). Here we can say the use of 4 rubber is best choice while use of 3 rubber strips also a good choice to reduce vibration at 2nd mode.

The amplitude along X-axis and Y-axis for both the attachments except the use of 3 rubber strips and 4 rubber increases Fig. 4.2.4.3 (a) and Fig. 4.2.4.3 (a). But similarly along Z axis the amplitudes increase for three attachments while for the use of 3 rubber strips amplitude reduces Fig. 4.2.4.3 (c). So, at this 3rd mode the use of 3 rubber strips should be the only choice over other attachments.

The 4th mode along X-axis shows us only the use of 2 side strips increases vibration amplitude while the use of other two attachments reduces vibration Fig. 4.2.4.4 (a). And along Y-axis use of 2 bottom strips and 2 side strips both increase vibration while use of 3 rubber strips and 4 rubber literally shows no peak of vibration amplitude. Lastly along Z-axis of this mode similarly both cases increase vibration amplitude a lot while use of 3 rubber strips and 4 rubber literally shows no vibration amplitude Fig. 4.2.4.4 (c). So, the use of 3 rubber strips and 4 rubber at this mode is best attachments.

The amplitude along X-axis at the 5th mode for the use of 2 bottom strips increases while for other three attachments it decreases Fig. 4.2.4.5 (a). For the use of 3 rubber strips the reduction is very much. And for the vibration along Y-axis for all the attachments amplitude reduces being lowest for the use of 3 rubber strips Fig. 4.2.4.5 (b). Lastly, though most reduction along Z-axis is observed for the use of 2 side strips but other three attachments also reduce the vibration amplitude Fig. 4.2.4.5 (c). In conclusion, the use of 3 rubber strips is better choice than any other at this 5th mode.

The summary of this section should be that the use of 3 rubber strips to reduce vibration amplitude along with 4 rubber should be considered over any other attachments as they reduce vibration amplitudes at most natural frequencies comparatively than other attachments. Over this conclusion next two cases were developed and the use of thickness and materials are discussed and studied in later sections.

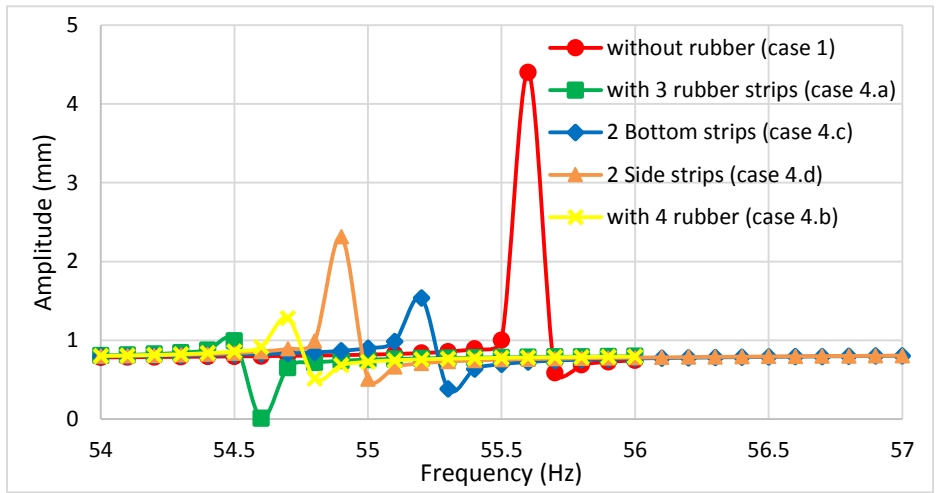


Fig. 4.2.4.1 (a) Amplitudes along X-Direction at 1st mode for case 4 compared with case 1.

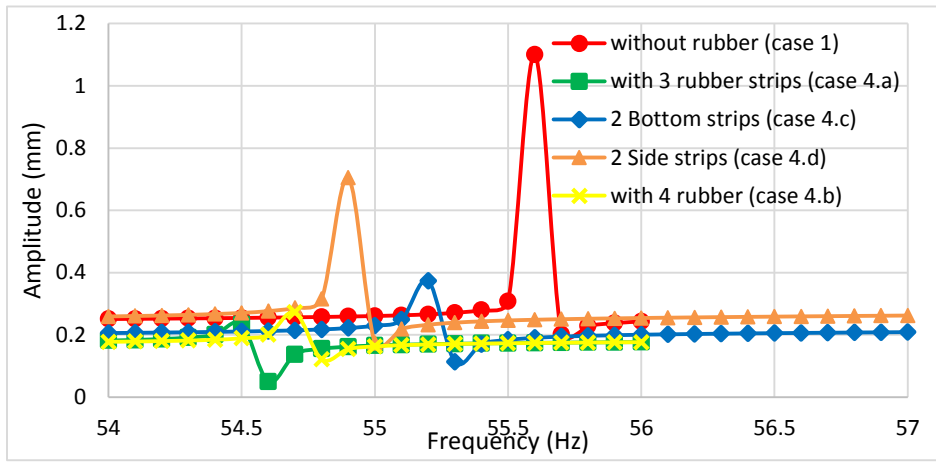


Fig. 4.2.4.1 (b) Amplitudes along Y-Direction at 1st mode for case 4 compared with case 1.

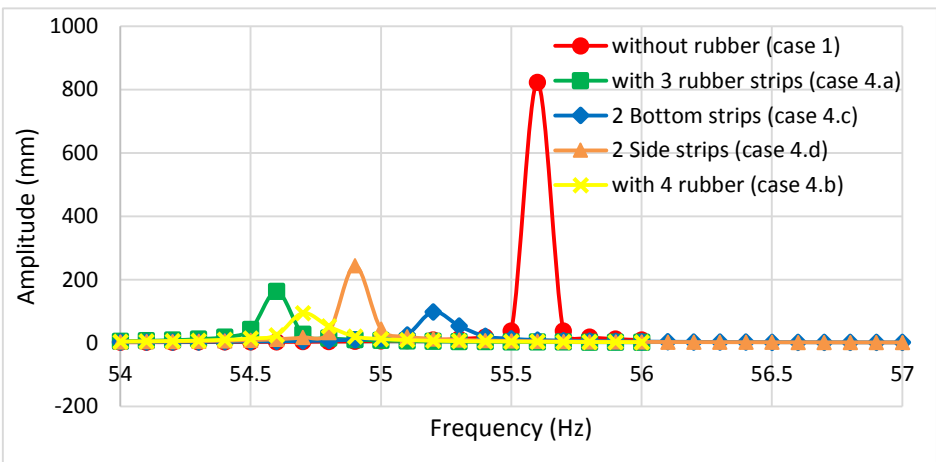


Fig. 4.2.4.1 (c) Amplitudes along Z-Direction at 1st mode for case 4 compared with case 1.

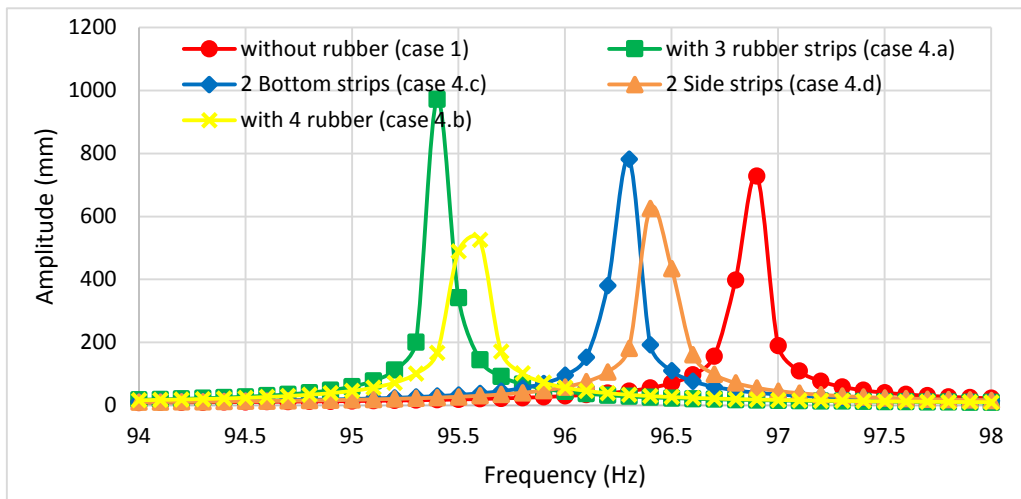


Fig. 4.2.4.2 (a) Amplitudes along X-Direction at 2nd mode for case 4 compared with case 1.

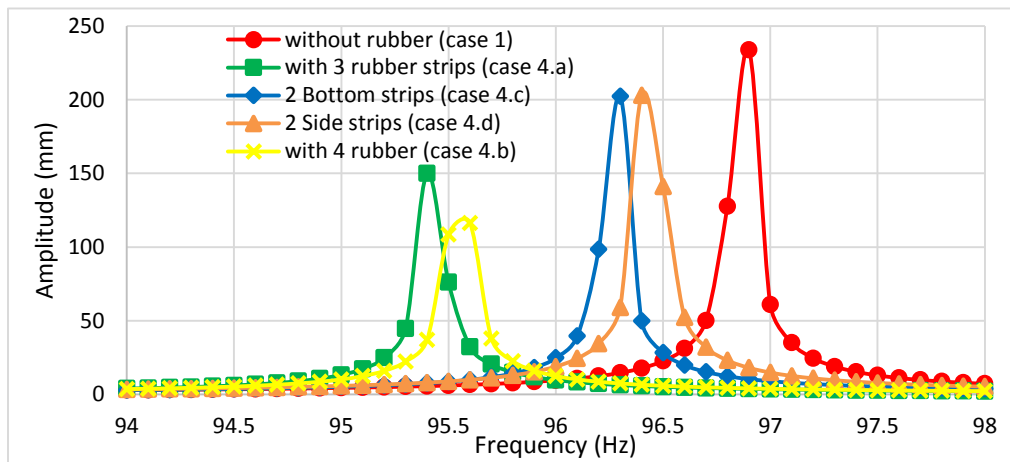


Fig. 4.2.4.2 (b) Amplitudes along Y-Direction at 2nd mode for case 4 compared with case 1.

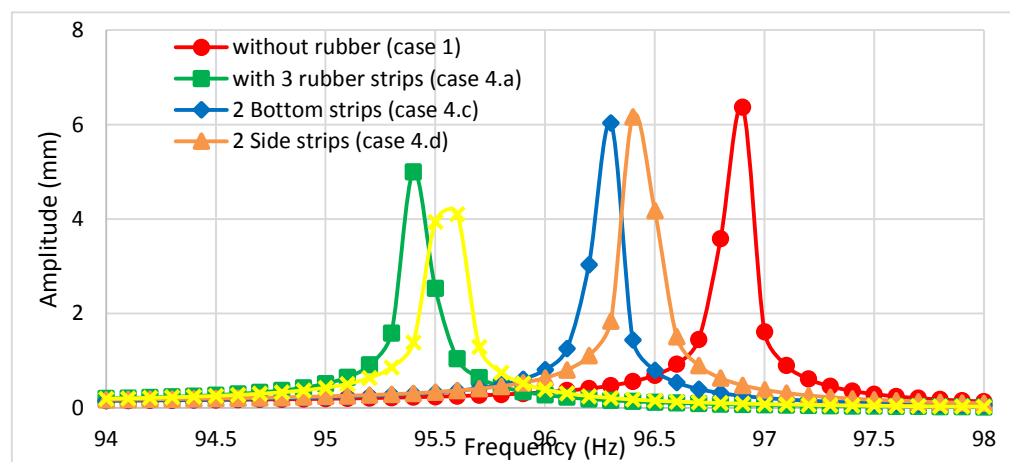


Fig. 4.2.4.2 (c) Amplitudes along Z-Direction at 2nd mode for case 4 compared with case 1.

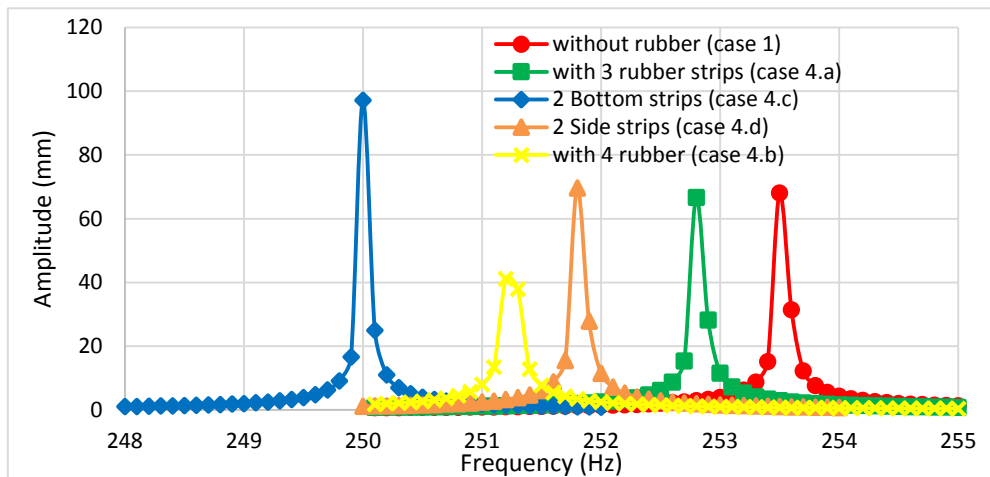


Fig. 4.2.4.3 (a) Amplitudes along X-Direction at 3rd mode for case 4 compared with case 1.

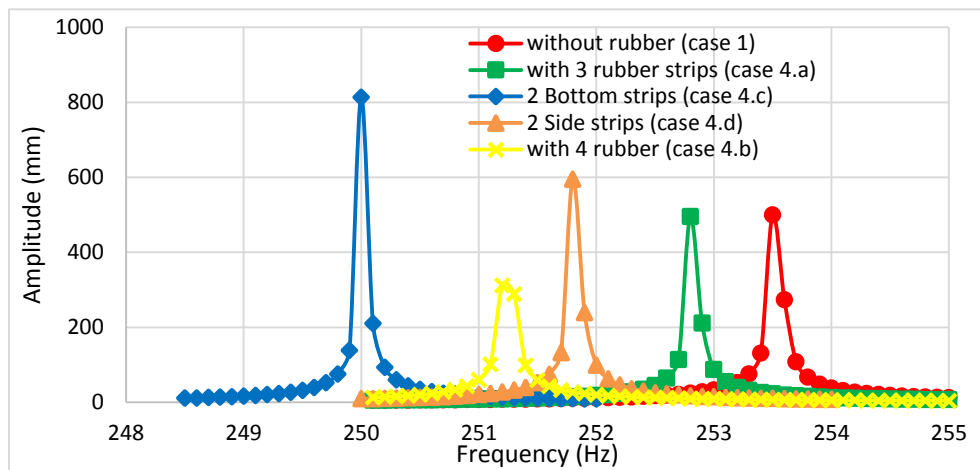


Fig. 4.2.4.3 (b) Amplitudes along Y-Direction at 3rd mode for case 4 compared with case 1.

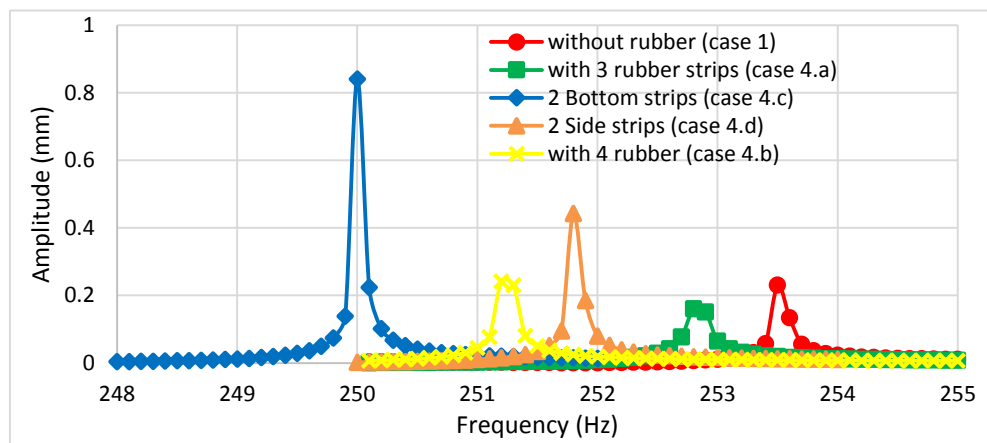


Fig. 4.2.4.3 (c) Amplitudes along Z-Direction at 3rd mode for case 4 compared with case 1.

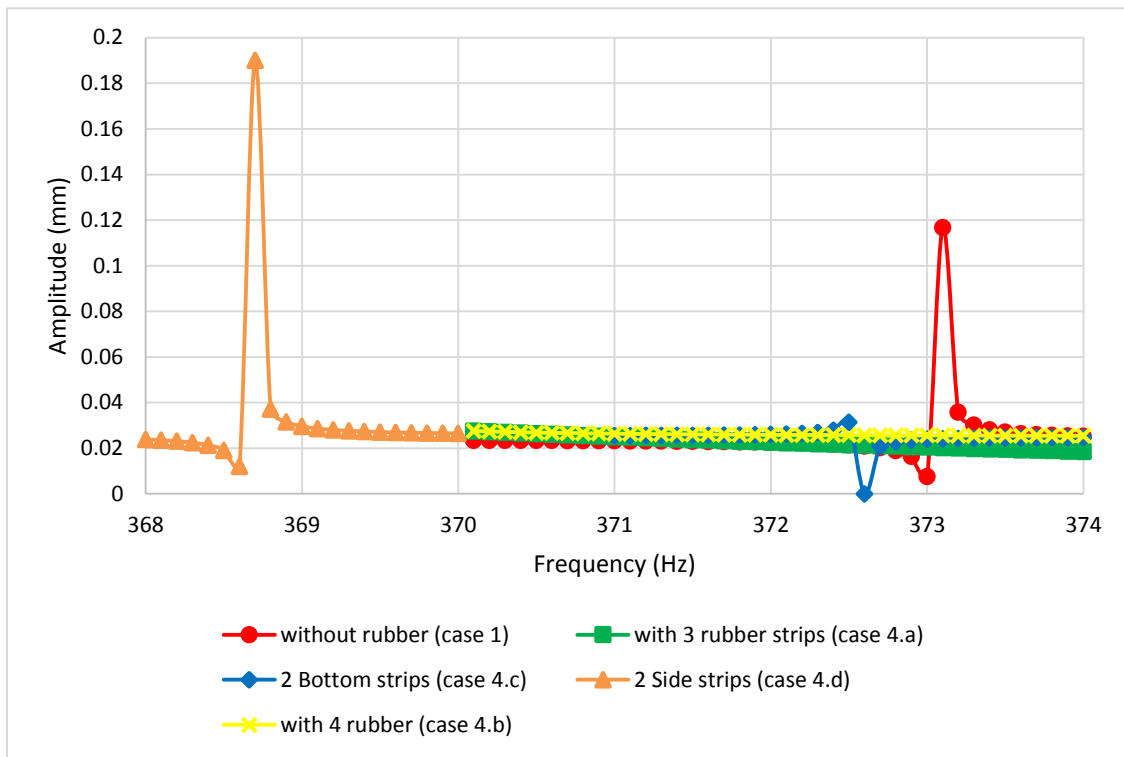


Fig. 4.2.4.4 (a) Amplitudes along X-Direction at 4th mode for case 4 compared with case 1.

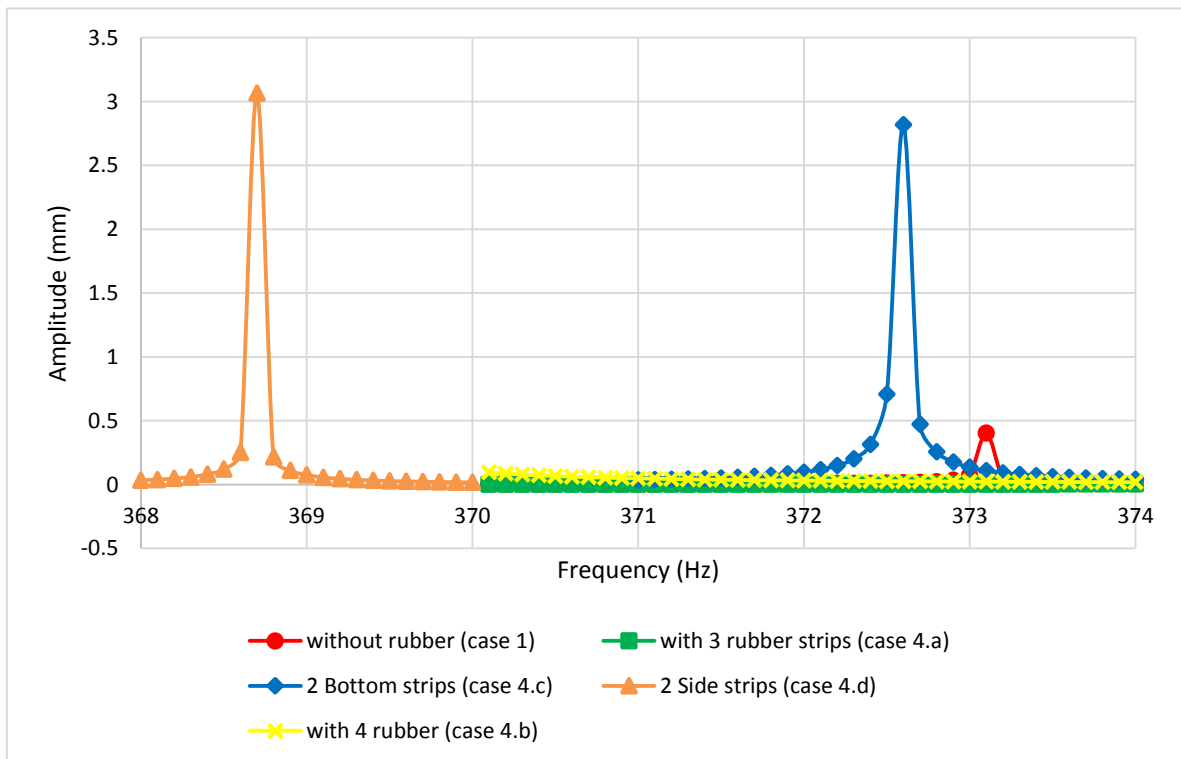


Fig. 4.2.4.4 (c) Amplitudes along Y-Direction at 4th mode for case 4 compared with case 1.

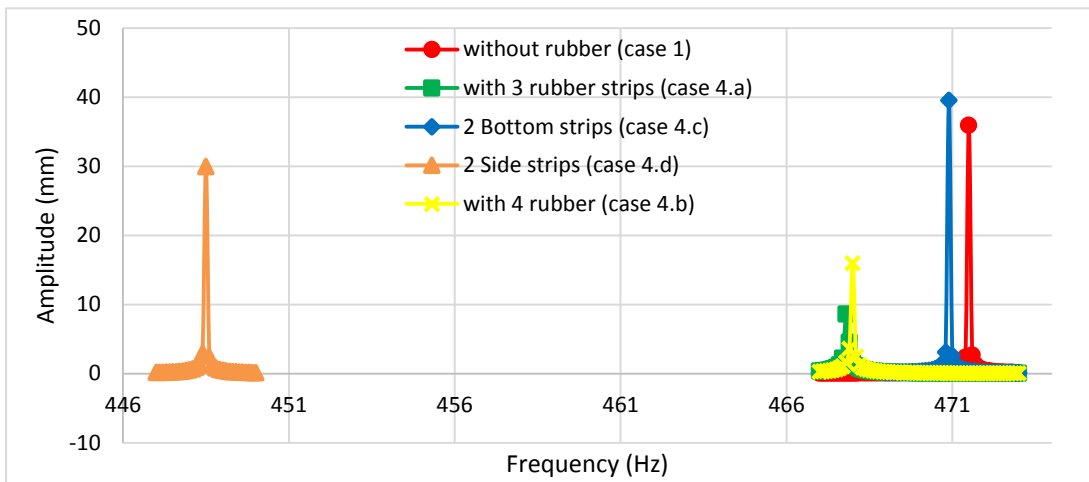


Fig. 4.2.4.5 (a) Amplitudes along X-Direction at 5th mode for case 4 compared with case 1.

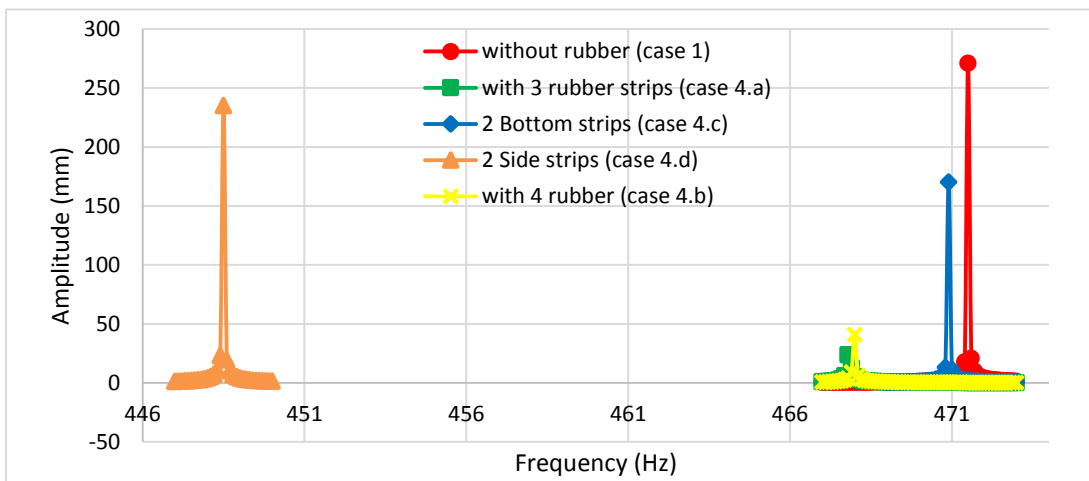


Fig. 4.2.4.5 (b) Amplitudes along X-Direction at 5th mode for case 4 compared with case 1.

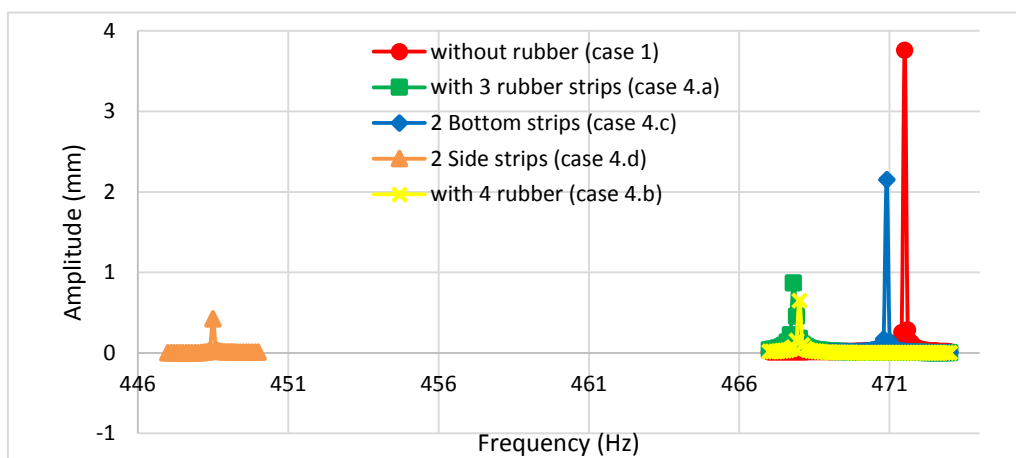


Fig. 4.2.4.5 (c) Amplitudes along X-Direction at 5th mode for case 4 compared with case 1.

4.2.5. Harmonic Response of Case 5

The vibration amplitudes along X-axis and Y-axis of the 1st mode reduce for all the attachments of the case but when use 3 rubber strips of 5mm thickness then it reduces most Fig. 4.2.5.1 (a) and Fig. 4.2.5.1 (b). And along Z-axis though all the modification reduce amplitude, the use of half thickness and double thickness of 3 rubber strips give lesser amplitudes Fig. 4.2.5.1 (c). However combining all three figures we can still say that the use of 3 rubber strips of 5 mm thickness is comparatively better choice at this 1st mode.

The amplitude for the use of double thickness (10 mm) case 5 (c) of 3 rubber strips increases along all the axis of this 2nd mode while the use of half thickness (2.5 mm) case 5 (b) reduces Fig. 4.2.5.2 (a), (b) and (c). And the use of 3 rubber strips of 5mm thickness along X-axis increases but for Y and Z-axis the amplitude decrease. So, we can conclude that the use of 3 rubber strips with half thickness is better choice at this 2nd mode then comes the choice of 3 rubber strips.

The amplitude at this 3rd mode along X-axis reduces most for the use of 3 rubber strips of double thickness (10 mm), then the use of half thickness (2.5 mm) and then the use of 3 rubber strips (5 mm) Fig. 4.2.5.3 (a). Similar pattern is observed along Y-axis Fig. 4.2.5.3 (b). And along Z-axis the use of half thickness and double thickness both increase vibration amplitude only reduction occurs for the use of 3 rubber strips Fig. 4.2.5.3 (c). So, we can say the use of 3 rubber strips of 5mm is best choice at this 3rd mode.

Huge vibration occurs for the use of Double thickness 3 rubber strips (10 mm) along X-axis and Y-axis of the 4th mode but literally no amplitude along Z-axis Fig. 4.2.5.4 (a), (b) and (c). Also huge vibration occurs for the use of 3 rubber strips of half thickness along X-axis and Z-axis of this mode. But no vibration amplitude is seen for the use of 3 rubber strips along all the axis. So, the use of 3 rubber strips is the best choice here also.

The vibration amplitude for the use of double thickness is not seen here as the mode's natural frequency shifts to the left so much that it actually overlaps with 4th mode's natural frequency. However the use of other two attachments reduces vibration amplitude along all the axis while the use of 3 rubber strips reduces most Fig. 4.2.5.5 (a), (b) and (c). So, at the 5th mode the use of 3 rubber strips is better choice.

From all these discussion we can say use of double thickness can be critical as it shows abrupt behavior of overlapping modes. And from all comparisons we can say use of 3 rubber strips of 5 mm thickness is a very good choice over other attachments. The study suggests the importance of thickness should be considered reinforcing rubber materials with bucket and also show the opportunity of wide future works on the optimization of bucket model design based on thickness considerations.

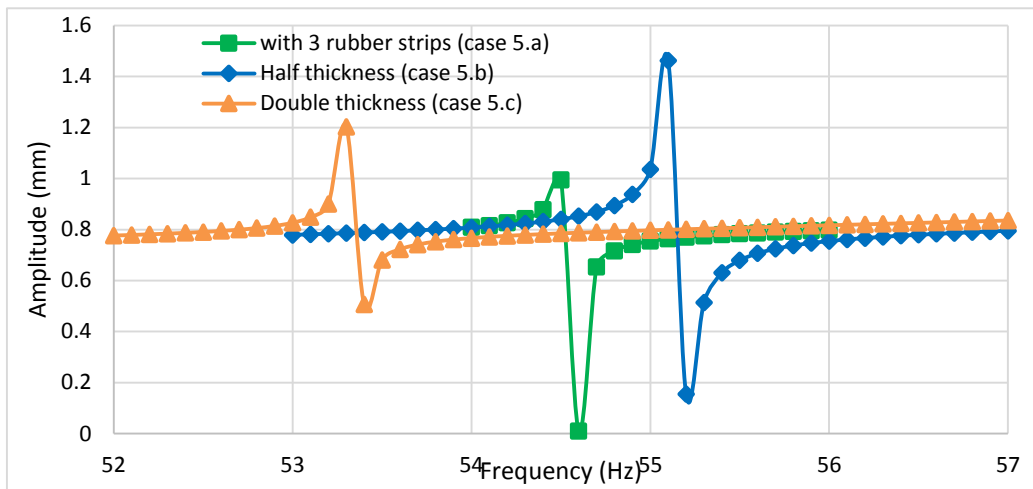


Fig. 4.2.5.1 (a) Amplitudes along X-Direction at 1st mode for case 5.

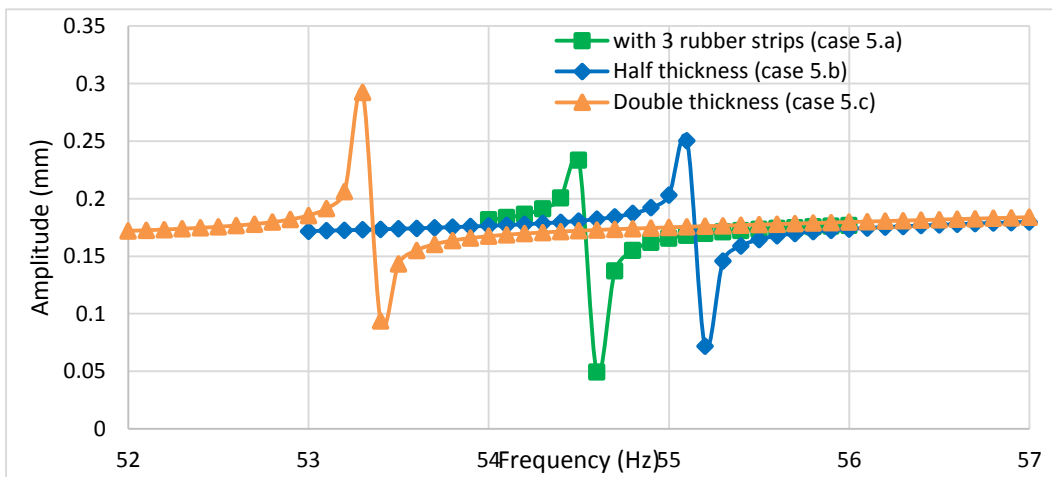


Fig. 4.2.5.1 (b) Amplitudes along Y-Direction at 1st mode for case 5.

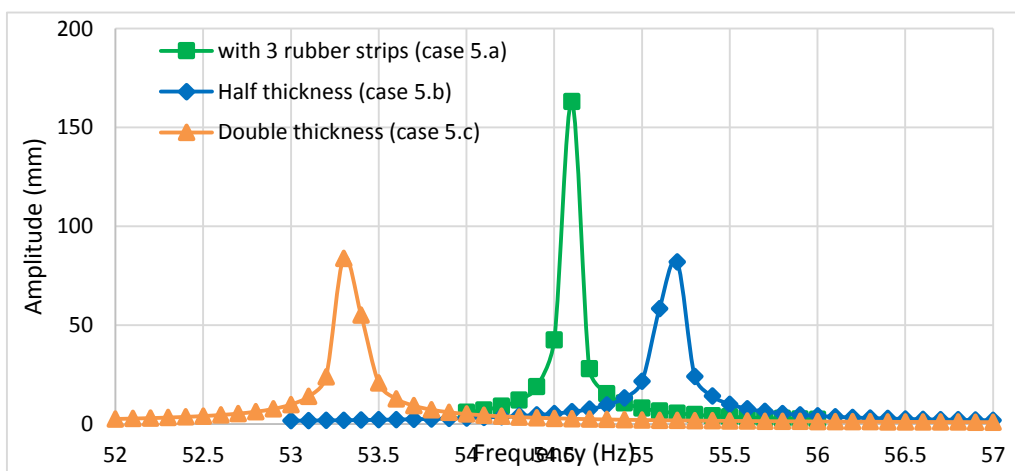


Fig. 4.2.5.1 (c) Amplitudes along Z-Direction at 1st mode for case 5.

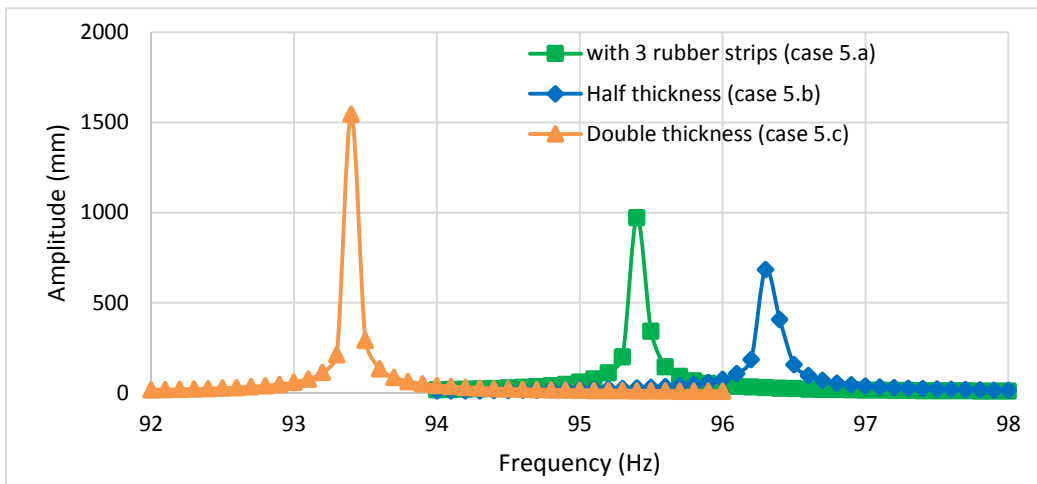


Fig. 4.2.5.2 (a) Amplitudes along X-Direction at 2nd mode for case 5.

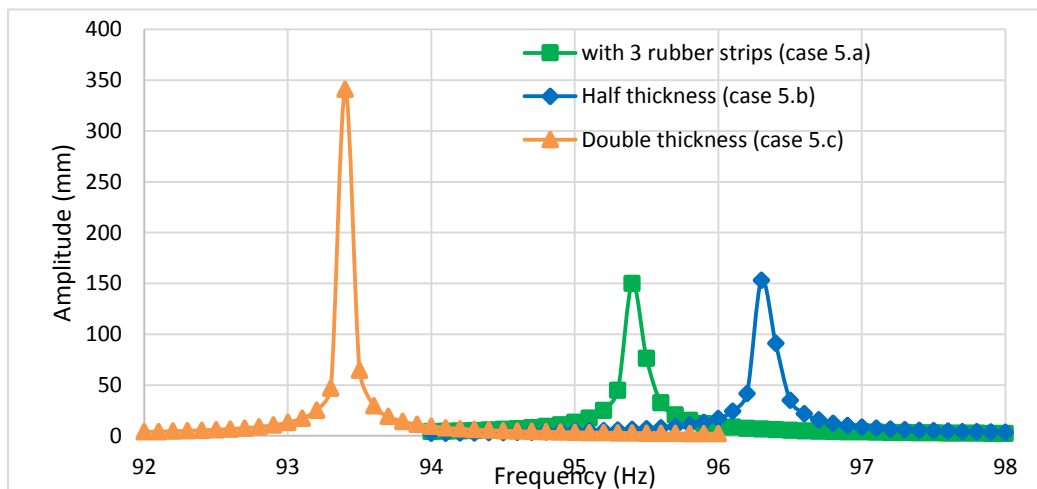


Fig. 4.2.5.2 (b) Amplitudes along Y-Direction at 2nd mode for case 5.

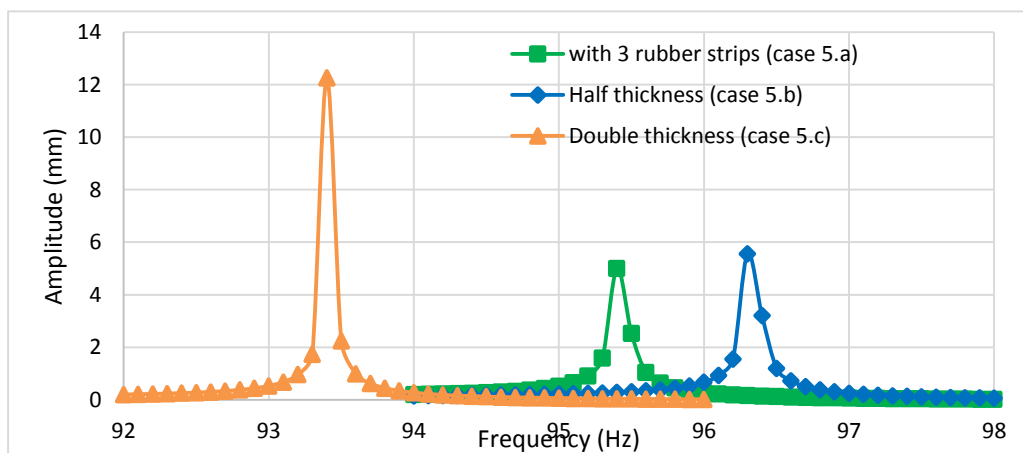


Fig. 4.2.5.2 (c) Amplitudes along Z-Direction at 2nd mode for case 5.

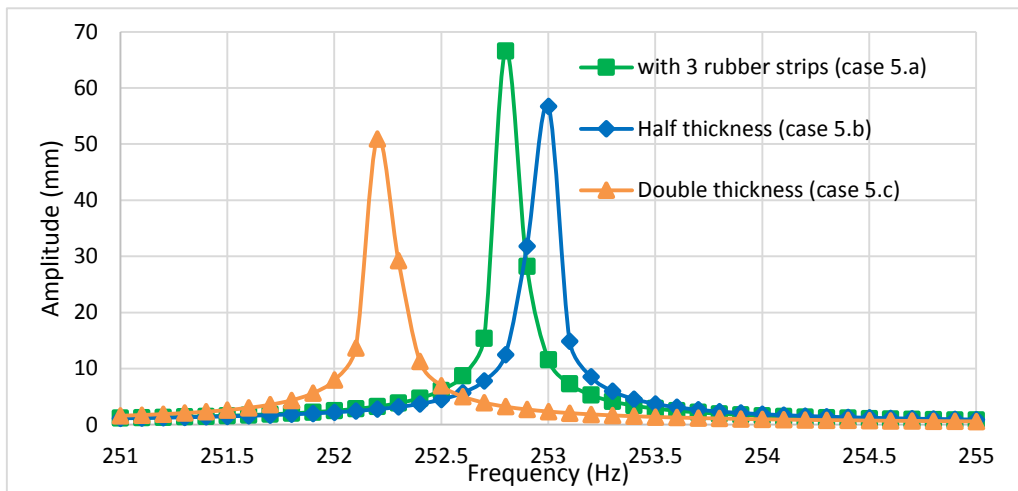


Fig. 4.2.5.3 (a) Amplitudes along X-Direction at 3rd mode for case 5.

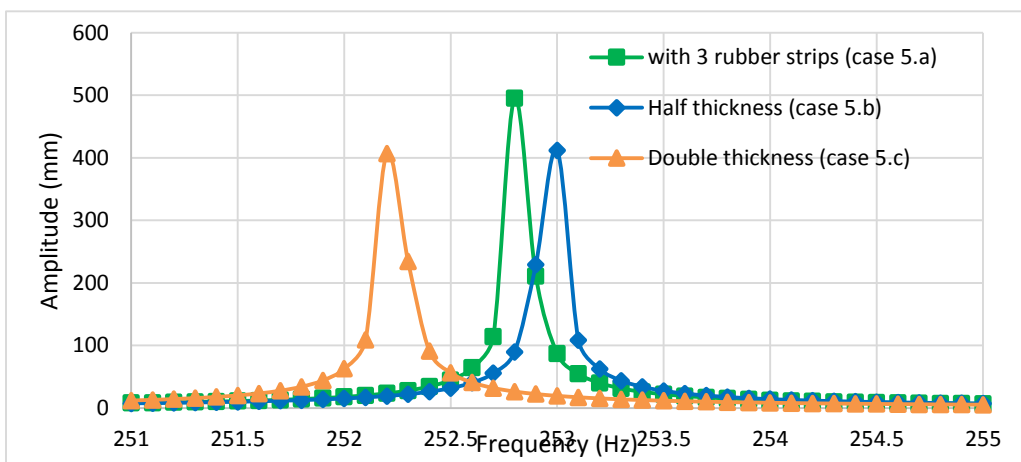


Fig. 4.2.5.3 (b) Amplitudes along Y-Direction at 3rd mode for case 5.

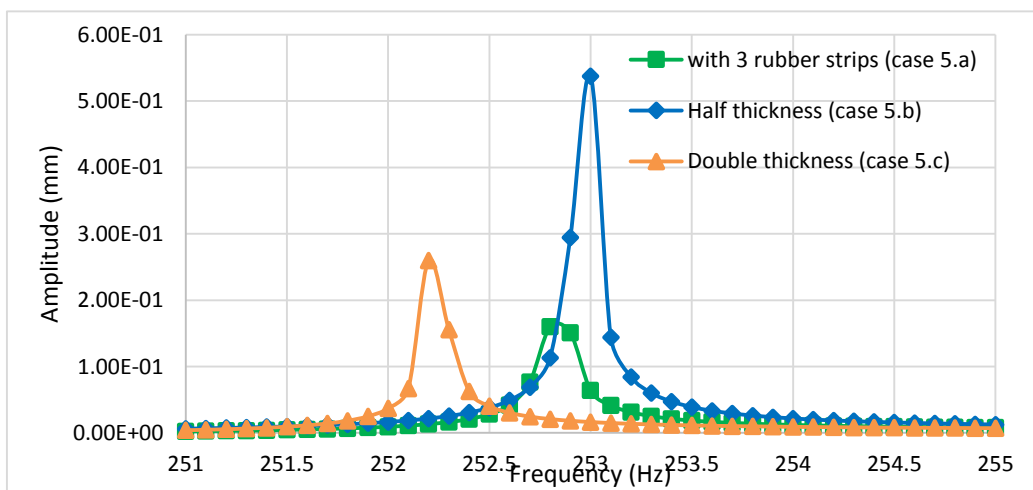


Fig. 4.2.5.3 (c) Amplitudes along Z-Direction at 3rd mode for case 5.

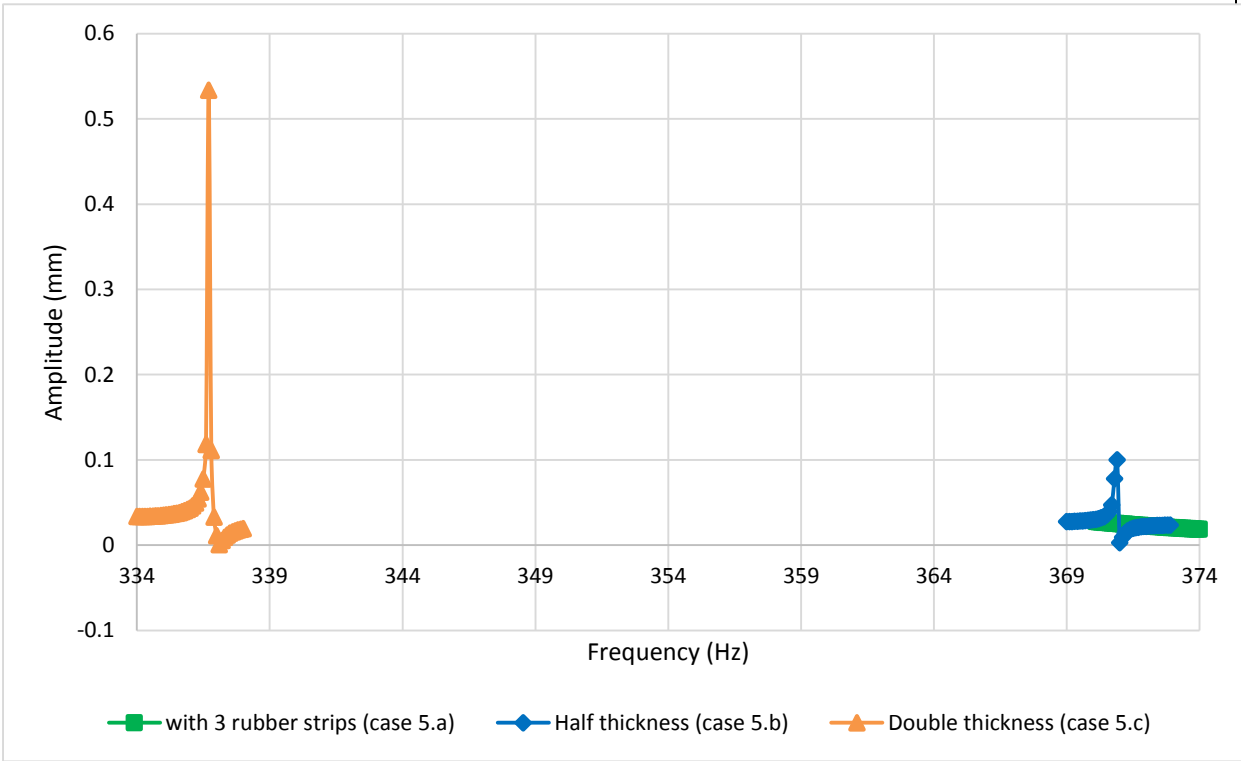


Fig. 4.2.5.4 (a) Amplitudes along X-Direction at 4th mode for case 5.

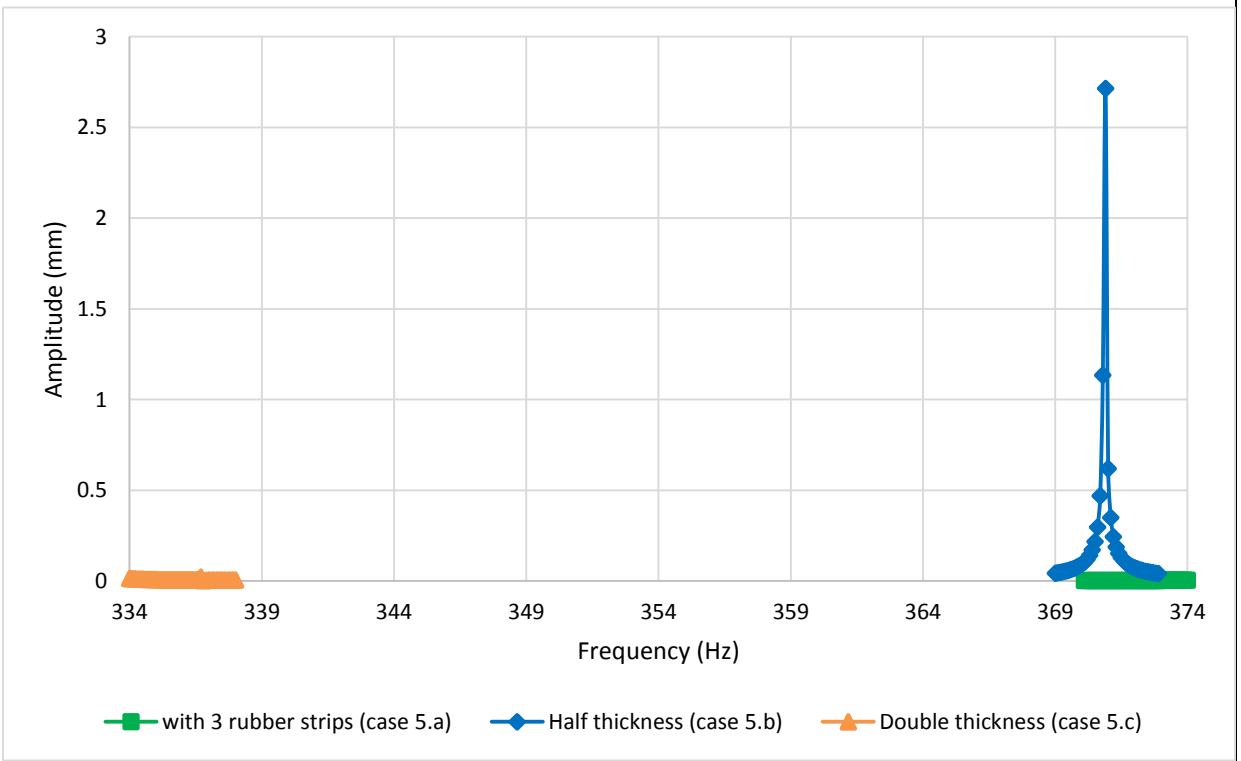


Fig. 4.2.5.4 (c) Amplitudes along Z-Direction at 4th mode for case 5.

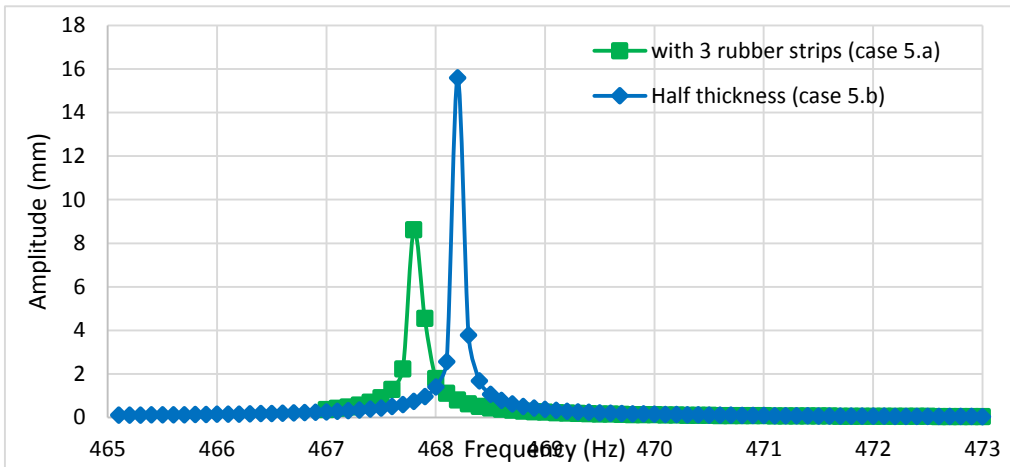


Fig. 4.2.5.5 (a) Amplitudes along X-Direction at 5th mode for case 5.

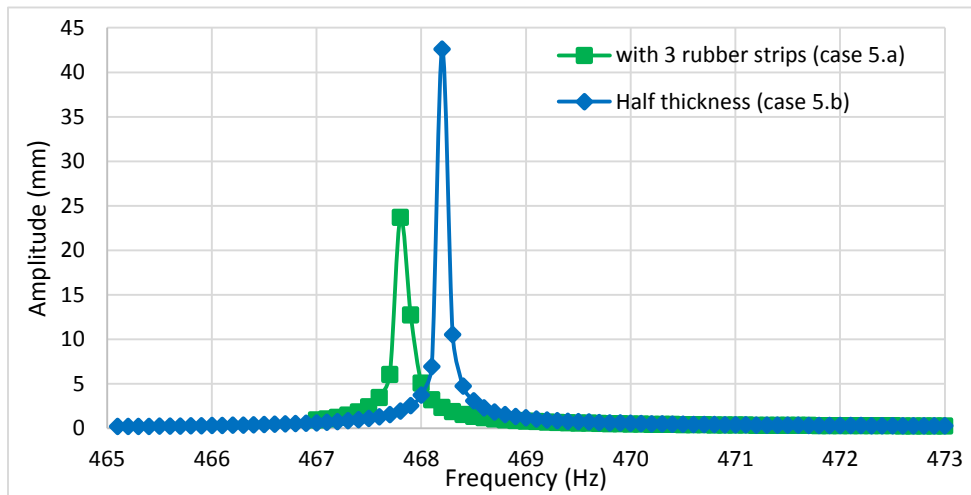


Fig. 4.2.5.5 (b) Amplitudes along Y-Direction at 5th mode for case 5.

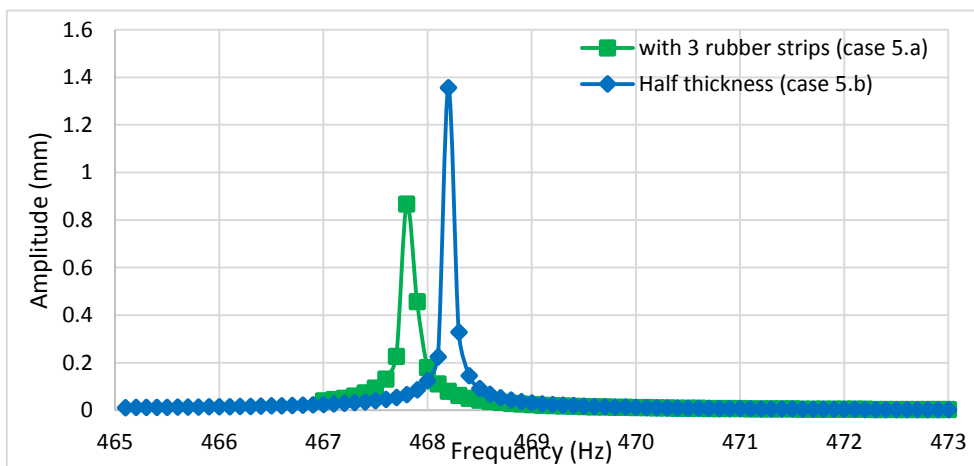


Fig. 4.2.5.5 (c) Amplitudes along Z-Direction at 5th mode for case 5.

4.2.6. Harmonic Response of Case 6

The vibration along X-axis and Y-axis of the 1st mode show very less vibration amplitude when use 3 rubber strips compared to the other attachments Fig. 4.2.6.1 (a) and Fig. 4.2.6.1 (b). But along Z-axis most reduction occurs for the use of 3 aluminum strips Fig. 4.2.6.1 (c). However we can still say the use of 3 rubber strips is better choice compared to other attachments at this mode.

The use of 3 aluminum strips increases vibration amplitude along all the axis of 2nd mode Fig. 4.2.6.2 (a), (b) and (c). With the use of 3 rubber strips the vibration amplitude increases along X-axis but decreases along Y-axis and Z-axis. And the use of 3 steel strips literally shows no vibration along any of the axis. So the use of 3 steel strips is the best choice at this 2nd mode while use of 3 rubber strips is the next.

At the 3rd mode along X-axis and Y-axis though the amplitude reduces for all the case but natural frequency shifts to the right while using 3 aluminum and steel strips Fig. 4.2.6.3 (a) and (b). And along Z-axis the use of aluminum and steel increases vibration while 3 rubber strips decreases the vibration amplitude Fig. 4.2.6.3 (c). So, the 3 rubber strips is the best choice at this 3rd mode.

The use 3 aluminum strips increases vibration amplitude along X-axis and Z-axis of 4th mode while no vibration is observed along Y-axis Fig. 4.2.6.4 (a), (b) and (c). And the use of steel strips increases amplitude along Y-axis and Z-axis but reduces along X-axis. But the use of 3 rubber strips literally shows no vibration amplitude along any of the axis at this mode. So, the use of rubber is still better choice at this mode.

Though the vibration amplitude decreases for the materials along all the axis of this 5th mode the use of aluminum and steel shift the natural frequency to the right side of the natural frequency of the bucket's natural frequency Fig. 4.2.6.5 (a), (b) and (c). However here also we can say that the use of 3 rubber strips is the best choice.

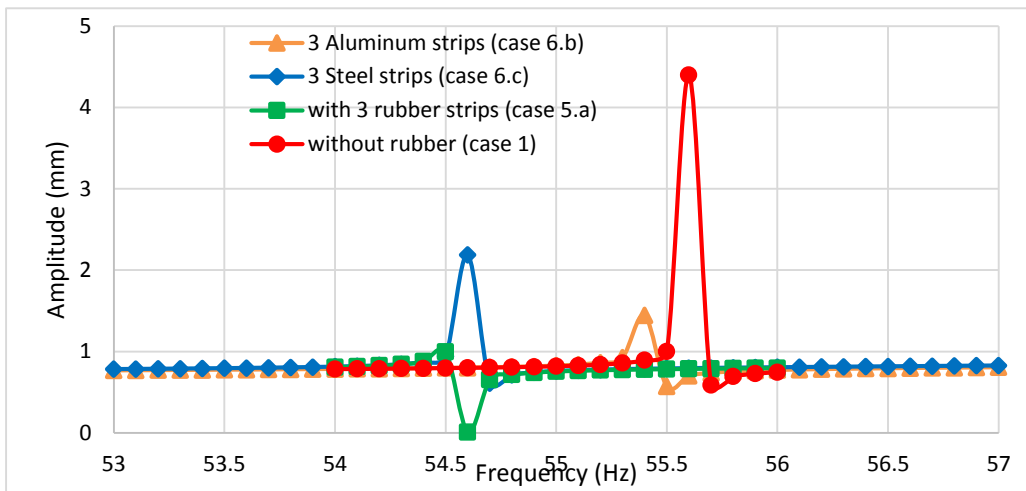


Fig. 4.2.6.1 (a) Amplitudes along X-Direction at 1st mode for case 6.

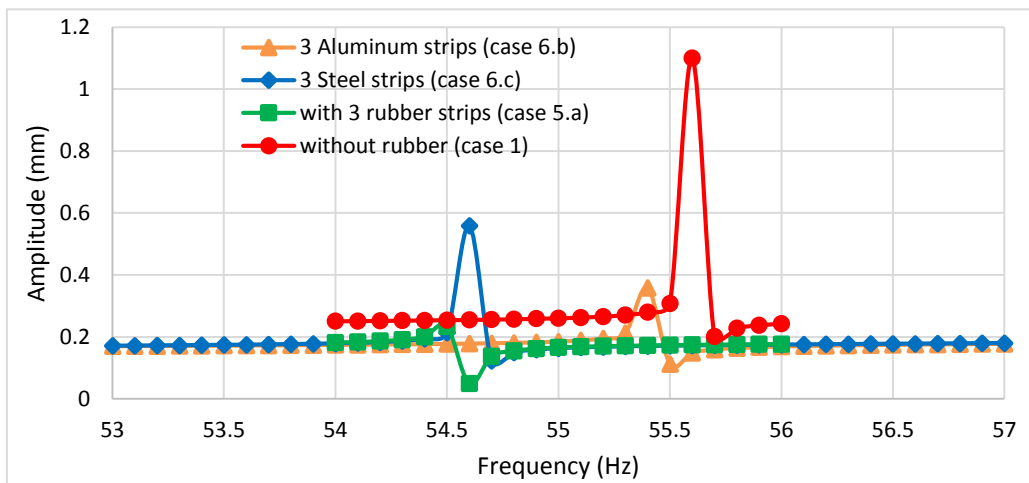


Fig. 4.2.6.1 (b) Amplitudes along Y-Direction at 1st mode for case 6.

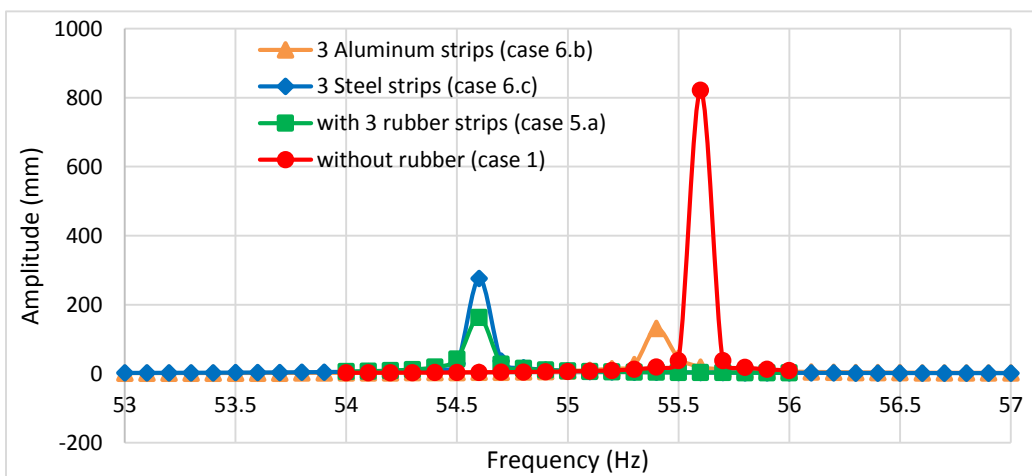


Fig. 4.2.6.1 (c) Amplitudes along Z-Direction at 1st mode for case 6.

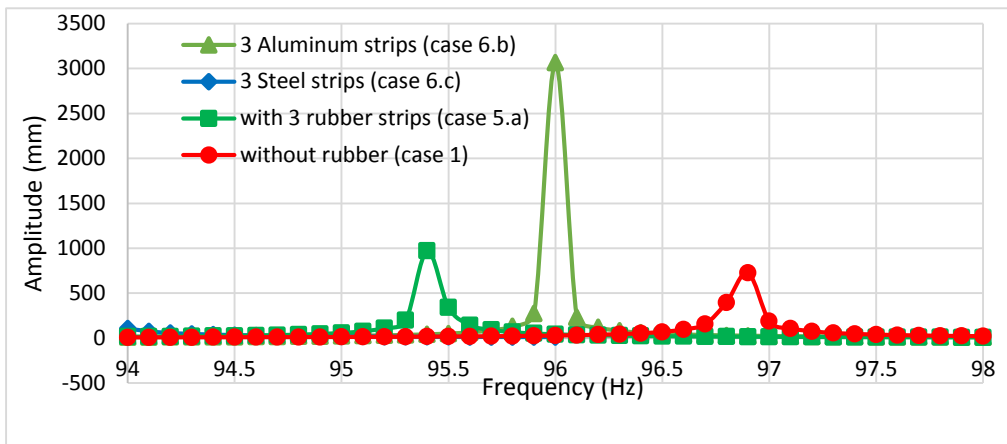


Fig. 4.2.6.2 (a) Amplitudes along X-Direction at 2nd mode for case 6.

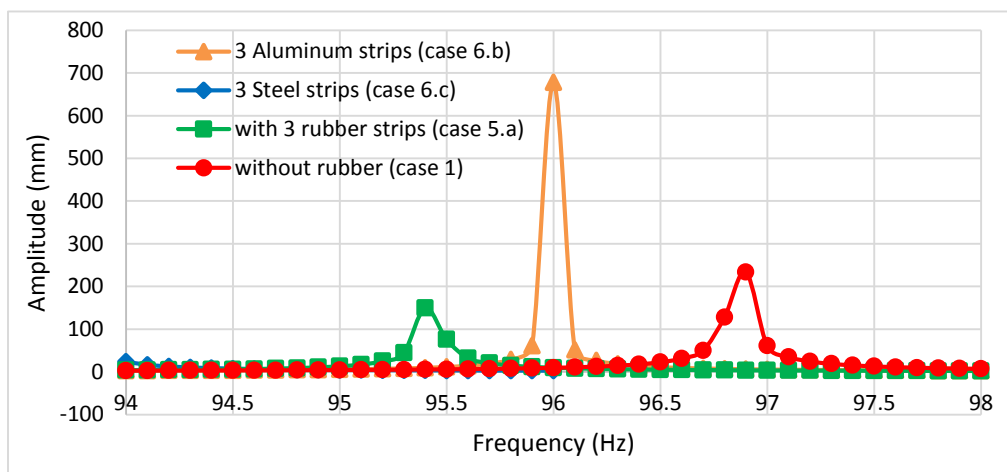


Fig. 4.2.6.2 (b) Amplitudes along Y-Direction at 2nd mode for case 6.

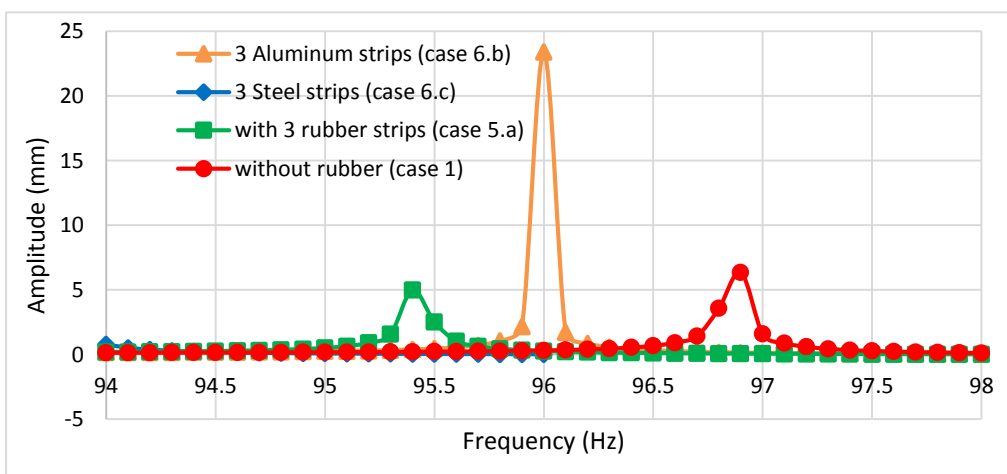


Fig. 4.2.6.2 (c) Amplitudes along Z-Direction at 2nd mode for case 6.

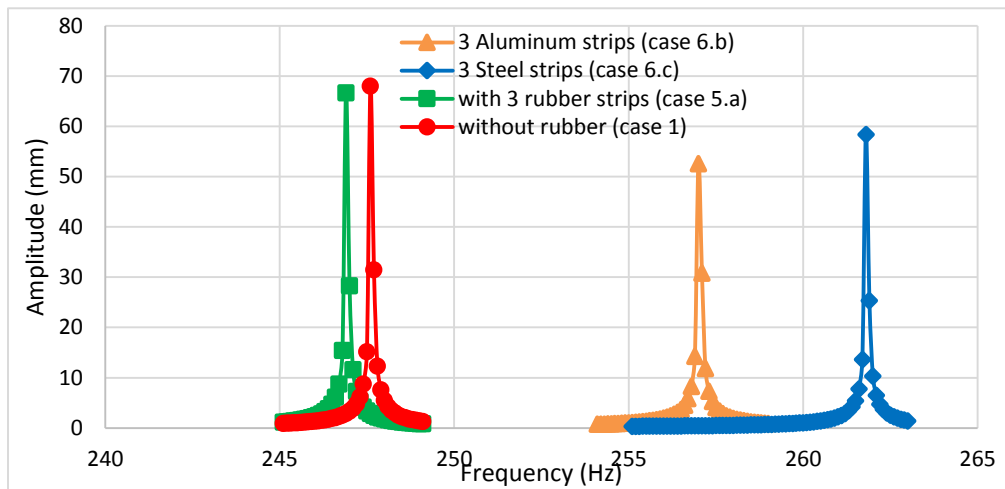


Fig. 4.2.6.3 (a) Amplitudes along X-Direction at 3rd mode for case 6.

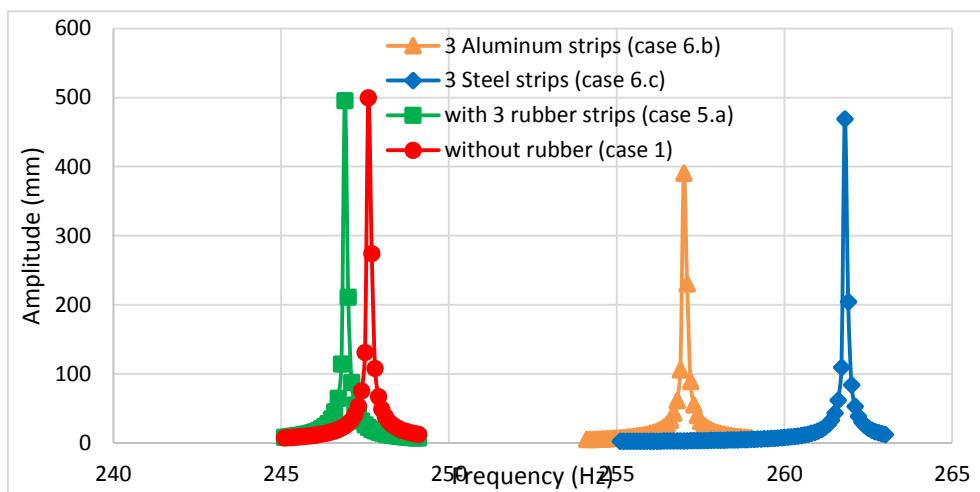


Fig. 4.2.6.3 (b) Amplitudes along Y-Direction at 3rd mode for case 6.

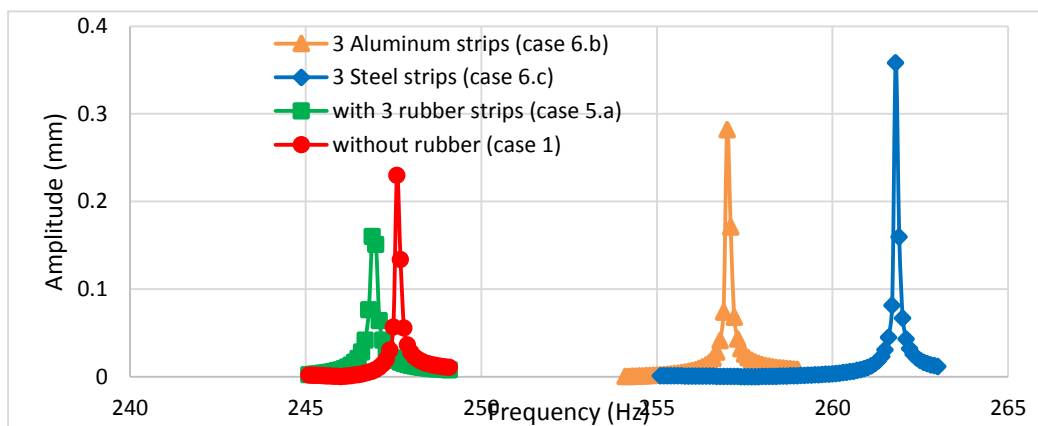


Fig. 4.2.6.3 (c) Amplitudes along Z-Direction at 3rd mode for case 6.

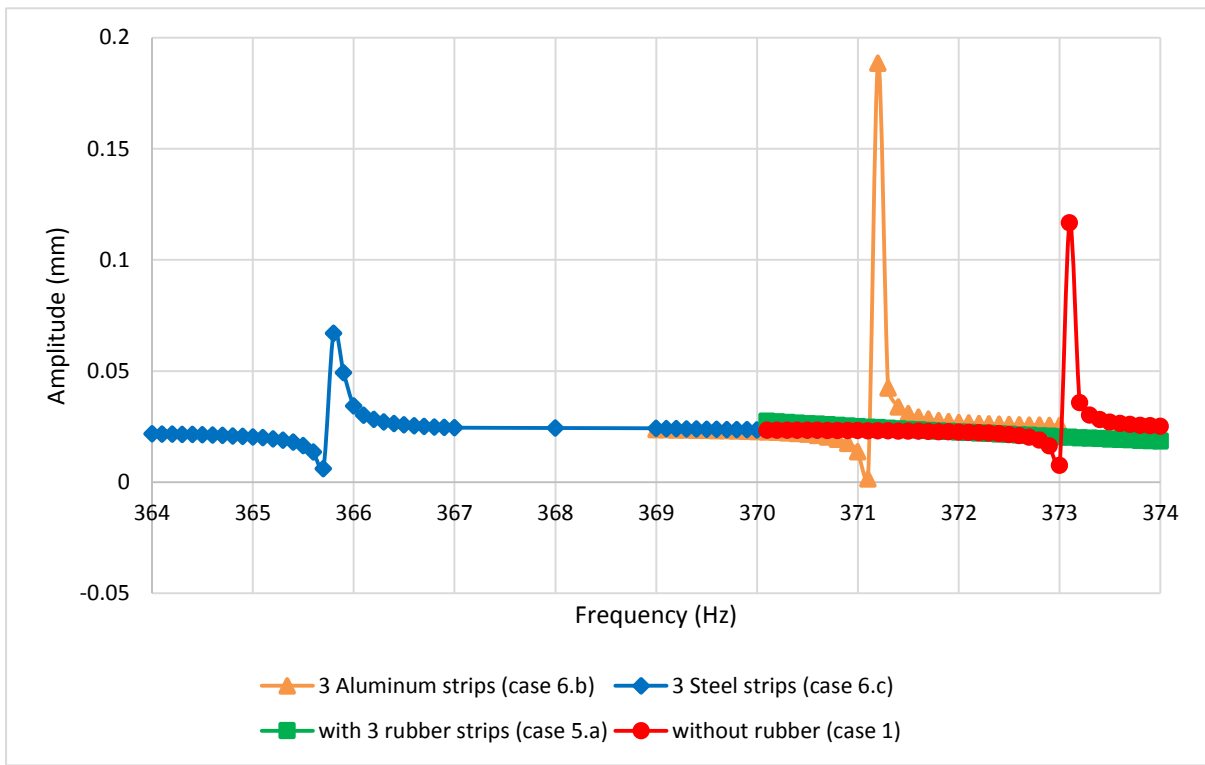


Fig. 4.2.6.4 (a) Amplitudes along X-Direction at 4th mode for case 6.

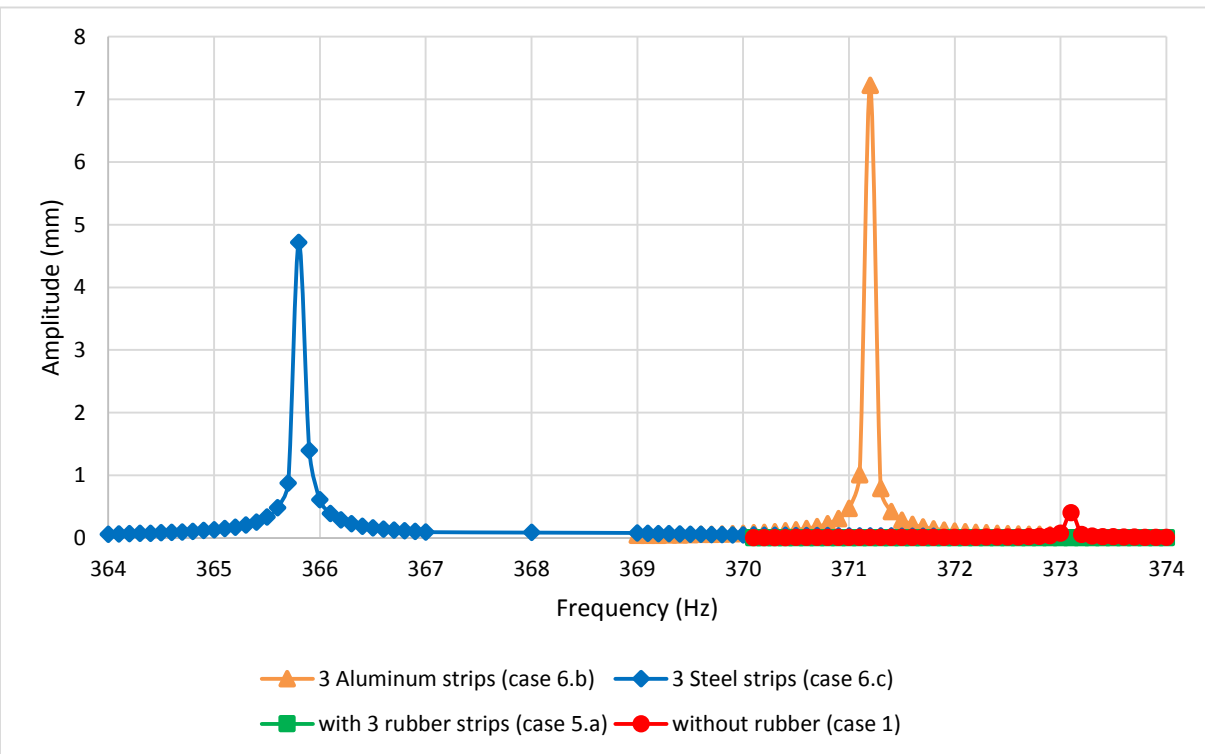


Fig. 4.2.6.4 (c) Amplitudes along Z-Direction at 4th mode for case 6.

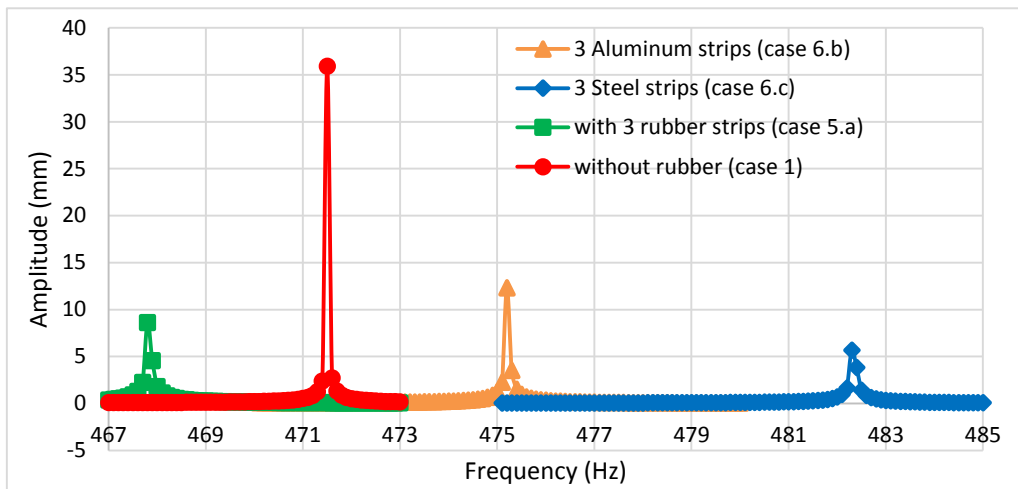


Fig. 4.2.6.5 (a) Amplitudes along X-Direction at 5th mode for case 6.

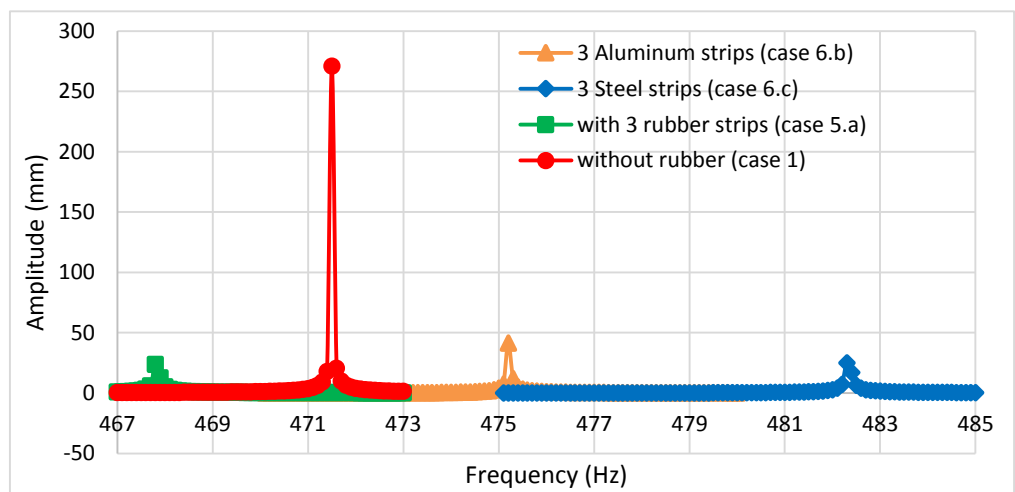


Fig. 4.2.6.5 (b) Amplitudes along Y-Direction at 5th mode for case 6.

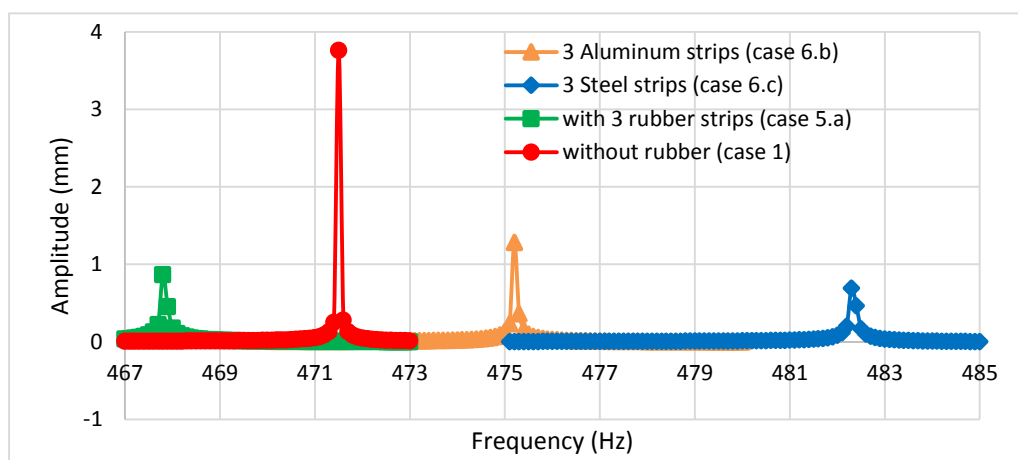


Fig. 4.2.6.5 (c) Amplitudes along Z-Direction at 5th mode for case 6.

4.3. Static Structure Analysis:

The static structure analysis give us different stresses and strains developed in the bucket. From the popular engineering procedure we know that the calculation of Von-mises stress is an important one to understand the strength of any device. So, we have measured the Von-mises stress and total deformation accordingly of the bucket (case 1) and bucket with attachments (case 2 to case 6). Then the change in the stresses is discussed at each section. To understand the changes in the buckets' Von-misses stress and total deformation, a table is also made and compared accordingly.

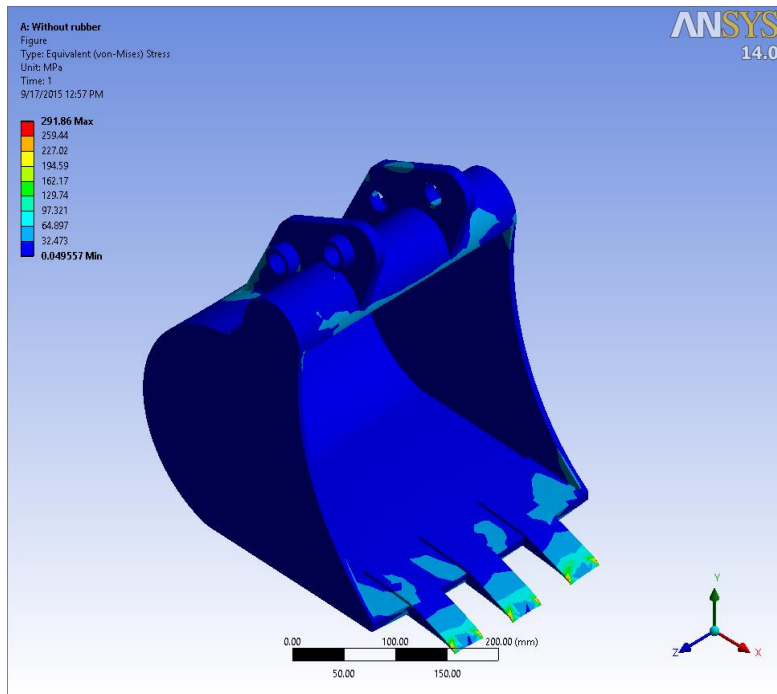
The boundary conditions for stress analysis are, fixed support at A and B of Fig. 3.4. The input load from the cylinder on C is 11380 N is parallel to the direction of Y and the reaction force from the soil/rock is static 2542 N distributed on the edges of three teeth (Fig. 3.4).

4.3.1. Von Mises Stress and Total Deformation for Case 1

The Von-mises stress developed at case 1 are mostly near the teeth (Fig. 4.3.1 (a)) and near fixed support and total deformation is mostly seen at the tip of the middle tooth (Fig. 4.3.1 (b)). The Yield Strength of Hardox 400 alloy steel is 1000 MPa which is way higher than the Von-Mises stress developed in the bucket because of the input load (11380 N) and reaction load (2542 N) which suggest the bucket will endure these loads under the boundary conditions.

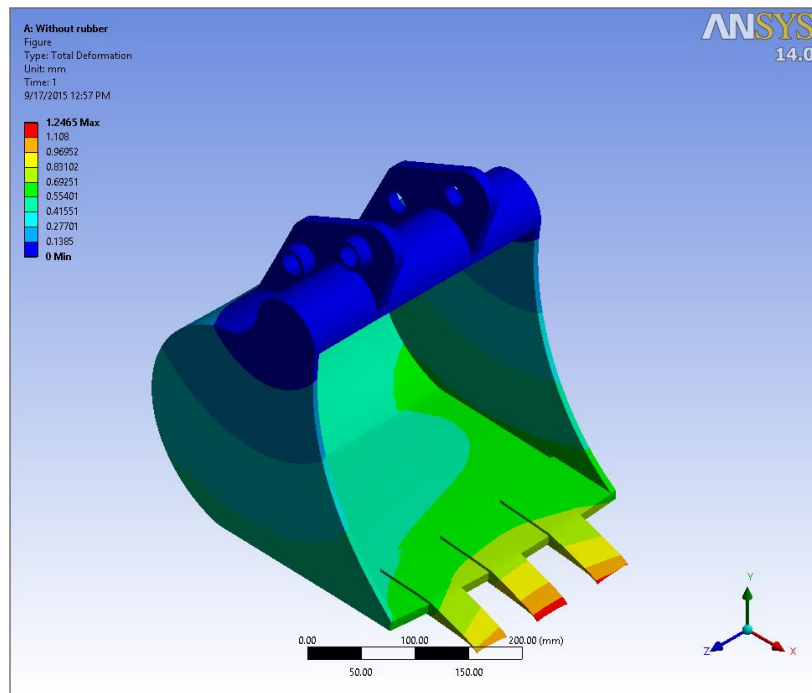
Table 4.3.1. Von-mises stress and Total Deformation at case 1.

	Calculated Von-Mises Stress (MPa)	Yield Strength of HARDOX 400 (MPa)	Calculated Total Deformation (mm)
a. Bare Bucket (case 1)	291	1000	1.2465



(a)

Fig. 4.3.1 (a) Von-mises stress for the bare bucket at case 1.



(b)

Fig. 4.3.1 (b) total deformation for the bare bucket at case 1.

4.3.2. Von Mises Stress and Total Deformation for Case 2

The Von-mises stress developed for all the attachments (Fig. 4.3.2.1) are slightly more than the von-mises stress of the actual bucket (case 1) which is negligible being maximum value 6.8%. Similarly the total deformation for all the modifications are almost similar to the deformation observed in the bucket without rubber at case 1 (Fig. 4.3.2.2). So these attachments will not reduce bucket's strength.

Table 4.3.2. Von-mises stress and Total Deformation comparison at case 2.

	Calculated Von-Mises Stress (MPa)	Calculated Total Deformation (mm)
a. Bucket (case 1)	291	1.2465
b. Bucket with whole side rubber sheets (case 2.a)	311.98	1.2593
c. Bucket with 1 whole rubber sheet at the back (case 2.b)	291.85	1.2504

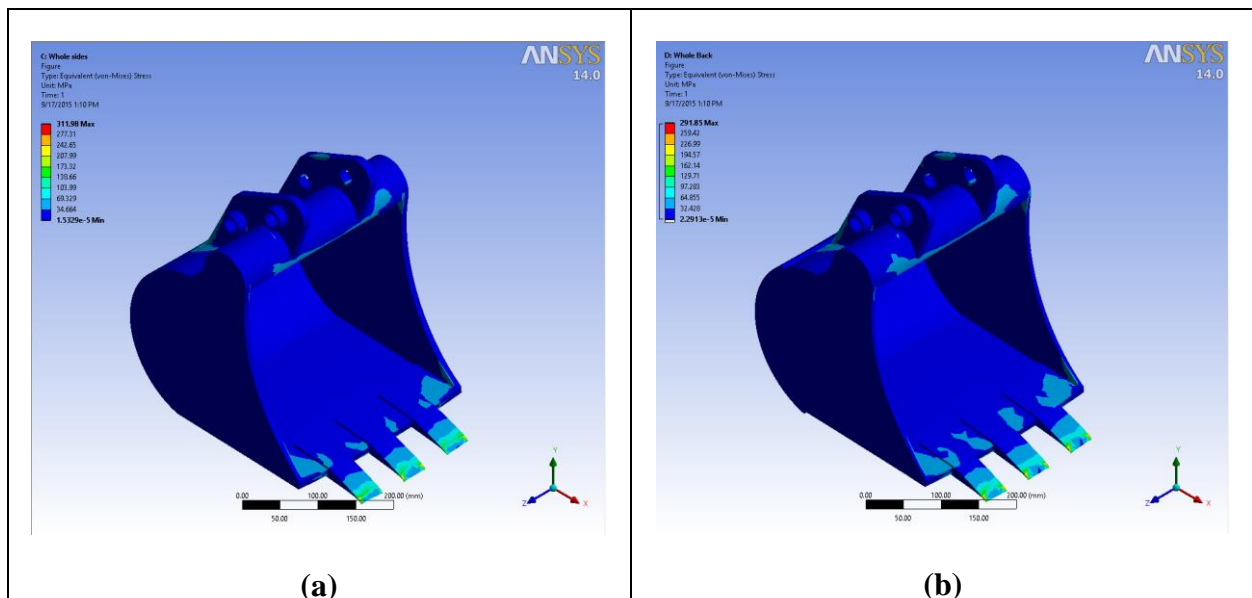


Fig. 4.3.2.1. Von-mises stress for case 2.

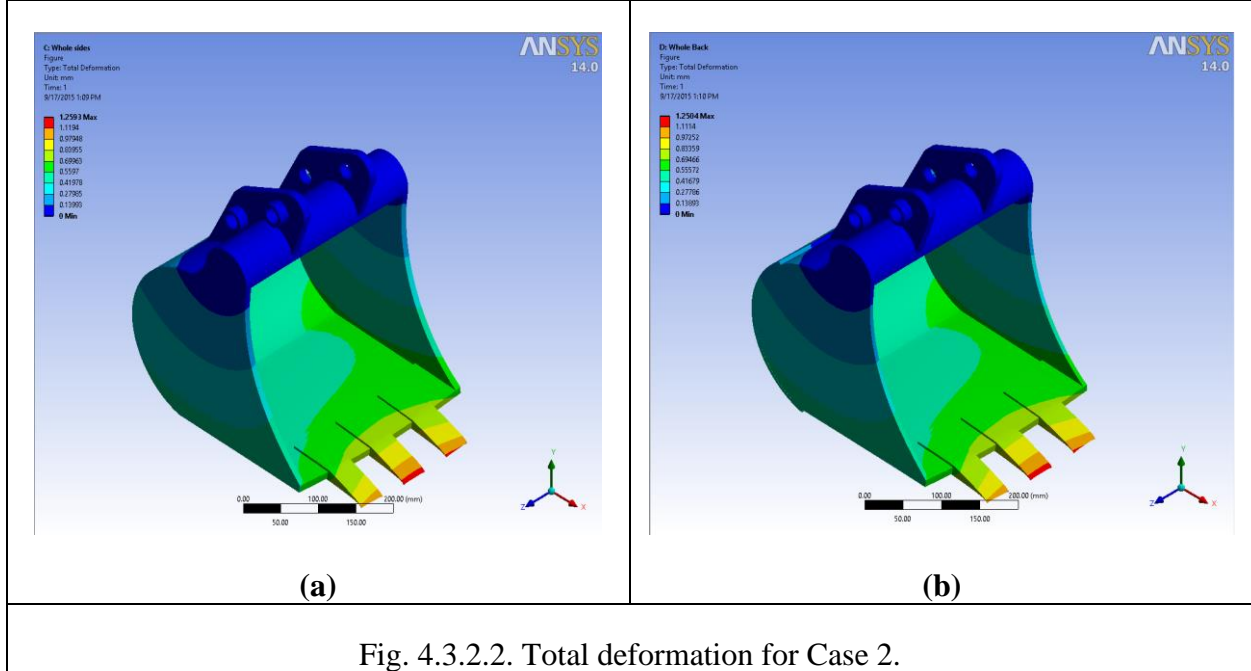


Fig. 4.3.2.2. Total deformation for Case 2.

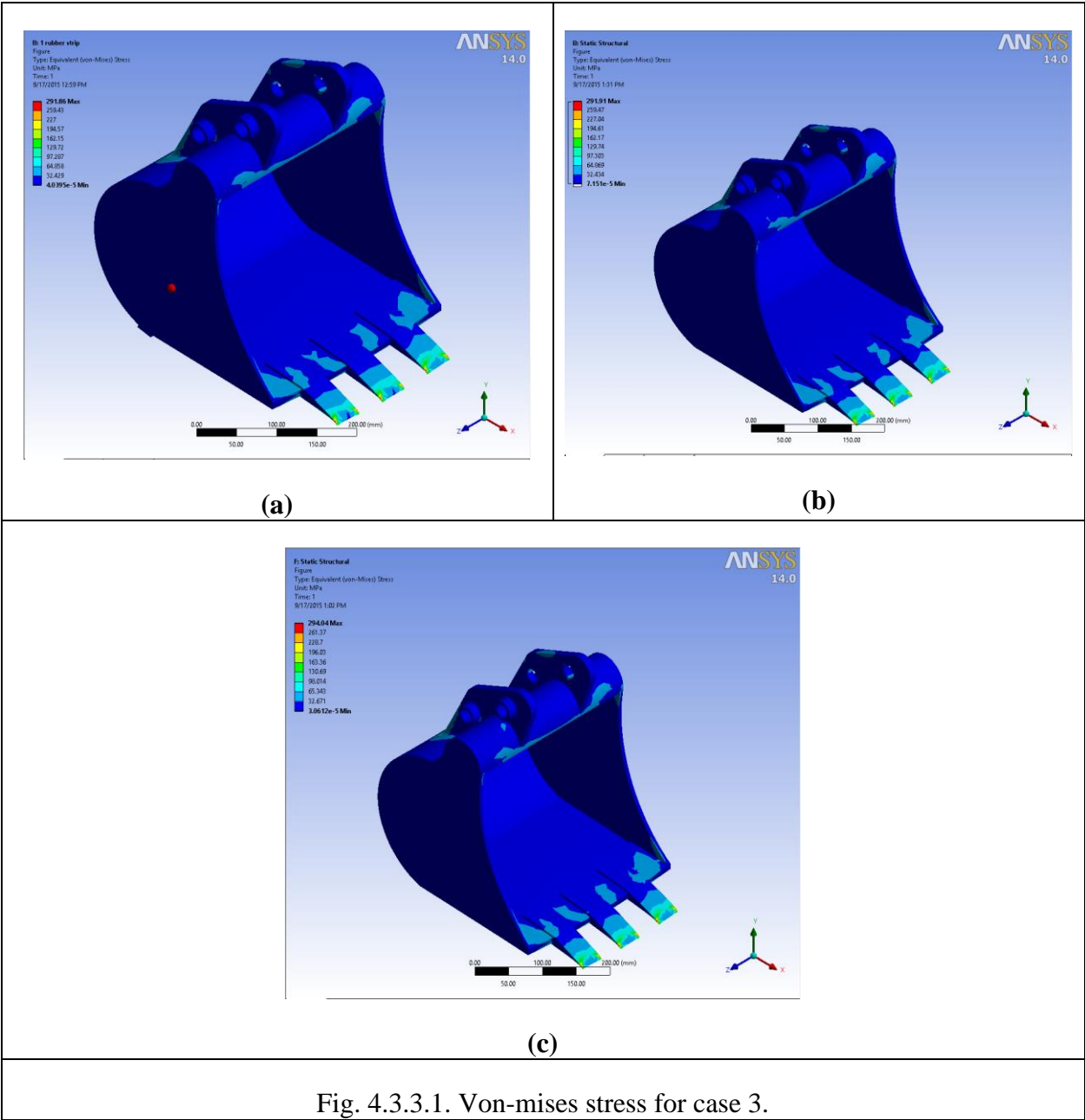
4.3.3. Von-mises stress and Total Deformation for Case 3

The Von-mises stress developed for all the attachments of rubber strips (Fig. 4.3.3.1.) are slightly more than the von-mises stress of the actual bucket which is negligible being maximum value 1%. Similarly the total deformation (Fig. 4.3.3.2) for all the attachments are almost similar to the deformation observed in the bucket without rubber case 1.

Table 4.3.3. Von-mises stress and Total Deformation comparison at case 3.

	Calculated Von-Mises Stress (MPa)	Calculated Total Deformation (mm)
a. Bucket (case 1)	291	1.2465
b. Bucket with 1 rubber strip (case 3.a)	291.86	1.2465

<p>c. Bucket with 1 round rubber (case 3.b)</p>	<p>291.91</p>	<p>1.2499</p>
<p>d. Bucket with 1 back rubber strip (case 3.c)</p>	<p>294.04</p>	<p>1.2473</p>



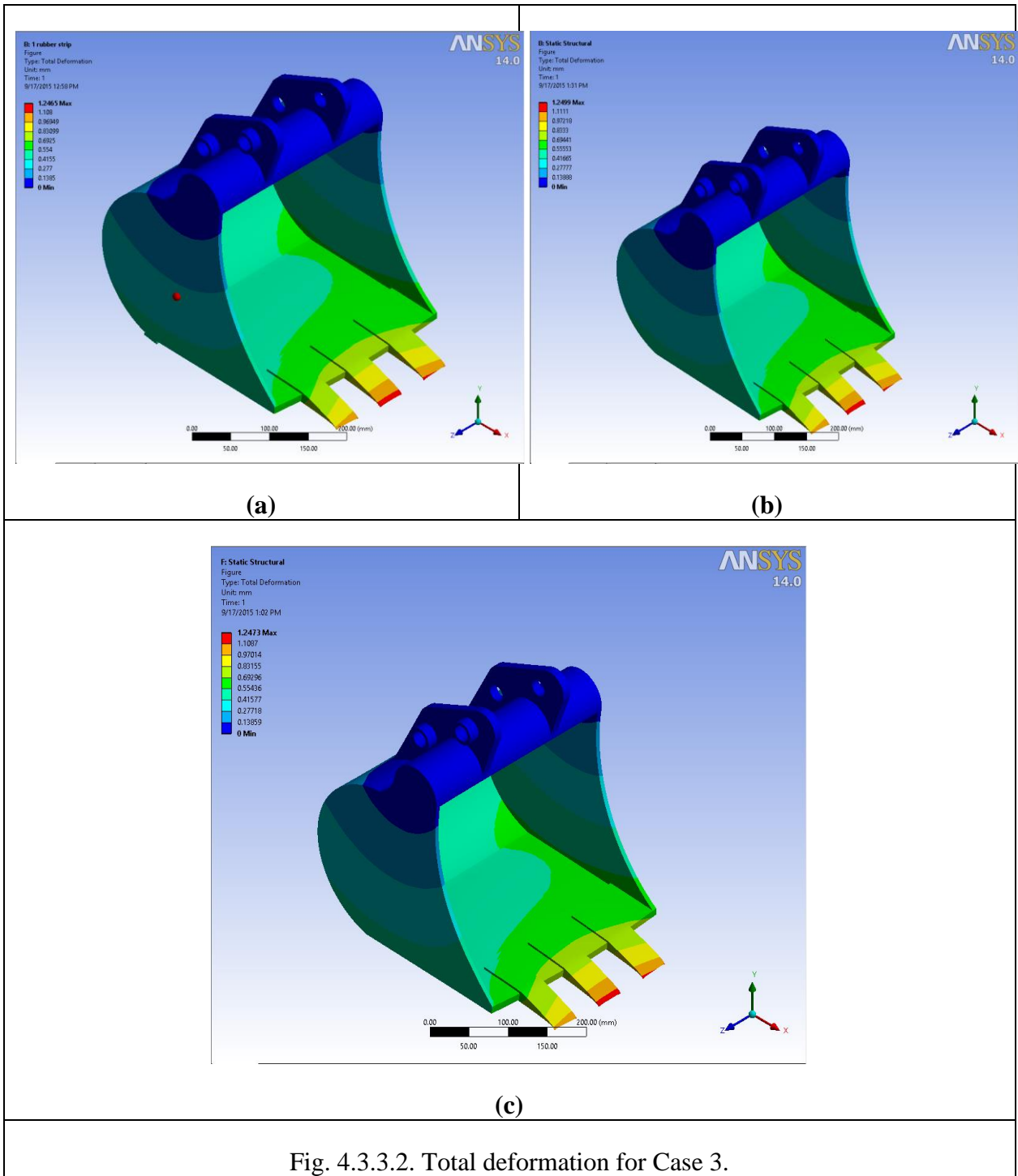


Fig. 4.3.3.2. Total deformation for Case 3.

4.3.4. Von-mises stress and Total Deformation for Case 4

The Von-mises stress developed for all the rubber attachment (Fig. 4.3.4.1.) are slightly more than the von-mises stress of the actual bucket which is negligible being maximum value 4.5%. Similarly the total deformation (Fig. 4.3.4.2.) for all the attachments are almost similar to the deformation observed in the bucket without rubber case 1.

Table 4.3.4. Von-mises stress and Total Deformation comparison at case 4.

	Calculated Von-Mises Stress (MPa)	Calculated Total Deformation (mm)
a. Bucket (case 1)	291	1.2465
b. Bucket with 3 rubber strips (case 4.a)	294.01	1.251
c. Bucket with 4 rubber (case 4.b)	291.91	1.2523
d. Bucket with 2 bottom rubber strips (case 4.c)	304.74	1.248
e. Bucket with 2 side rubber strips (case 4.d)	291.86	1.2502

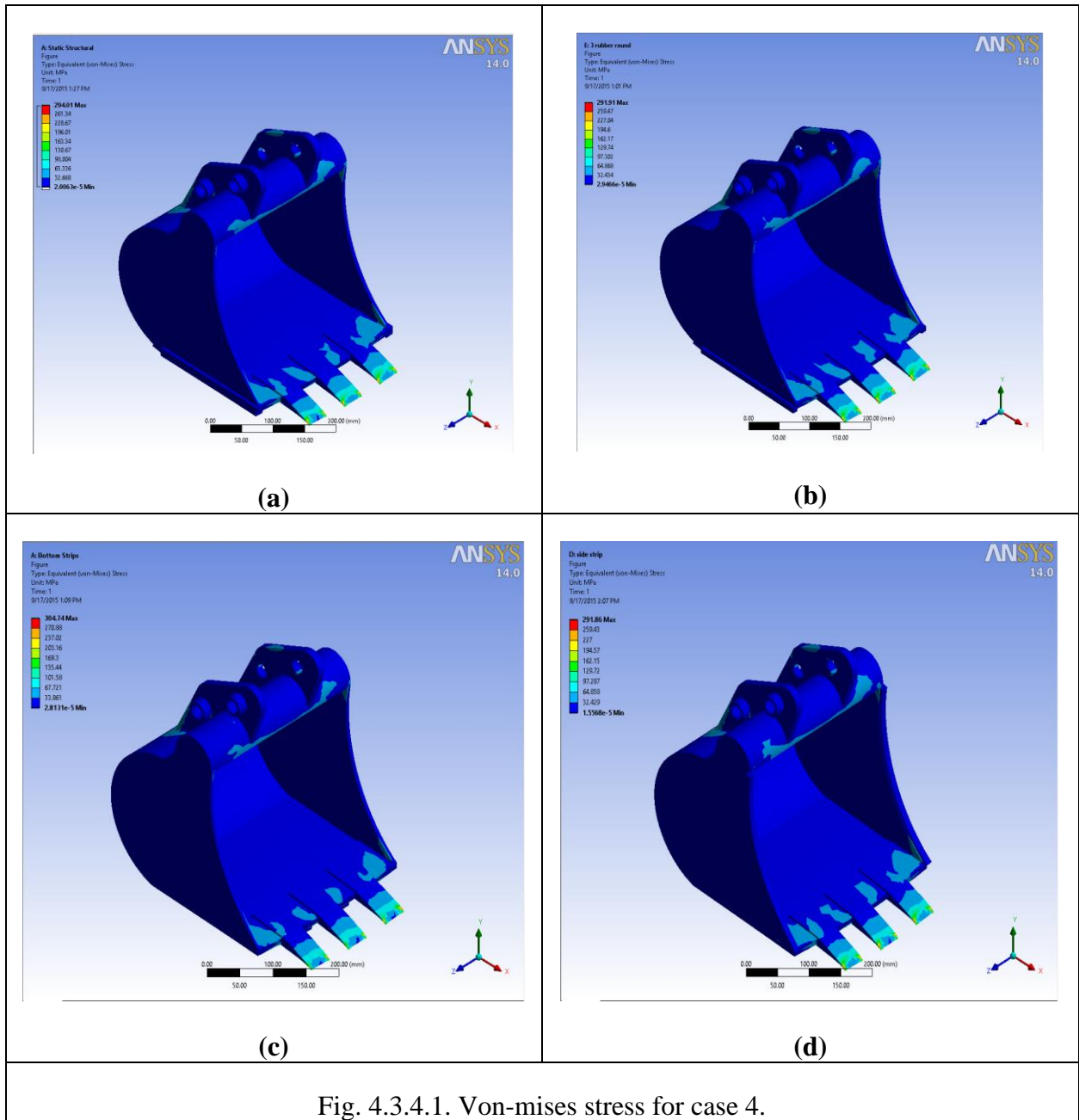


Fig. 4.3.4.1. Von-mises stress for case 4.

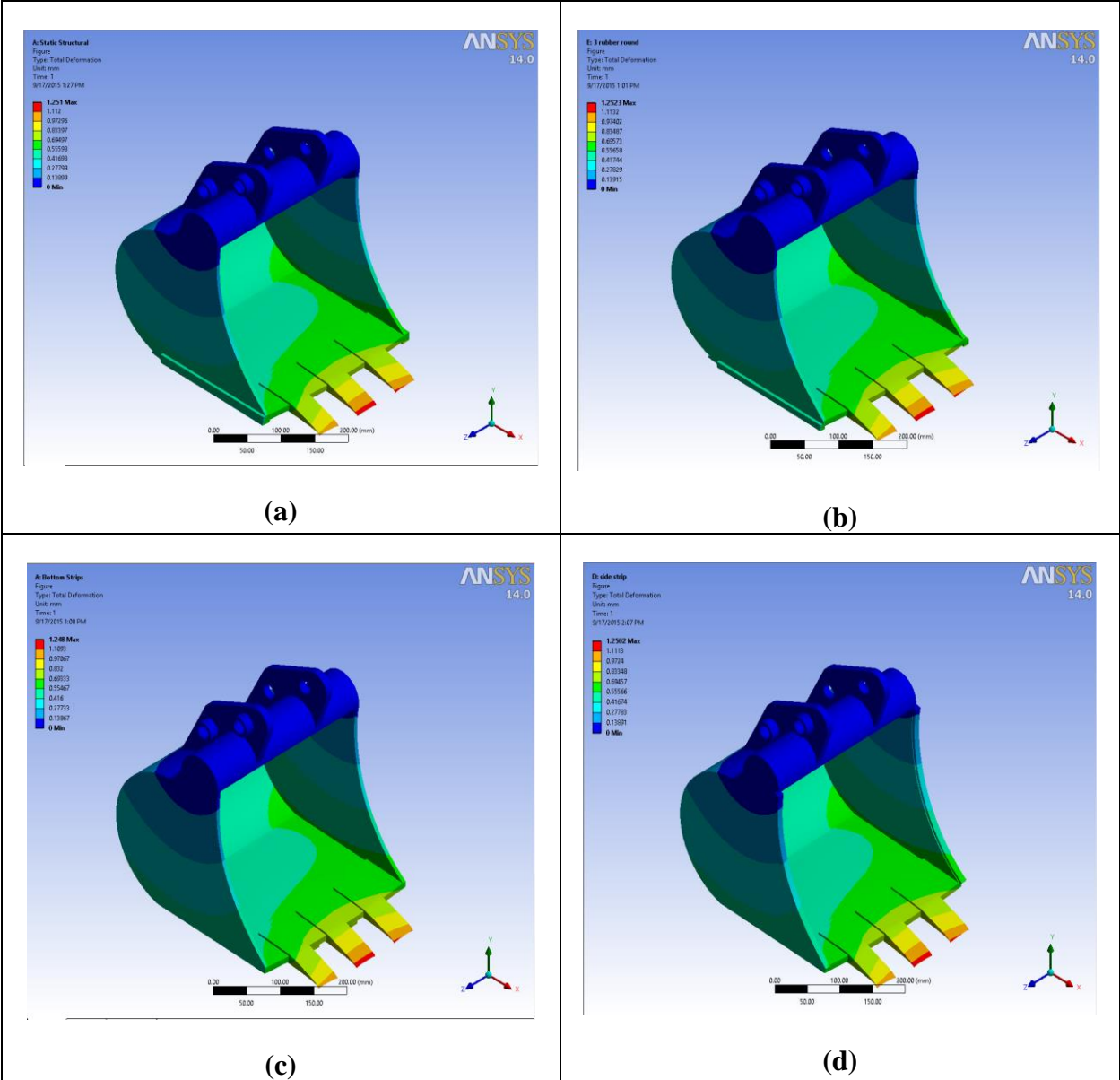


Fig. 4.3.4.2. Total deformation for Case 4.

4.3.5. Von-mises stress and Total Deformation for Case 5

At the case 5 the Von-mises stress developed for all the attachments (Fig. 4.3.5.1.) are slightly more than the von-mises stress of the actual bucket which is negligible being maximum value 1%. Similarly the total deformation for all the attachments (Fig. 4.3.5.2.) are similar to the total deformation observed in the bucket without rubber case 1.

Table 4.3.5. Von-mises stress and Total Deformation comparison at case 5.

	Calculated Von-Mises Stress (MPa)	Calculated Total Deformation (mm)
a. Bucket	291	1.2465
b. Bucket with 3 rubber strips (case 5.a)	294.01	1.251
c. Bucket with 3 rubber strips half thickness (case 5.b)	291.89	1.2525
d. Bucket with 3 rubber strips Double thickness (case 5.c)	291.85	1.2453

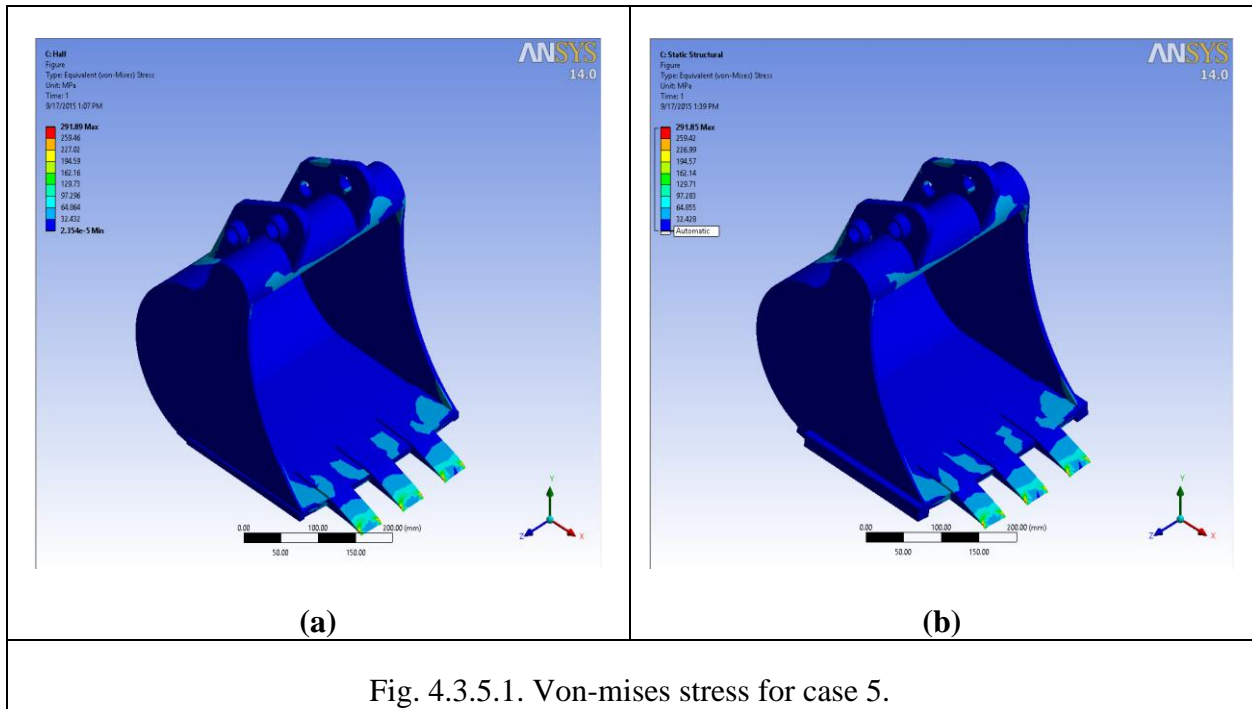


Fig. 4.3.5.1. Von-mises stress for case 5.

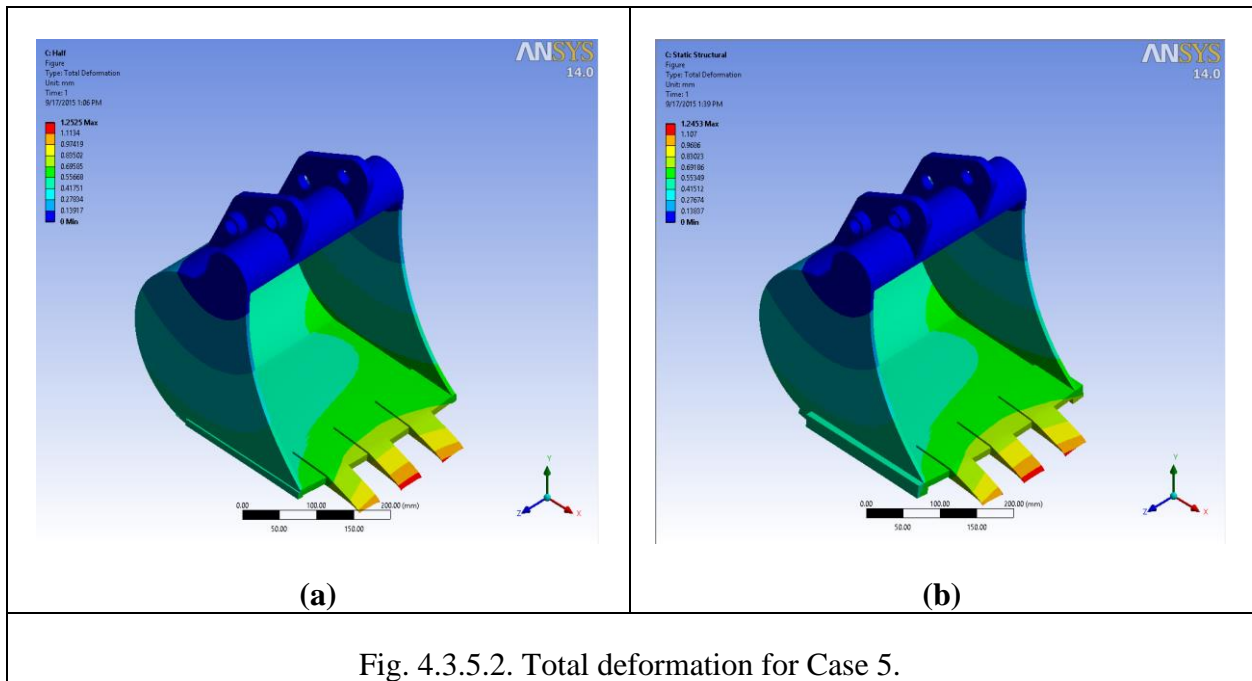


Fig. 4.3.5.2. Total deformation for Case 5.

4.3.6. Von-mises stress and Total Deformation for Case 6

The case 6 shows that the Von-mises stress developed for all the attachments (Fig. 4.3.6.1.) are slightly more than the von-mises stress of the actual bucket which is negligible being maximum value 1%. Similarly the total deformation for all the attachments (Fig. 4.3.6.2.) are very less than the deformation observed in the bucket without rubber.

Table 4.3.6. Von-mises stress and Total Deformation comparison at case 6.

	Calculated Von-Mises Stress (MPa)	Calculated Total Deformation (mm)
a. Bucket (case 1)	291	1.2465
b. Bucket with 3 rubber strips (case 6.a)	294.01	1.251
c. Bucket with 3 aluminum strips (case 6.b)	294.01	1.2299
d. Bucket with 3 steel strips (case 6.c)	294.01	1.2068

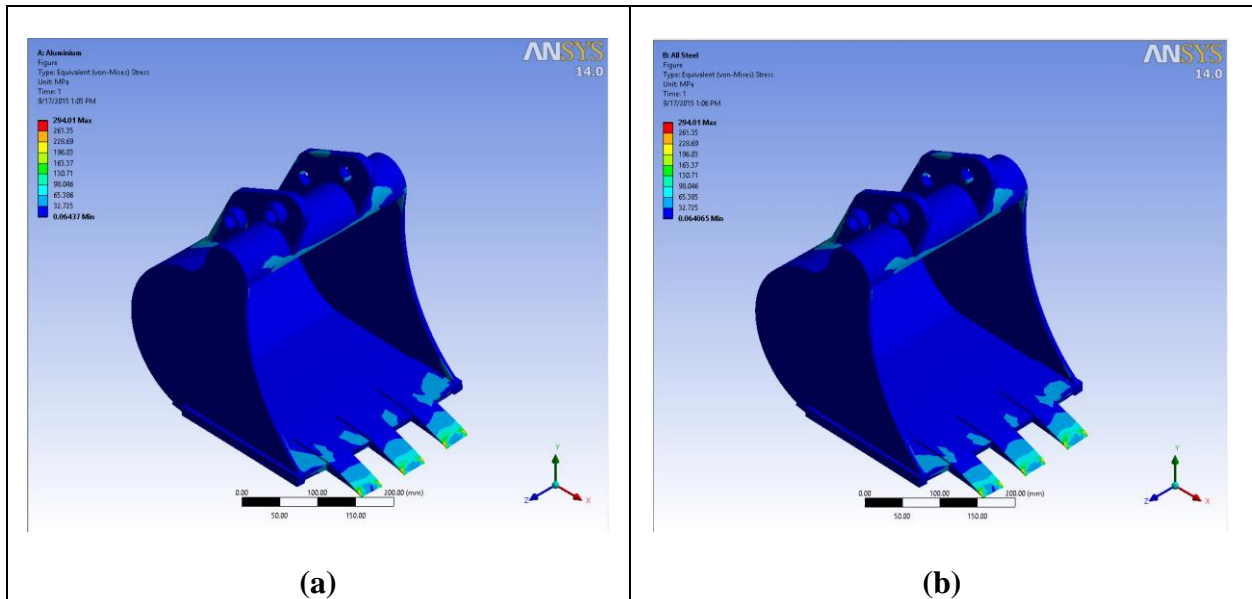


Fig. 4.3.6.1. Von-mises stress for case 6.

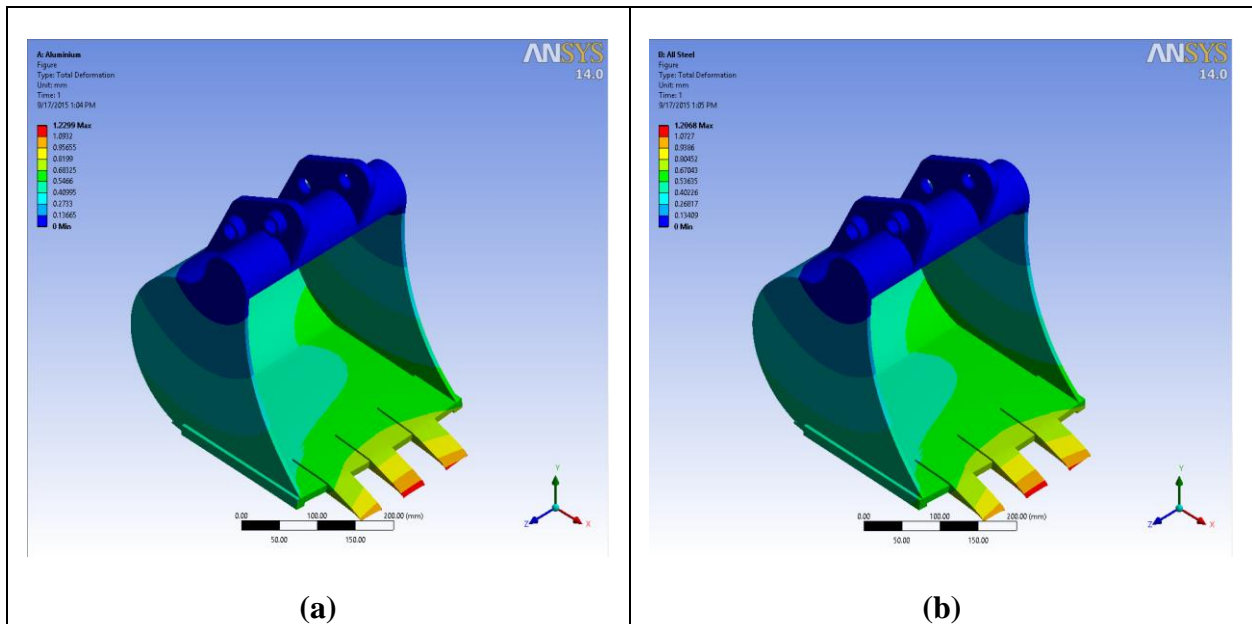


Fig. 4.3.6.2. Total deformation for Case 6.

Chapter 5

Experimental Results and Validation

5.1. Introduction

The thesis includes detailed analysis of different techniques of using rubber materials and other metals with excavator bucket to study its modified behavior in vibration and stress. That includes a lot of experiment to be done which in practice takes a lot of time to perform and not economical. That is why Chapter 3 is introduced where a lot of simulations have been performed to study the bucket's modified behavior from different angles. However the numerical simulation performed by ANSYS Software is validated in this chapter with experimentation. For the purpose of experiment a model is manufactured and both modal and harmonic analysis is performed on it. Similar model is developed in SOLIDWORKS Software and analysis is performed on it in ANSYS Software and these results are compared with experimental results.

5.2. Experimental Set-up

5.2.1. Bucket Model

A model excavator bucket is made in the workshop using 2.5 mm thickness sheet metal and using different cutting tools, welding and rolling etc. A fixture is also made and fixed with a rigid structure using royal bolt.

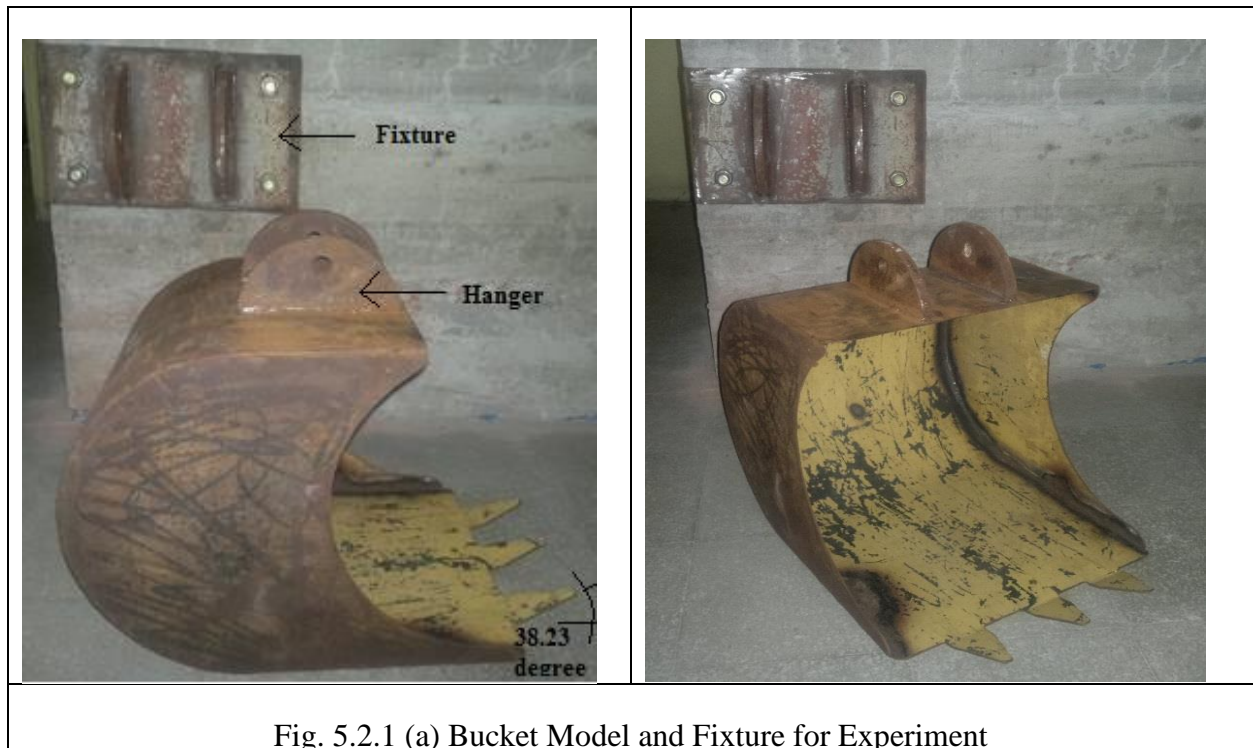


Fig. 5.2.1 (a) Bucket Model and Fixture for Experiment

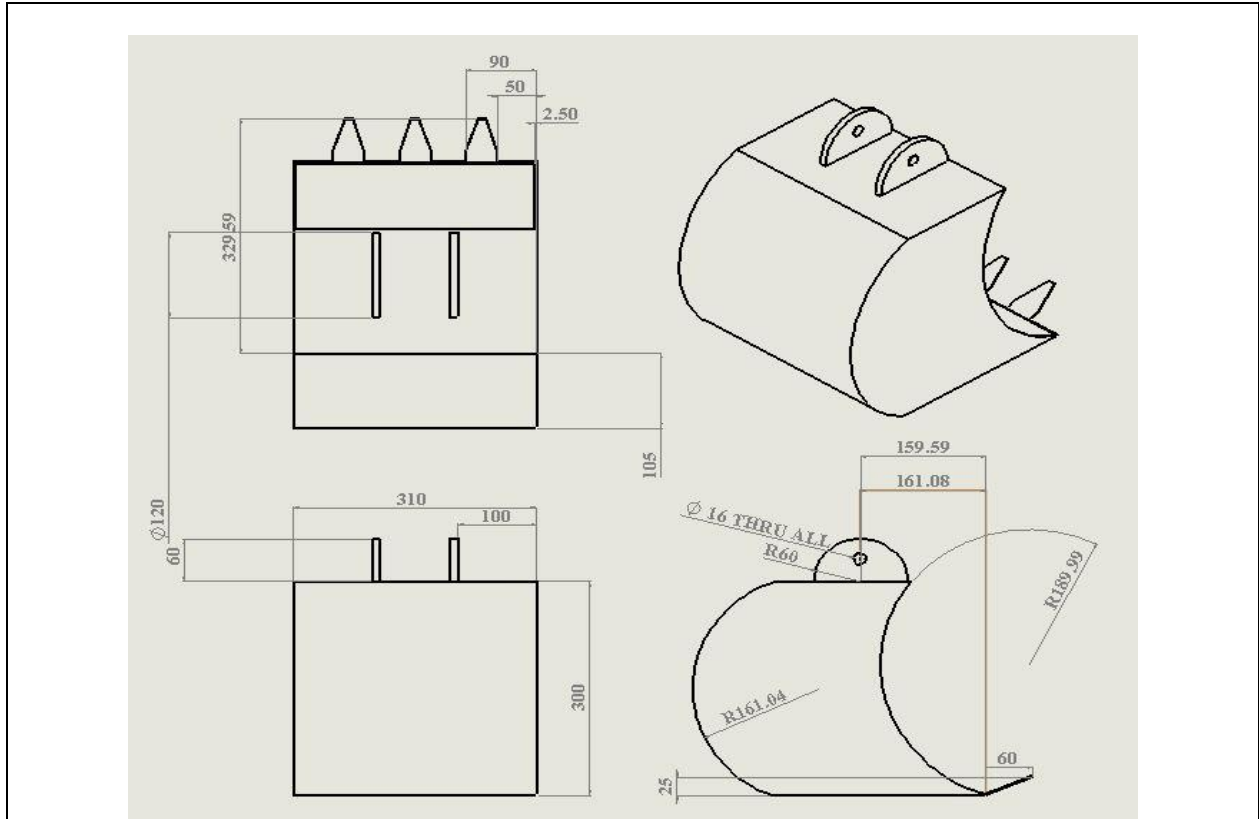


Fig. 5.2.1 (b) Experimental Bucket model specifications.

5.2.2. SmartShaker K2007E01

This electrodynamic exciter is a small, portable permanent magnet shaker with a new generation of ultra compact precision power amplifier integrated in its base. The revolutionary SmartShaker™ eliminates the need for a separate, cumbersome power amplifier - just plug the excitation signal from a dynamic signal analyzer or function generator directly into the BNC on the base of the shaker. SmartShaker provides up to 7 pounds (31 N) pk sine force during testing. The unit is supplied with a DC power supply but can be run directly from any 12-21 VDC supply.



Fig. 5.2.2. Shaker K2007E01

5.2.3. ICP® Force Sensor Model 208C01

ICP force sensors incorporate a built-in MOSFET microelectronic amplifier. This serves to convert the high impedance charge output into a low impedance voltage signal for analysis or recording. They are powered from a separate constant current source, operate over long ordinary coaxial or ribbon cable without signal degradation. The low impedance voltage signal is not affected by triboelectric cable noise or environmental contamination.



Fig. 5.2.3. Force Sensor

5.2.4. ICP® signal conditioner 485B36

2-channel, USB-powered, ICP® signal conditioner, unity gain

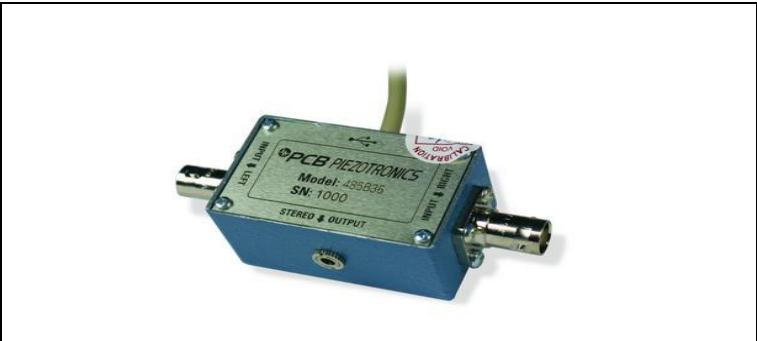




Fig. 5.2.4. Signal Conditioner


5.2.5. Low-noise coaxial cable 003C03

Low-noise coaxial cable, blue TFE jacket, 3-ft, 10-32 coaxial plug to BNC plug	
Fig. 5.2.5. Cable	

5.2.6. Kenwood FG-281 Function Generator

Kenwood FG-281, FG SERIES Function Generators 0.01Hz to 15MHz	
Fig. 5.2.6. Function Generator	

5.2.7. Oscilloscope GDS1000-U Series

The GDS-1000-U provides an excellent balance of performance between memory length and sampling speed. Other major features include user-friendly menu tree operations, compact size, ergonomic design, USB host for PC connectivity and USB device port support.	
Fig. 5.2.7. Oscilloscope	

5.3. Experiment and Simulation Case:

Three of the cases were taken to perform experiment.

- a. Bucket (without rubber).
- b. Bucket with whole rubber sheet at the back.
- c. Bucket with 3 rubber strips.

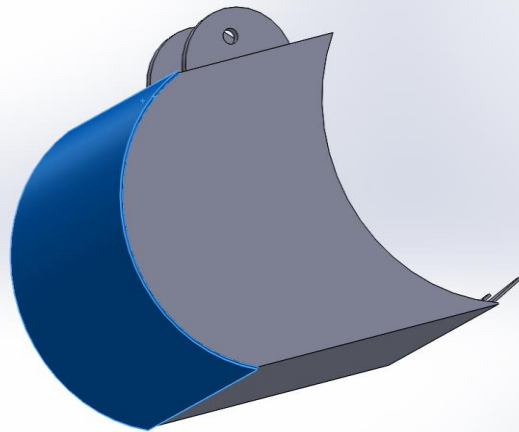
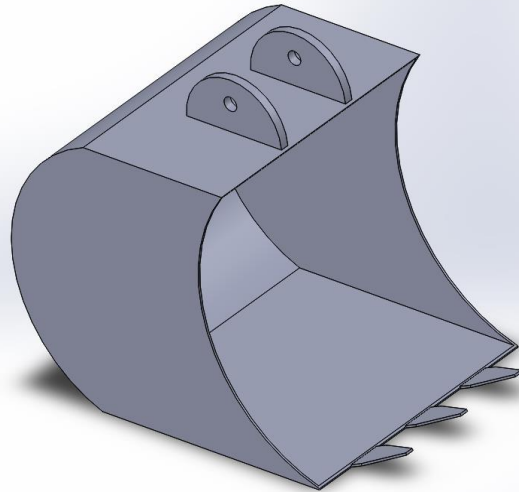




Fig. 5.3. The Cases of Experiment and Simulation.

5.4. Experimental Procedure:

The hanger of the bucket was fixed using a fixture as shown in the Fig. 5.4. The fixing was done with the hanger by using nut bolt. The three teeth are made with certain angle of 38.23 degree with respect to the bottom plate. The shaker was controlled using a signal generator and amplifier with a sinusoidal excitation at a range of frequencies $0-75$ Hz.. The force sensor was used in between the shaker and the teeth to measure the input force from the shaker to the bucket. The force sensor was connected to the oscilloscope through a signal conditioner. Another eddy current sensor was used to measure displacement of vibration at a certain position of the bucket shown in Figure 5.4. The output of the eddy current sensor was captured by the oscilloscope through a signal conditioner. A bucket model of approximately same dimension was taken from the SOLIDWORKS Software and harmonic analysis was performed in the ANSYS Software. In the experiment for convenience the excitation was implied on the middle tooth of the bucket.

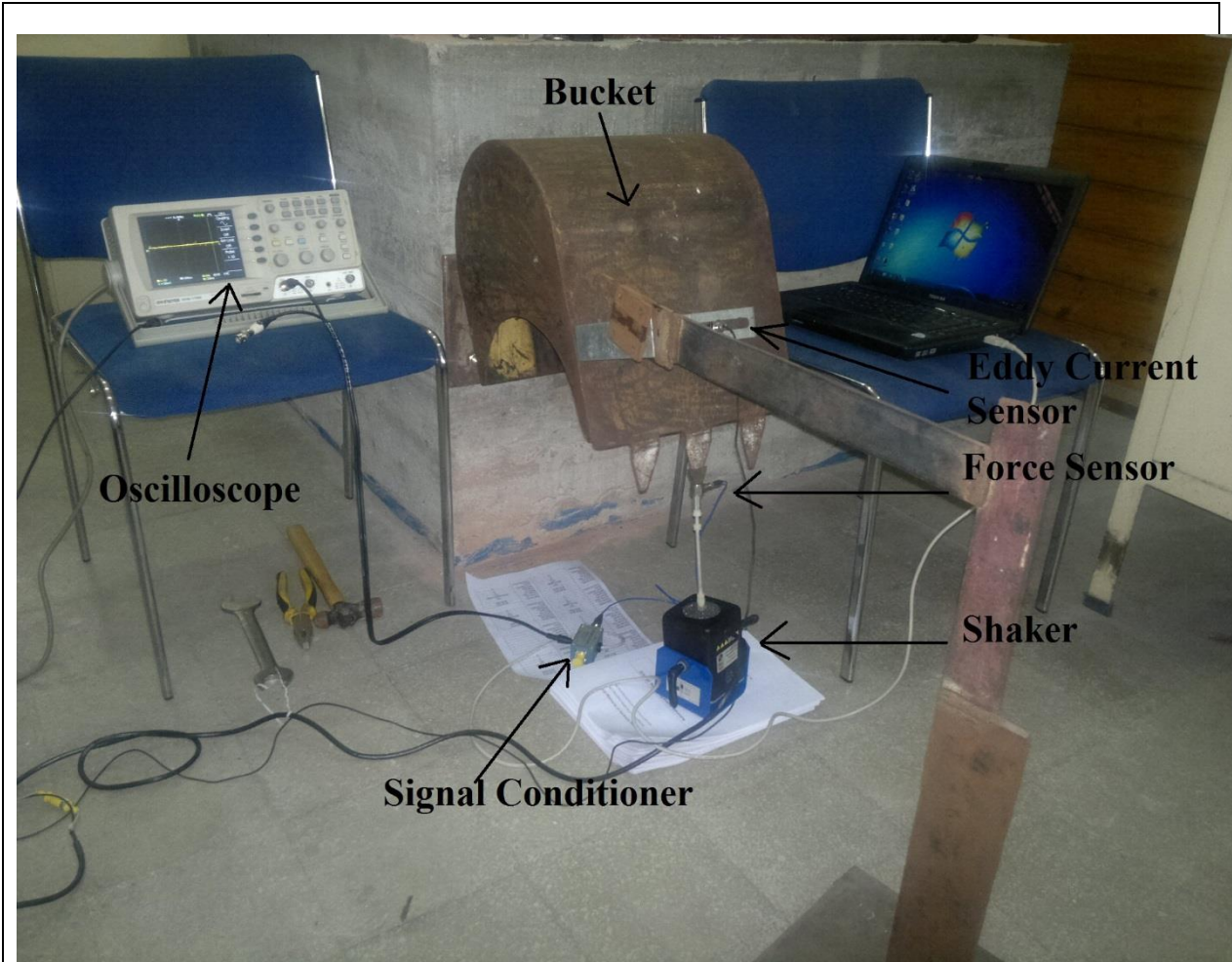


Fig. 5.4. Experimental Arrangement to perform vibration analysis of bucket.

5.5. Experiment and Simulation Results:

In the ANSYS Software fixing the inner surface of the pair of wholes of the hanger, excitation was given on the middle tooth of the bucket similar to the force given in the experiment.

The material properties assumed for the model in ANSYS Software are,

Steel	
Density (ρ)	7850 kg/m ³
Young's modulus of elasticity	170 GPa
Poisson's Ratio	0.35
Rubber	
Density ρ	1500 kg/m ³
Young's modulus of elasticity	8 MPa
Poisson's Ratio	0.41

Results of experiment and simulation are shown in Fig. 5.5.1, Fig. 5.5.2, Fig. 5.5.3 and Fig. 5.5.4 for 2nd and 3rd modes. The experimental results taken are the vibration response along Y-axis and also the simulation results are the amplitude response along Y-axis. Deviation in natural frequencies are observed in the simulation results from the actual experiment. The deviation at the 2nd natural frequency is 6.6 % and at the 3rd natural frequency is 6.5 %. These deviations occur because of the material properties taken for simulation do not perfectly match with the material properties of the experimental model. But the pattern from the frequency response in both experiment and simulation suggest that the simulation is in good agreement with experiment.

The frequency response from the experiment shows that for the 2nd mode Fig. 5.5.1 the vibration amplitude increases when a rubber sheet is attached at the back of the bucket and natural frequency shifts to the left from the natural frequency of the bare bucket. However, if 3 rubber strips are attached at the bottom then vibration amplitude reduces at the 2nd mode. A similar pattern in the frequency response is observed for the numerical simulation of the similar experimental model. From the analysis of the model in the 2nd mode Fig. 5.5.2, it is observed similar frequency response pattern as in the experiment. The use of 3 rubber strips at the bottom reduces the vibration

amplitude of the bucket in the 2nd mode whereas the sheet rubber at the back increases the vibration amplitude from the bare bucket amplitude.

For the 3rd mode (Fig. 5.5.3), the experiment showed that vibration amplitude increases for both cases of attaching a rubber sheet at the back and attaching 3 rubber strips at the bottom and both the natural frequencies shift to the left from the natural frequency of the bare bucket. And similarly for the 3rd mode of Simulation Fig. 5.5.4 both techniques of rubber used in the bucket increase the vibration amplitudes and natural frequencies shift to the left than that of the bare bucket.

The results found from the experiment can be explained from the mode shapes of the bucket shown in the Fig. 4.1.1. (b) and Fig. 4.1.1 (c). The amplitude reduction occurs when three rubber strips were attached at the 2nd mode because the rubber works as a damper at this mode. From the Fig. 4.1.1 (b) we see vibration occurs mostly in X and Y directions. At these directions 3 rubber strips dampen the vibration amplitude being near to the most deformation zone developed at the bottom plate and teeth. Use of whole rubber sheet at the back of the bucket does not reduce vibration amplitude because the rubber is attached away than the bottom plate and also it makes the back plate stiffer than the bottom plate, which is why an increase in vibration amplitude is observed here. In the 3rd mode Fig. 4.1.1 (c) it is seen that three teeth are more exposed to vibration because of force applied. The highest deformation zone at this 3rd mode is the three teeth. Both attachments are far away from the highest deformation zone, that is why for this mode vibration is not damped and amplitude increases.

Limitations:

Local steel material was used to manufacture the bucket and local rubber material was used for experimentation, which is why the material properties used in the numerical simulation does not match perfectly with the actual case of the experiment. Matching damping coefficient with the experiment in the simulation is very difficult. In addition the damping coefficient is also frequency dependent, so some deviation of the amplitude in the simulation results from the experimental results was observed.

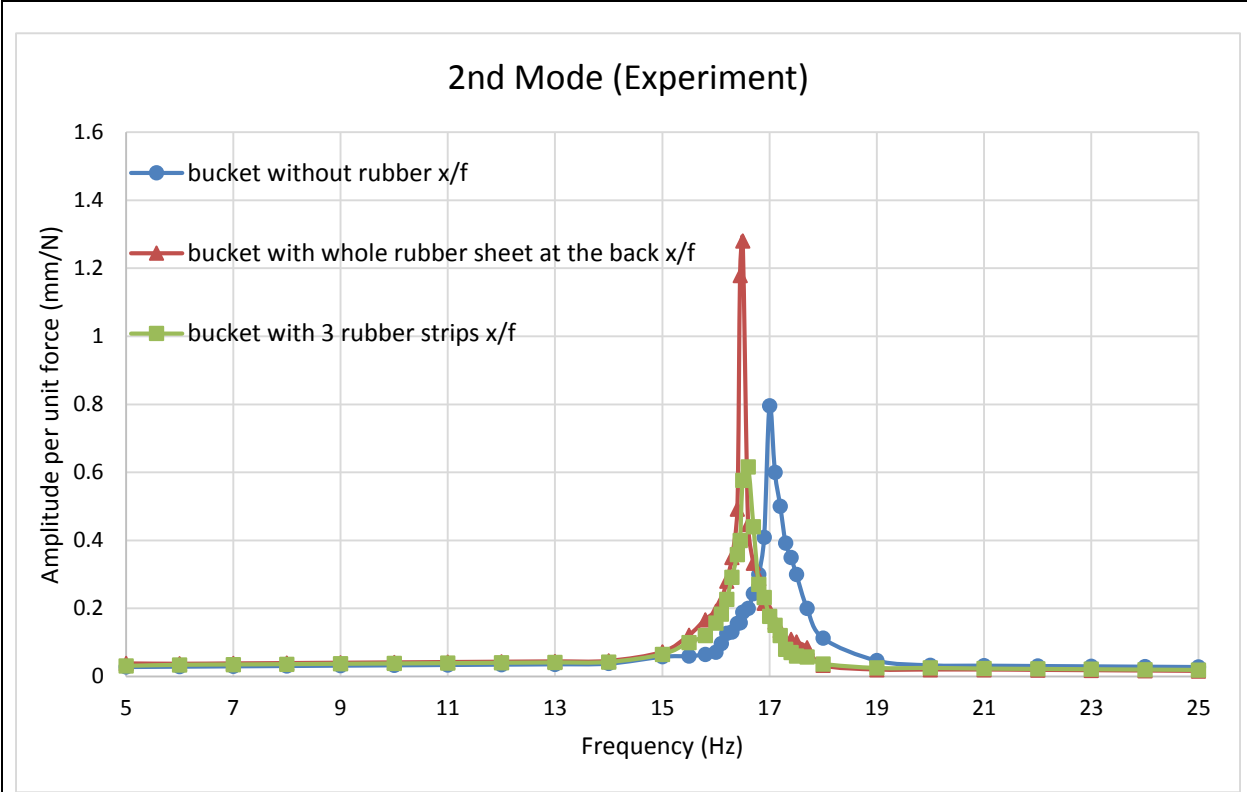


Fig. 5.5.1. Experimental Results Comparison at 2nd mode.

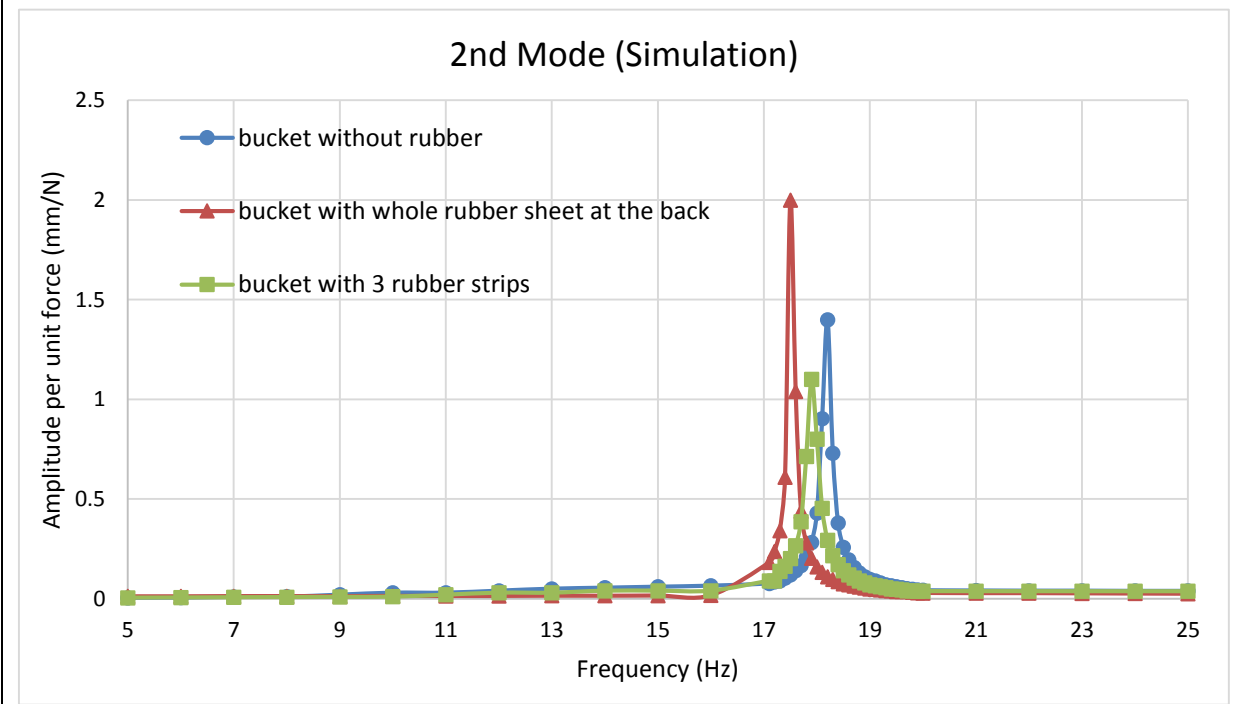


Fig. 5.5.2. Simulation Results Comparison at 2nd mode.

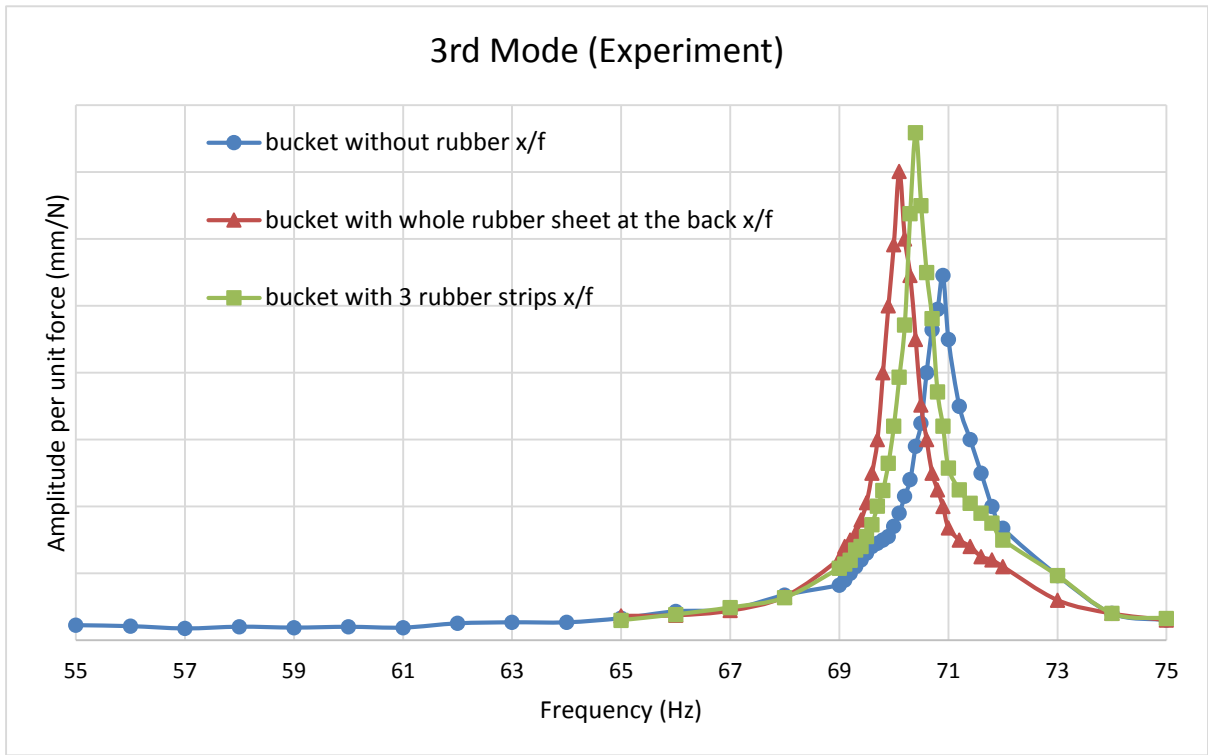


Fig. 5.5.3. Experimental Results Comparison at 3rd mode.

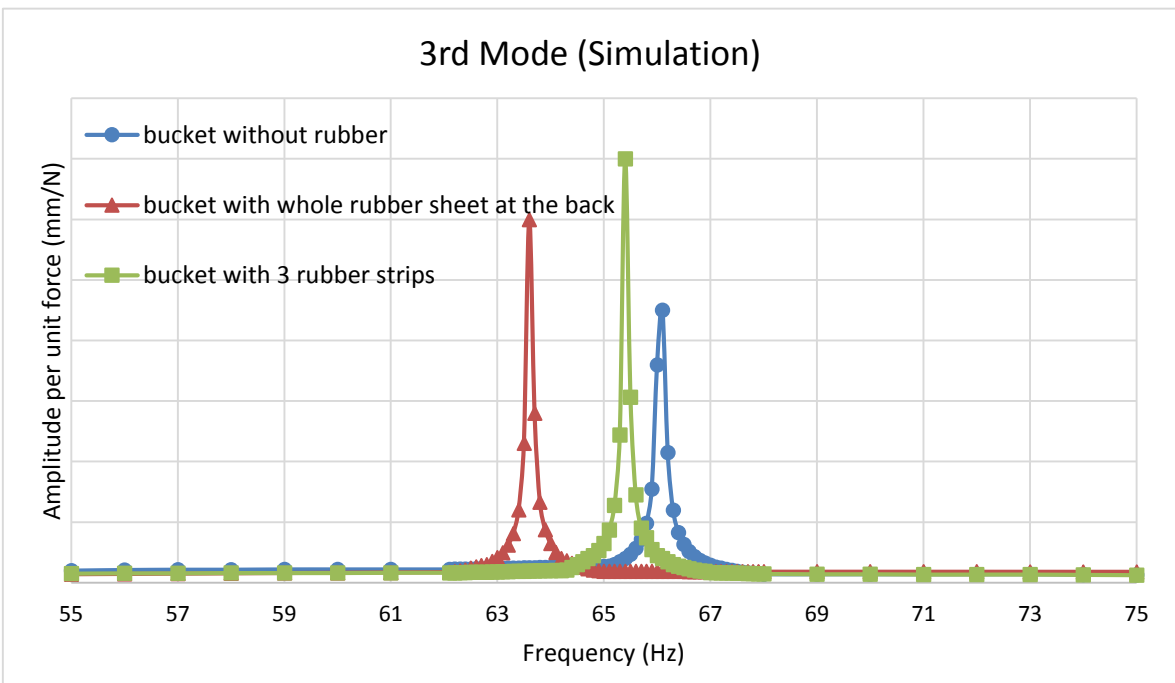


Fig. 5.5.4. Simulation Results Comparison at 3rd mode.

Chapter 6

Conclusion and Recommendation

6.1. Conclusion

- The modal analysis represents the mode shapes and change in natural frequencies of the bucket. These mode shapes can show us the vulnerable places of vibration amplitude in the bucket. Then the modal analysis is performed on the bucket with different techniques of using rubber sheets or strips. The results found from the bucket with rubber are compared with case 1 and discussed the change in natural frequencies with change in mode shapes obtained. Then the thickness of rubber is considered to perform analysis and found different thickness is an important factor to change the mode shapes and natural frequencies. Lastly the materials of the attachments also changed and for that the change in mode shape and natural frequencies in the bucket observed and discussed.
- The harmonic analysis for different cases can be used to modify a bucket for certain operating natural frequencies. The techniques of using different sized rubber with the bucket is analysed and the results were compared with case 1 amplitudes. Though it is the operating natural frequencies that decides which techniques should be used to reduce vibration amplitudes of bucket but from the results of our analysis we can say the use of 4 rubber and 3 rubber strips with the bucket reduce vibration for most natural frequencies and preferred over other techniques. Thickness of the reinforced rubber can be an important aspect in reducing vibration amplitudes which is found and discussed in case 5. Material properties of reinforced materials should also be considered as it has important effect on the reduction of amplitudes discussed in case 6.
- The von-mises stress are found for employing different techniques and found that the use of techniques do not change the overall stress developed in the bucket which is why we can say these techniques are safe to use and will not damage the bucket under usual loads.

6.2. Recommendation

- Mode shapes of the bucket should be analysed to understand the buckets behaviour for certain operating conditions.
- Natural frequency should be checked when a modification is made to adjust with the operating frequency.
- Harmonic analysis can be done to reduce vibration for certain operating condition of the bucket.
- For all the modifications the stress analysis is important to know which will tell us if the bucket is prone to damage.

REFERENCE

- [1] Mehta Gaurav K, “Design and Development of an Excavator Attachment” M. tech Dissertation Thesis, Nirma University, Institute of Technology, Ahmedabad, May 2008, pp. 1.
- [2] Bhaveshkumar P. Patel, Dr. J. M. Prajapati, “Soil-Tool Interaction as a Review for Digging Operation of Mini Hydraulic Excavator”, International Journal of Engineering Science and Technology, Vol. 3 No. 2, February 2011, 894-901.
- [3] Bhargav J Gadhvi, B. P. Patel and P. M. Patel, “Development of a Controller for Mini Hydraulic Excavator as a Review”, Proceeding of National Conference on Recent Advances in Manufacturing, SVNIT, Surat, 19th - 21st July, 2010, pp. 198-203.
- [4] Mehmet Yener, “Design of a Computer Interface for Automatic Finite Element Analysis of an Excavator Boom”, M.S. Thesis, The Graduate School of natural and Applied Sciences of Middle East Technical University, May 2005, pp. 1-4, 68-69.
- [5] Ju-Ho Kwak, Byung-Joo Kim, Jae-Ohk Lee, Hyun-Koo Cho, ‘A study on the determination of design load for excavator attachments from field measurement’. 15th International Conference on Experimental Mechanics.
- [6] Nareshkumar N. Oza, “Finite Element Analysis and Optimization of an Earthmoving Equipment Attachment – Backhoe”, M. tech Dissertation Thesis, Nirma University, Institute of Technology, Ahmedabad, May 2006, pp. 31-68.
- [7] MA Bromfield and WT Evans, “Computer modelling of microexcavator”, Computer Aided Design, Butterworth & Co (Publishers) Ltd., Vol. 20, No. 9, November 1988, pp. 549-554.
- [8] Ram Vadhe and Vrajesh Dave, “ Multi-Body Simulation of Earthmoving Equipment using Motionview/Motionsolve”, Driving Innovations with Enterprise Simulation, L & T e-engineering Solutions, 1993, pp. 1-5.
- [9] Tadeusz Smolnicki, Damian Derlukiewicz, and Mariusz Stańco, “Evaluation of load distribution in the superstructure rotation joint of single-bucket caterpillar excavators”, Automation in Construction, Elsevier, 2008, pp. 218-223.

- [10] Luigi Solazzi, "Design of aluminium boom and arm for an excavator", *Journal of Terramechanics*, Elsevier, Vol. 47, 2010, pp. 201–207.
- [11] J. Mottl, "Excavator optimization using the voting method", *Computer Methods in Applied Mechanics and Engineering*, No. 98, North-Holland, 1992, pp. 227-250.
- [12] Yefei Li, Xianghong Xu and Qinying Qiu, "FEM-Based Structure Optimization with Grid-Enabled Analysis Environment", *Proceedings of the 6th World Congress on Intelligent Control and Automation*, IEEE, Dalian, China June 21 - 23, 2006, pp. 6915-6919.
- [13] Bipin N. Patel, "Finite Element Analysis and Optimization of Arm and Boom of Excavator", M. Tech. Thesis, Institute of Technology, Nirma University of Science and Technology, Ahmedabad, May 2007, pp. 40-72.
- [14] Jakub Gottvald (2012), "Analysis of Vibrations of Bucket Wheel Excavator Schrs1320 During Mining Process", *FME Transactions*, Vol. 40, pp. 165-170.
- [15] Jakub Gottvald (2011), "Measuring and Comparison of Natural Frequencies of Bucket Wheel Excavators Sch Rs. 1320 and K 2000", ISBN: 978-1-61804-022-0.
- [16] Bhaveshkumar P. PATEL, Jagdish M. PRAJAPATI, "structural optimization of mini hydraulic backhoe excavator attachment using FEA approach", *machine design*, Vol.5(2013) No.1, ISSN 1821-1259 pp. 43-56
- [17] Anil Jadhav, Vinayak Kulkarni, Abhijit Kulkarni, Prof. Ravi. K, 'Static, Modal and Kinematic Analysis of Hydraulic Excavator', *International Journal of Engineering Research & Technology (IJERT)* ISSN: 2278-0181, Vol. 3 Issue 5, May – 2014.
- [18] Kuniaki Nakada, Kazuya Imamura, Mitsuo Yabe, 'Research and Development of Low-noise Bucket for Construction Machinery', *Komatsu Technical Report*.
- [19] Bhaveshkumar P Patel and J M Prajapati, "Static analysis of mini hydraulic backhoe excavator attachment using FEA approach", *International Journal of Mechanical Engineering and RoboticS Research*, ISSN: 2278-0149, Vol 1, No. 3, October, 2012.

[20] Bhaveshkumar P Patel and Prajapati J M, “Evaluation of Bucket Capacity, Digging Force Calculations and Static Force Analysis of Mini Hydraulic Backhoe Excavator”, Machine Design—The Journal of Faculty of Technical Sciences, Vol. 4, No. 1, pp. 59-66, 2012.

[21] Ihsan Küçükrendeci, “Comparison of damping characteristics of polymer-stell and polymer-al composite structure”, Scientific Research and Essays, ISSN 1992-2248, Vol. 6(23), pp. 4870-4884, 16 October, 2011.

[22] Wikipedia the free encyclopedia.

APPENDIX A

Validation of the simulation for Static Structure Analysis

A.1. Results from Published Paper [16]

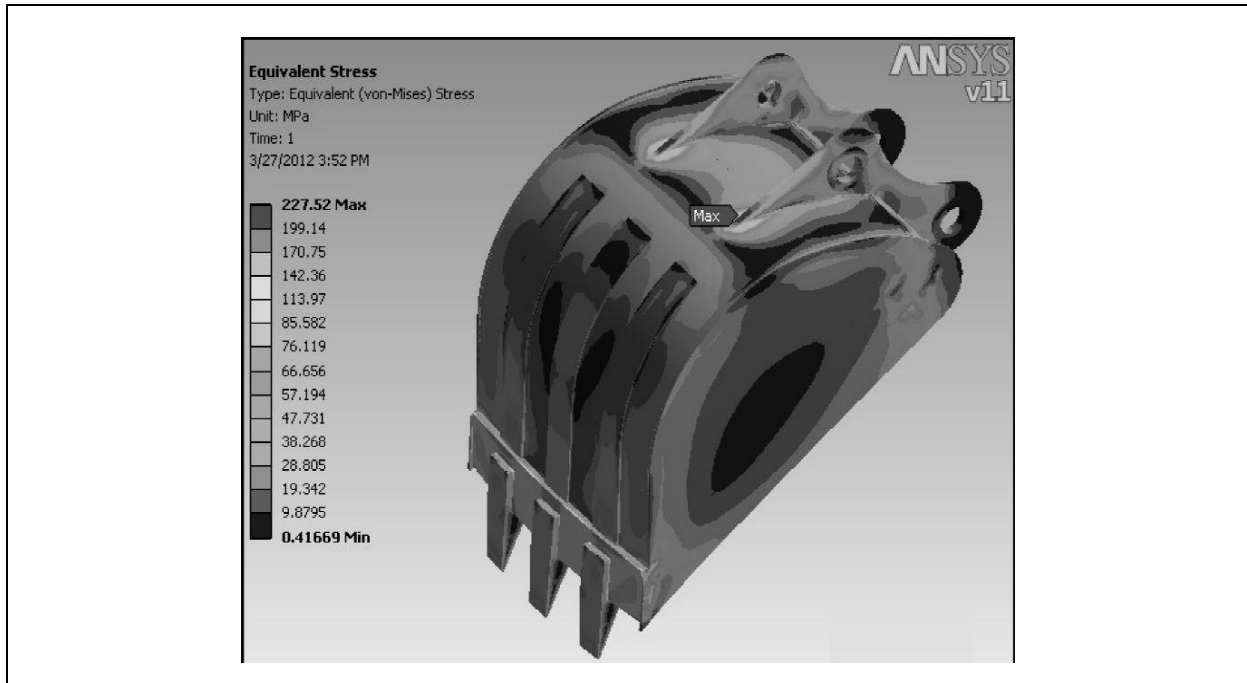


Fig A.1.1 Von Mises stress developed in the bucket. [16]

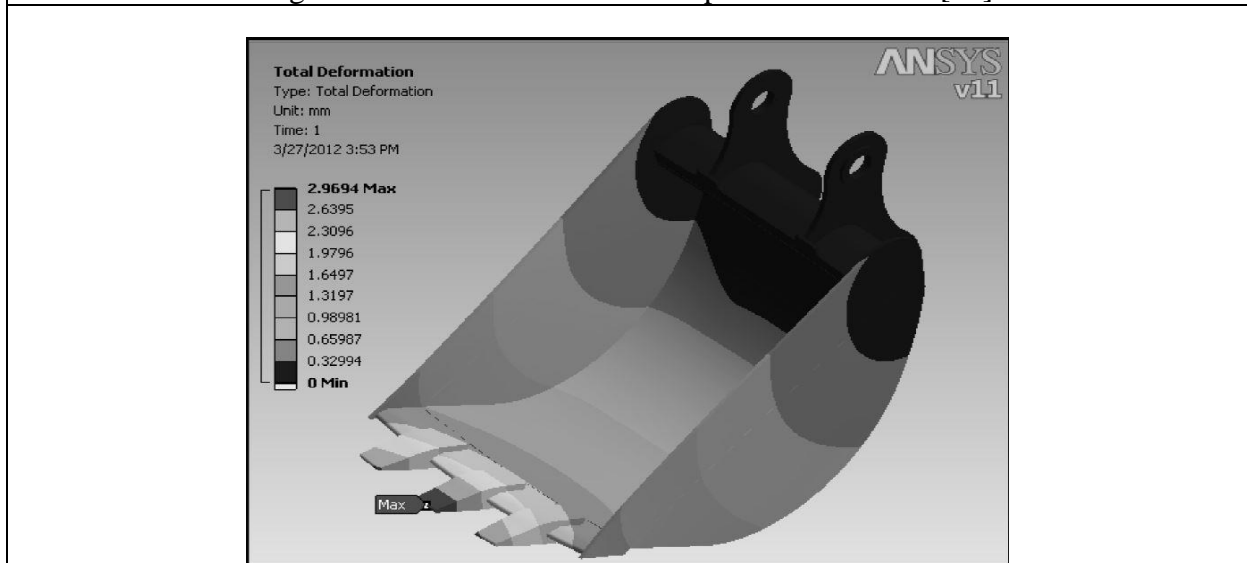


Fig A.1.2. Total deformation developed in the bucket. [16]

A.2. Results from FEA of this thesis:

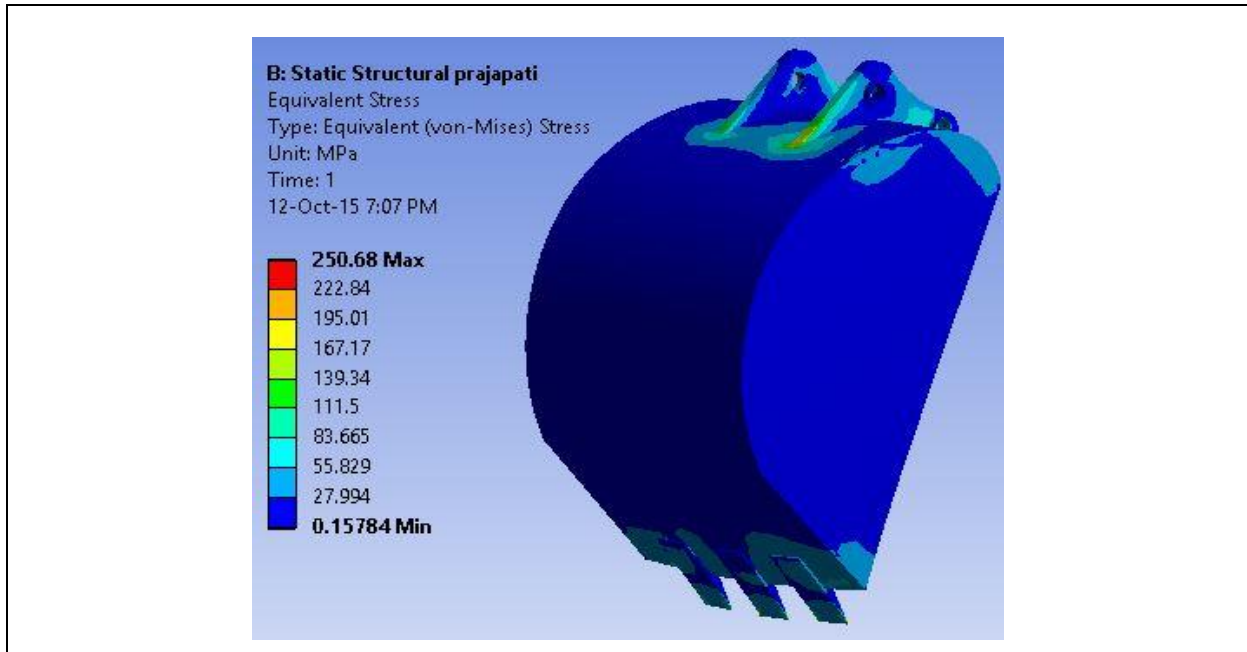


Fig A.2.1. Von Mises stress developed in the bucket.

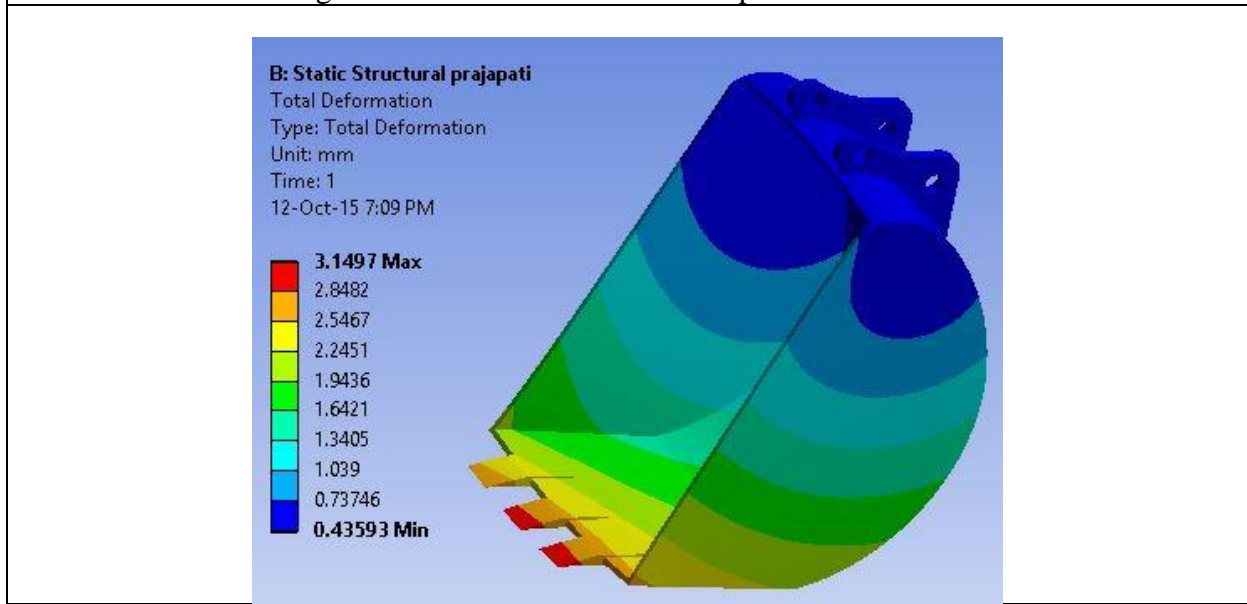


Fig A.2.2. Total deformation developed in the bucket.

The boundary conditions, forces and material properties are same for the A1 and A2. However slight changes in the results observed as the dimensions are not exactly identical.

APPENDIX B

Mode Shapes of Case 3

4.1.3.1. 1st mode Shapes

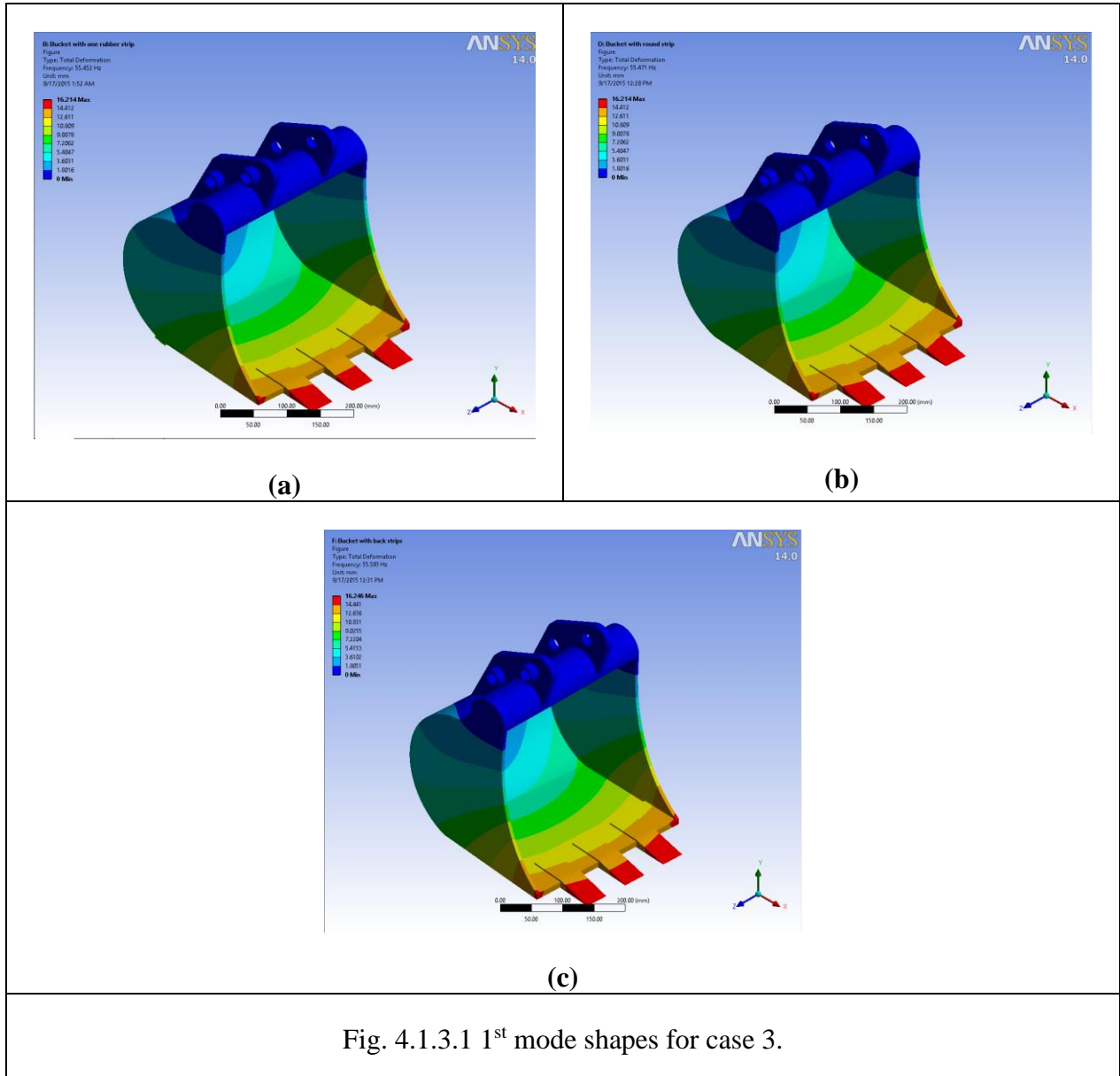
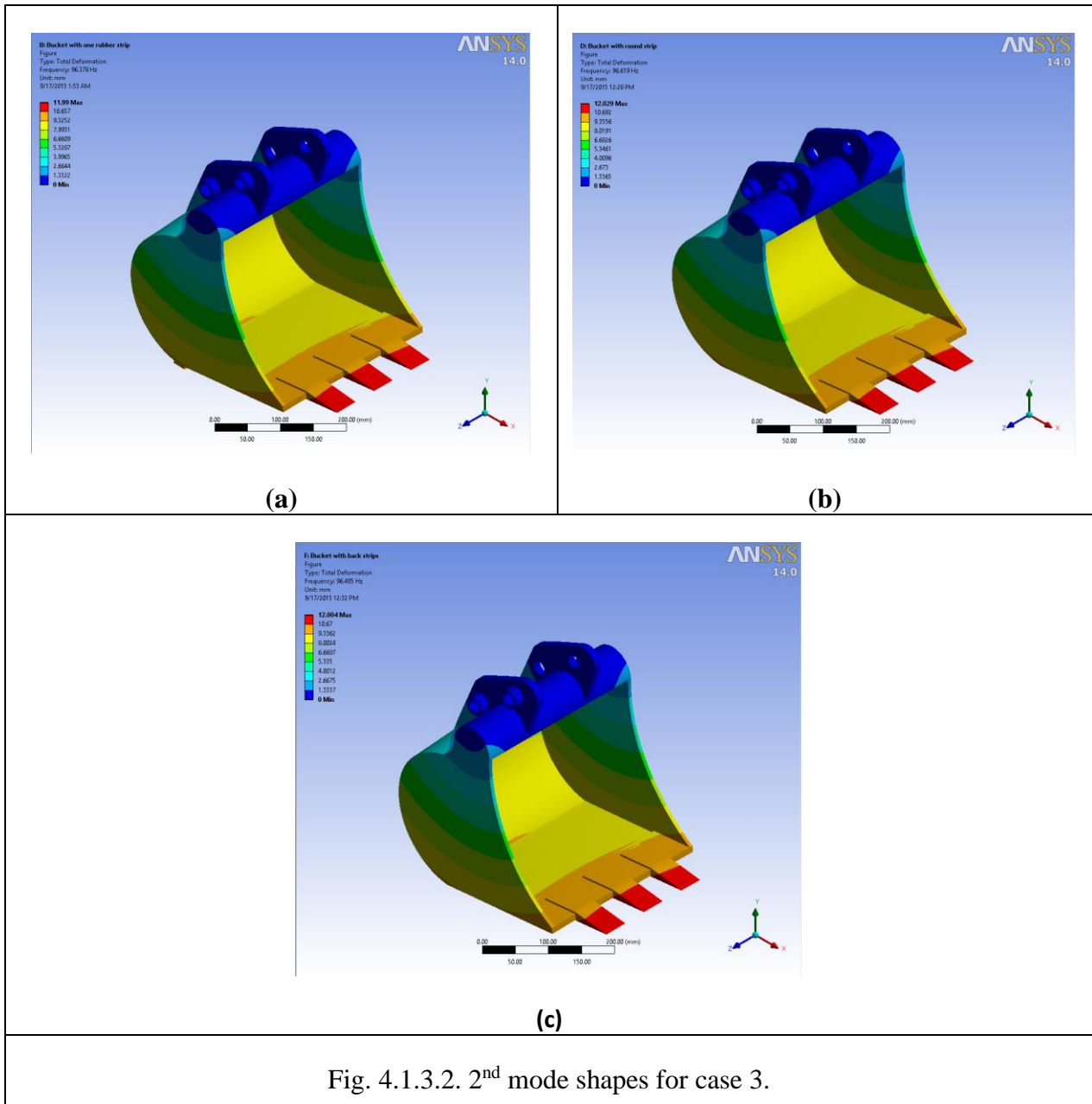


Fig. 4.1.3.1 1st mode shapes for case 3.

4.1.3.2. 2nd Mode Shapes



4.1.3.3. 3rd Mode Shapes

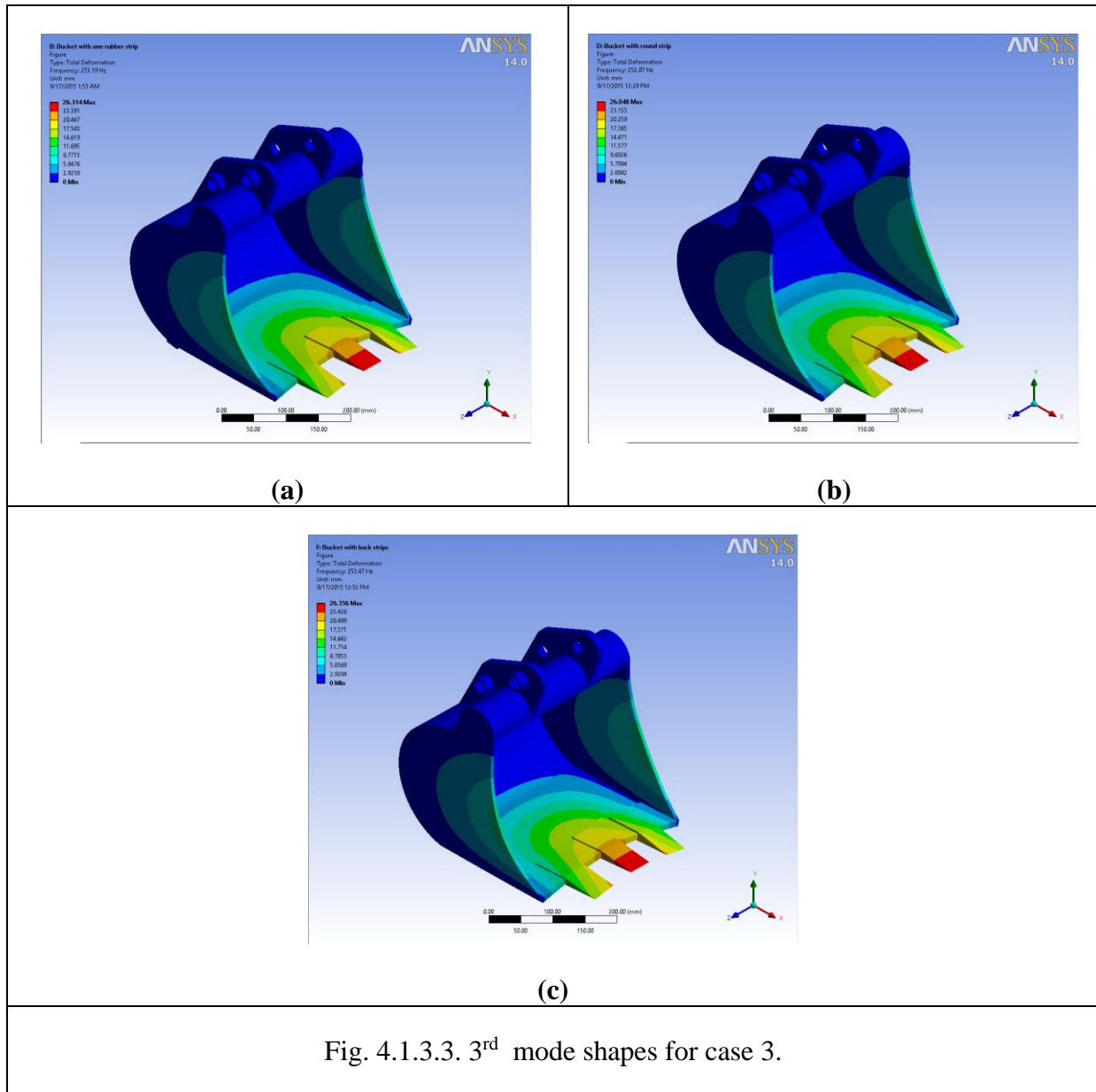
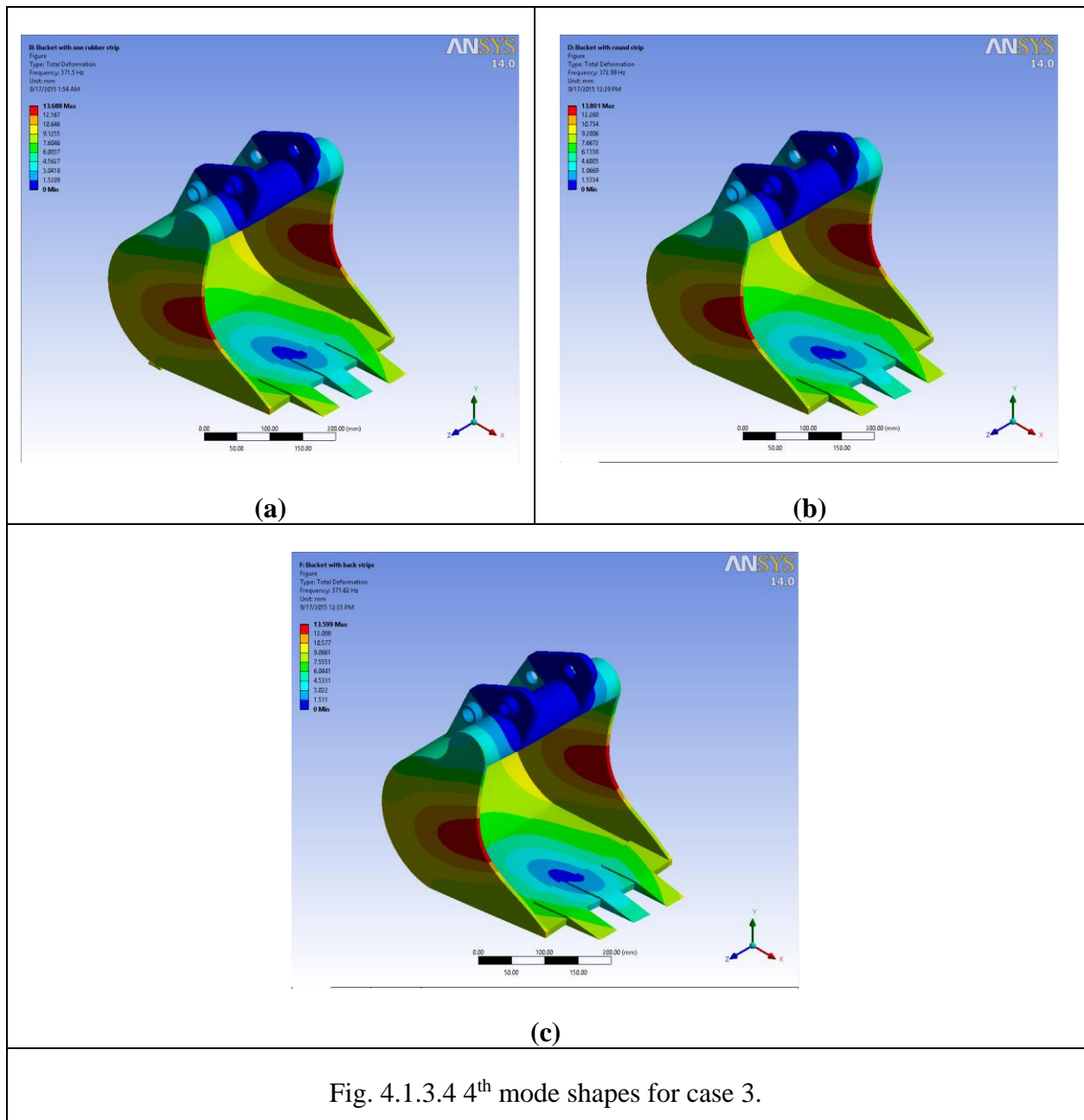
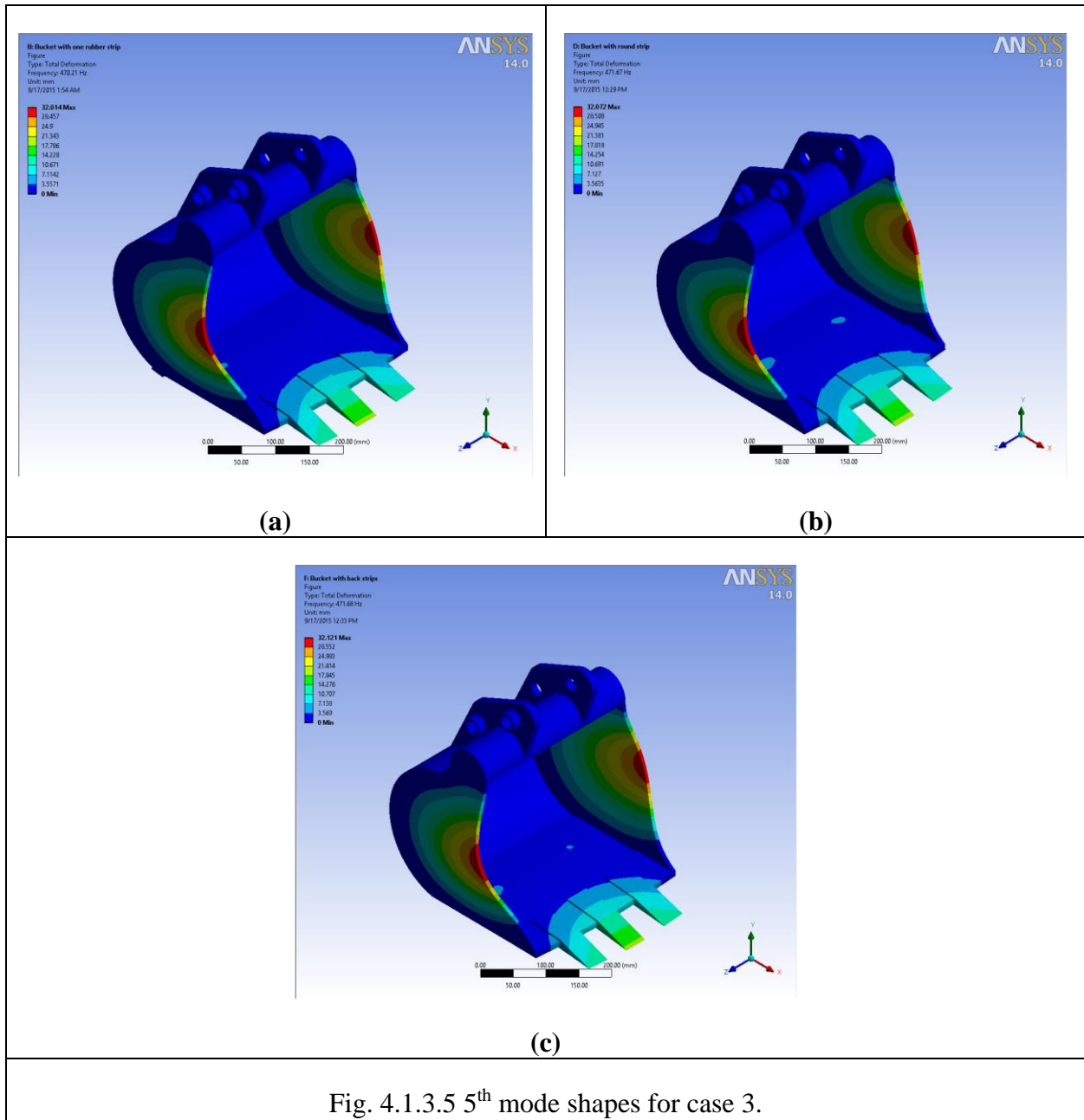


Fig. 4.1.3.3. 3rd mode shapes for case 3.

4.1.3.4. 4th Mode Shapes



4.1.3.5. 5th Mode Shapes



APPENDIX C

Mode shapes for Case 4

4.1.4.1. 1st Mode Shapes

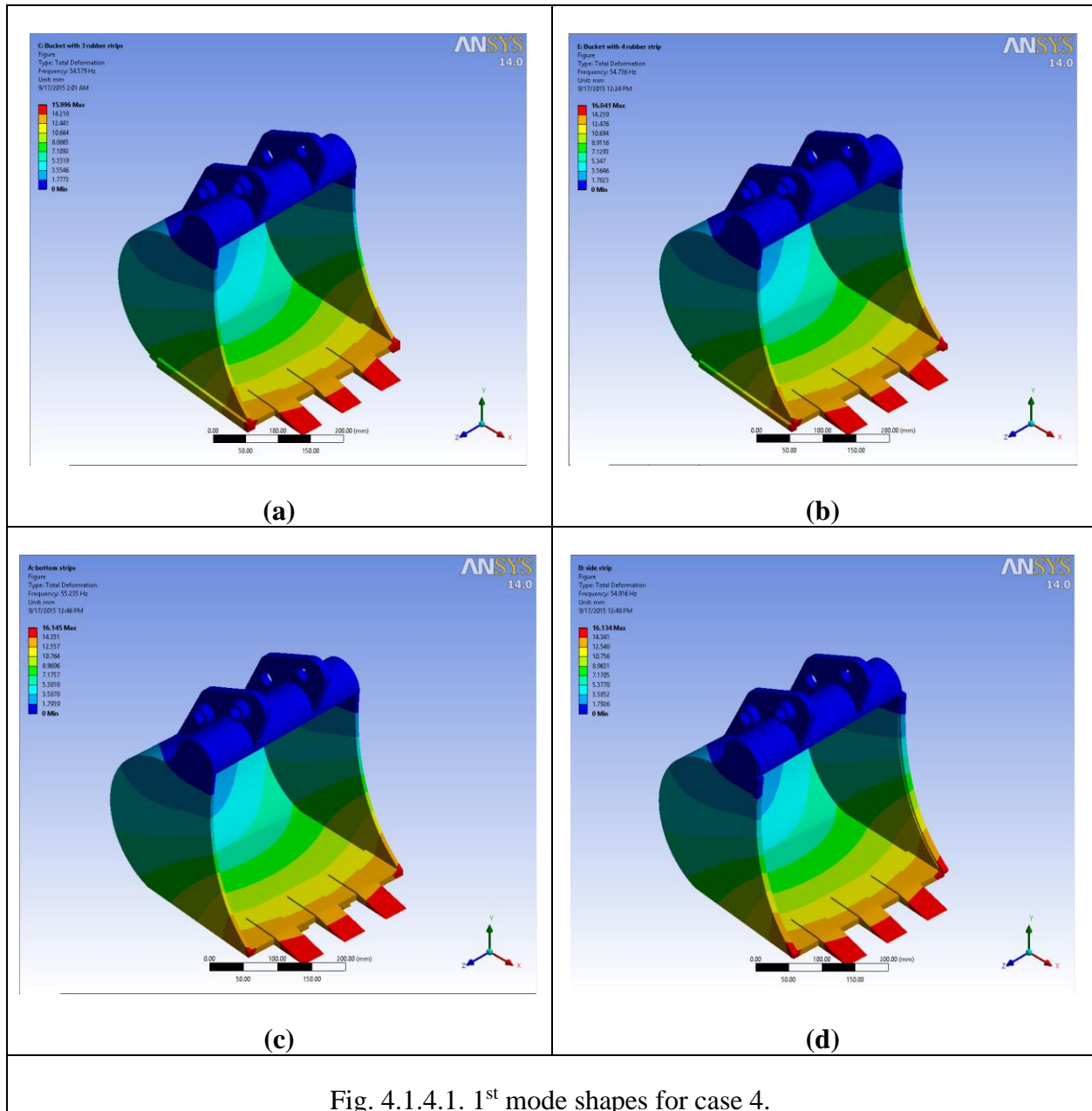


Fig. 4.1.4.1. 1st mode shapes for case 4.

4.1.4.2. 2nd Mode Shapes

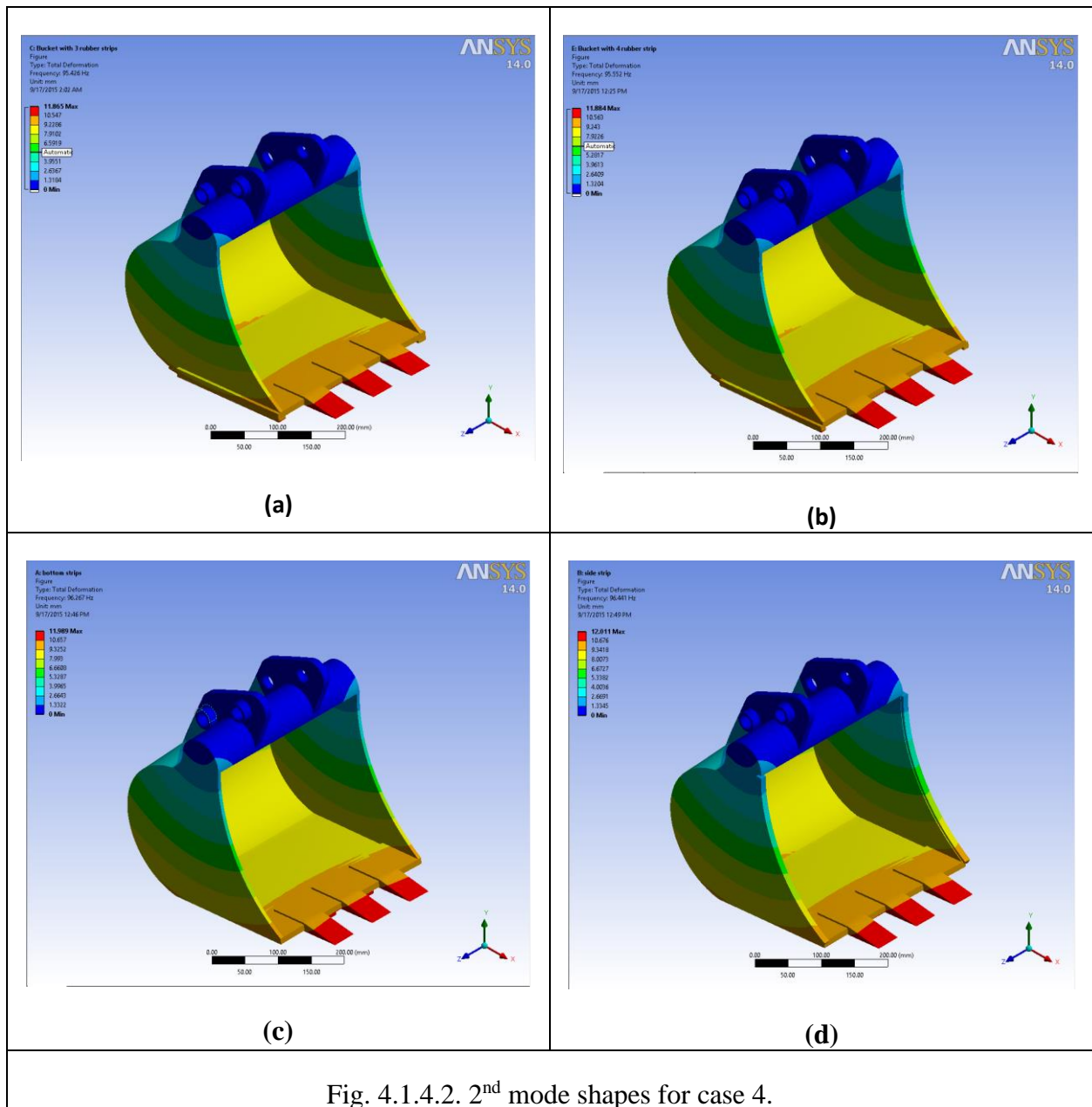


Fig. 4.1.4.2. 2nd mode shapes for case 4.

4.1.4.3. 3rd Mode Shapes

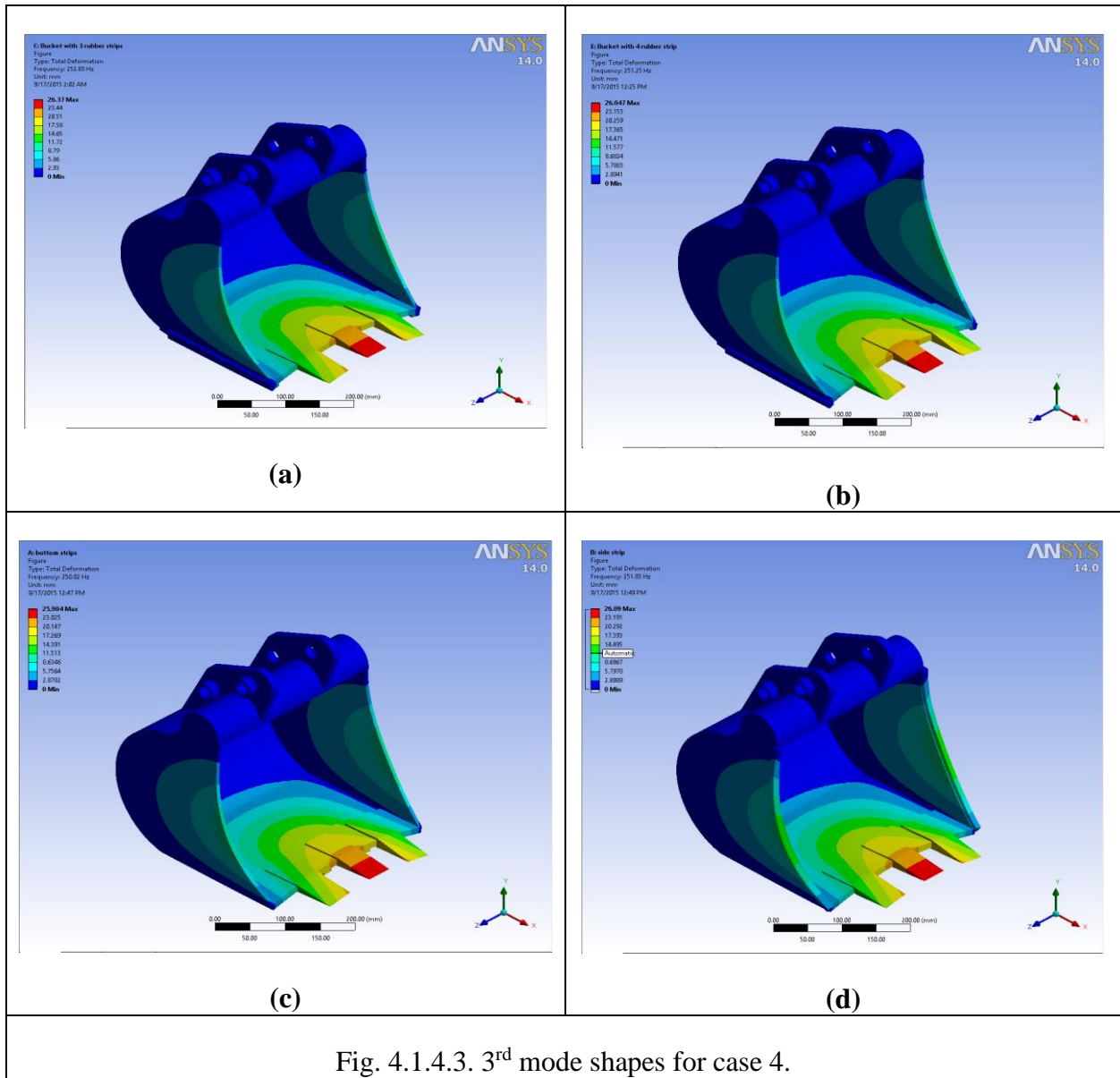
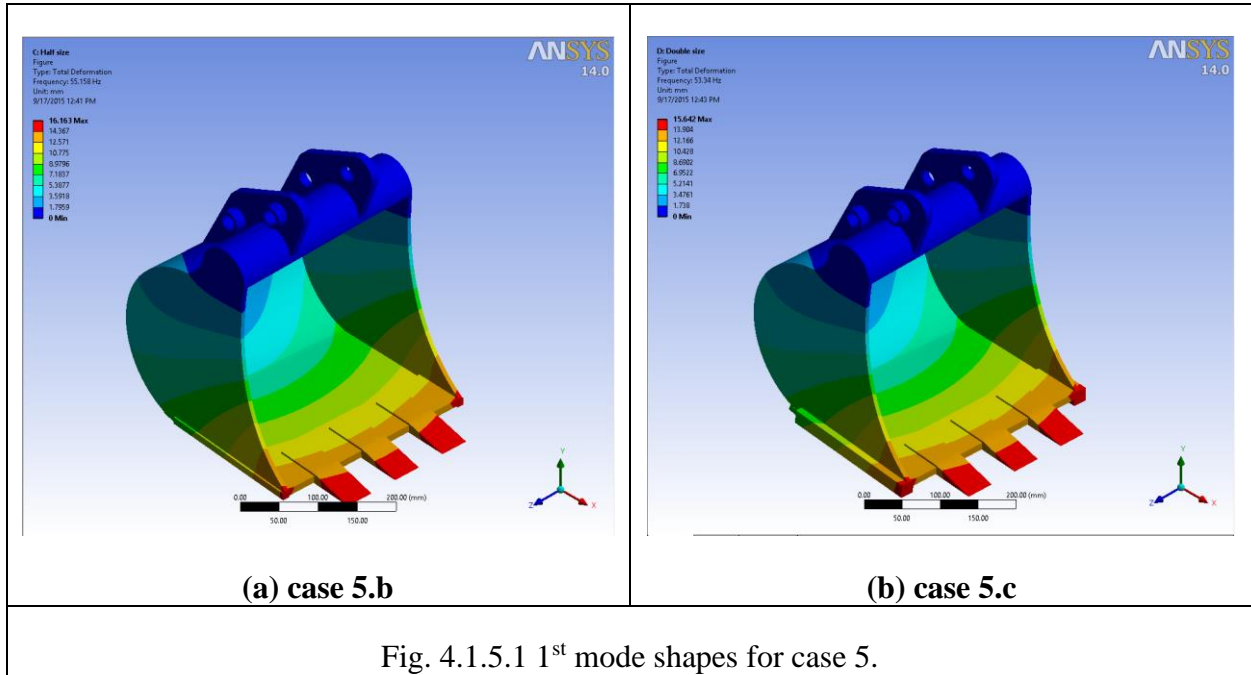


Fig. 4.1.4.3. 3rd mode shapes for case 4.

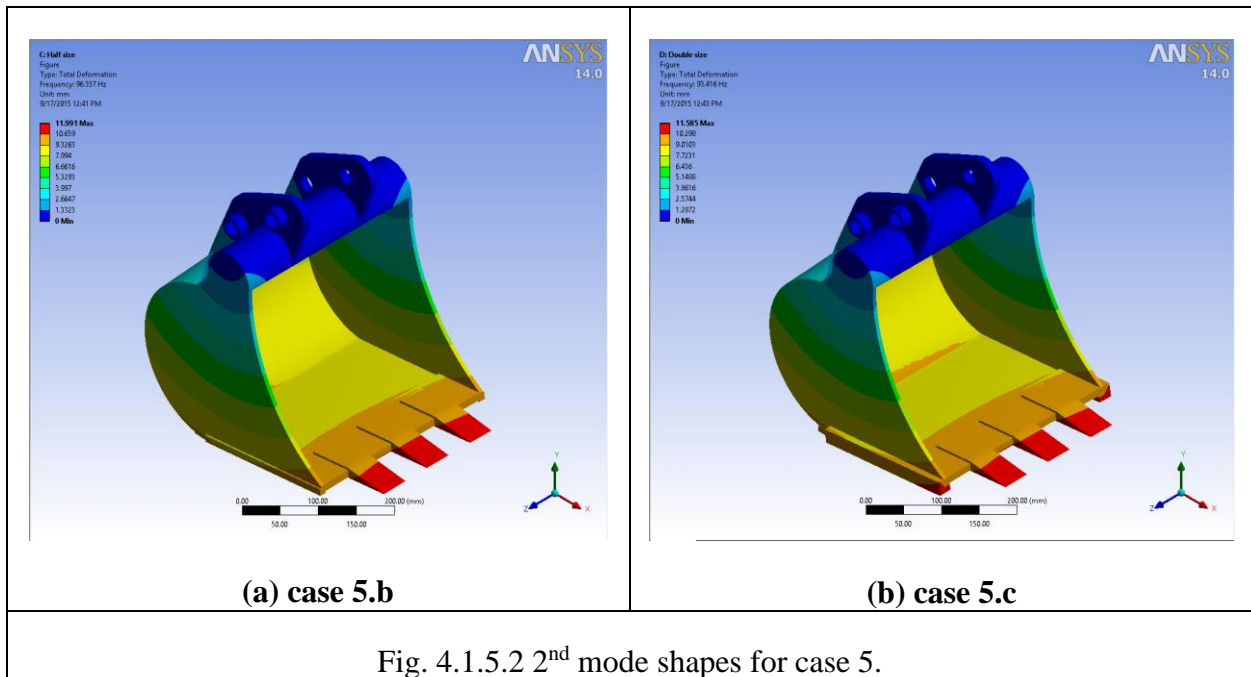
APPENDIX D

Mode Shapes of Case 5

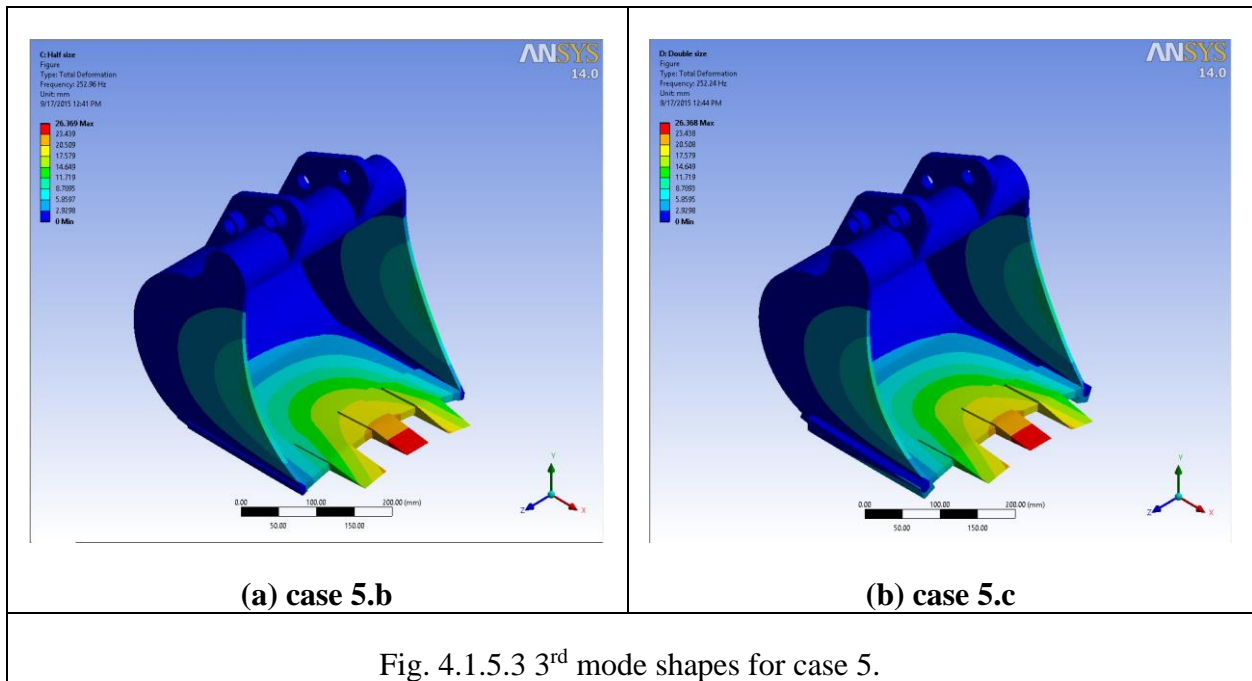
4.1.5.1. 1st Mode Shapes



4.1.5.2. 2nd Mode Shapes



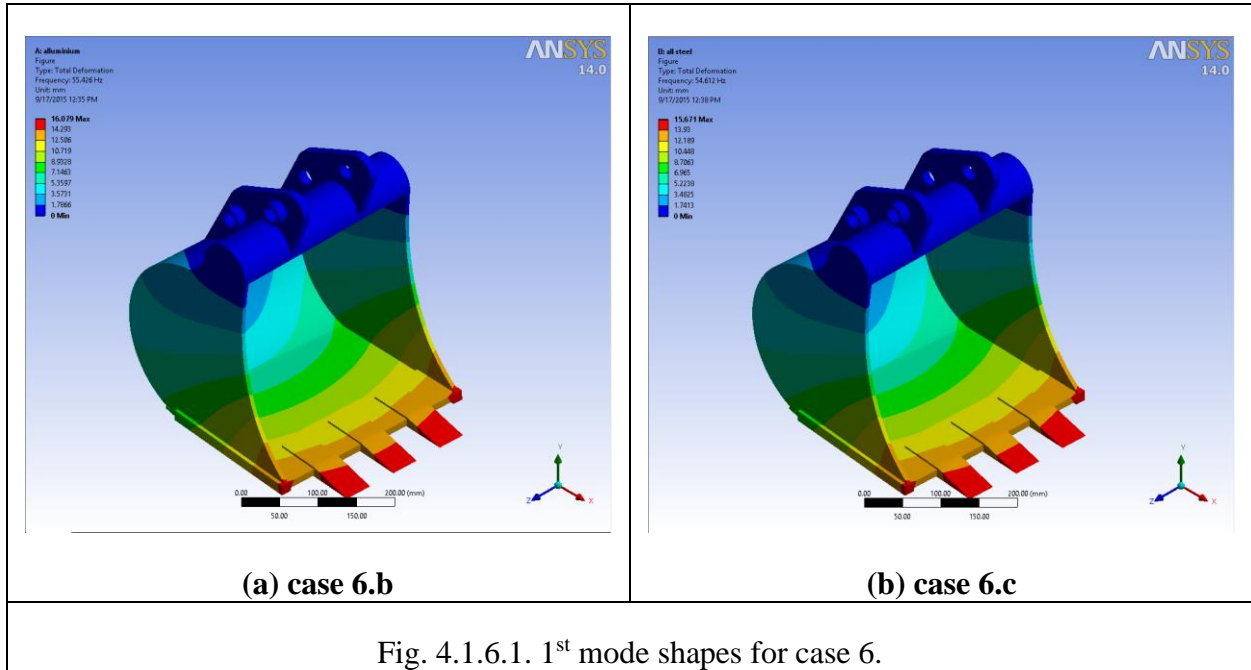
4.1.5.3. 3rd Mode Shapes



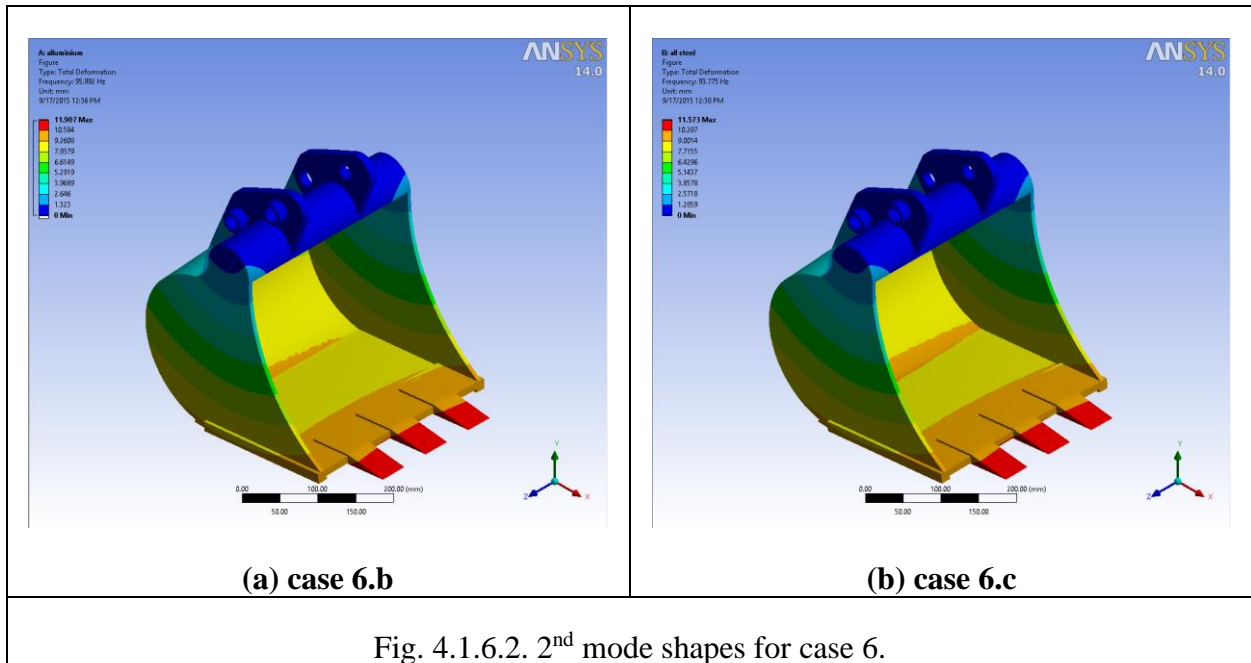
APPENDIX E

Mode Shapes of Case 6

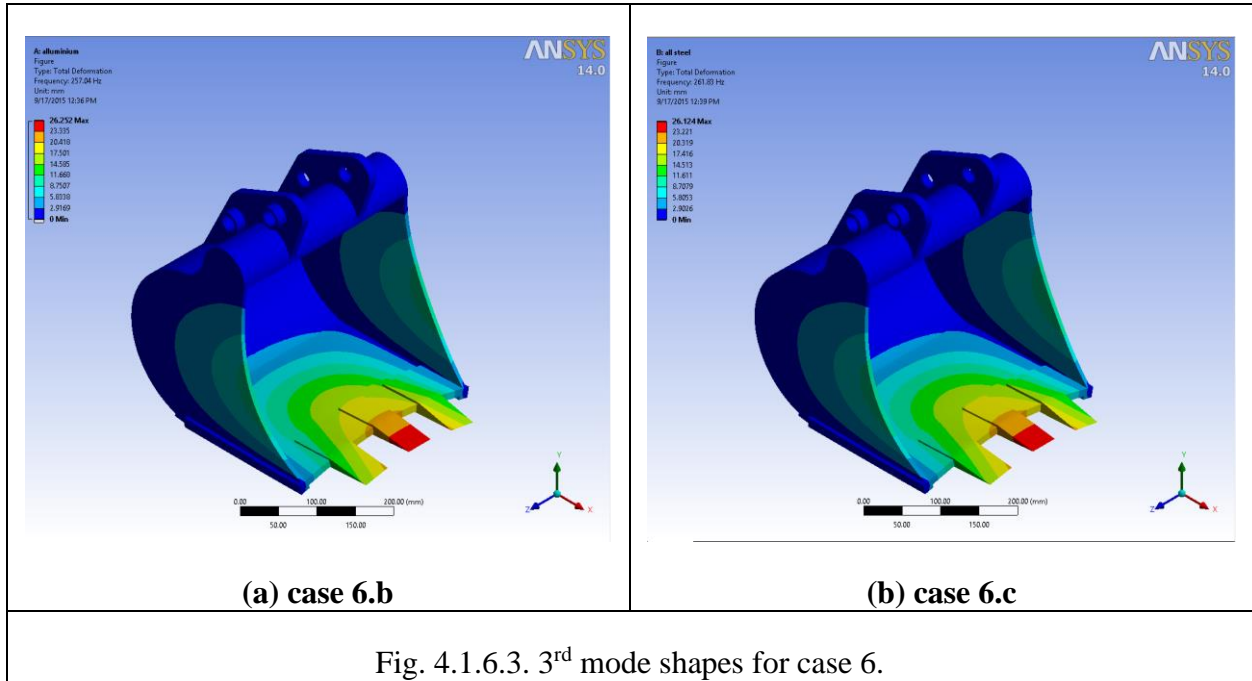
4.1.6.1. 1st Mode Shapes



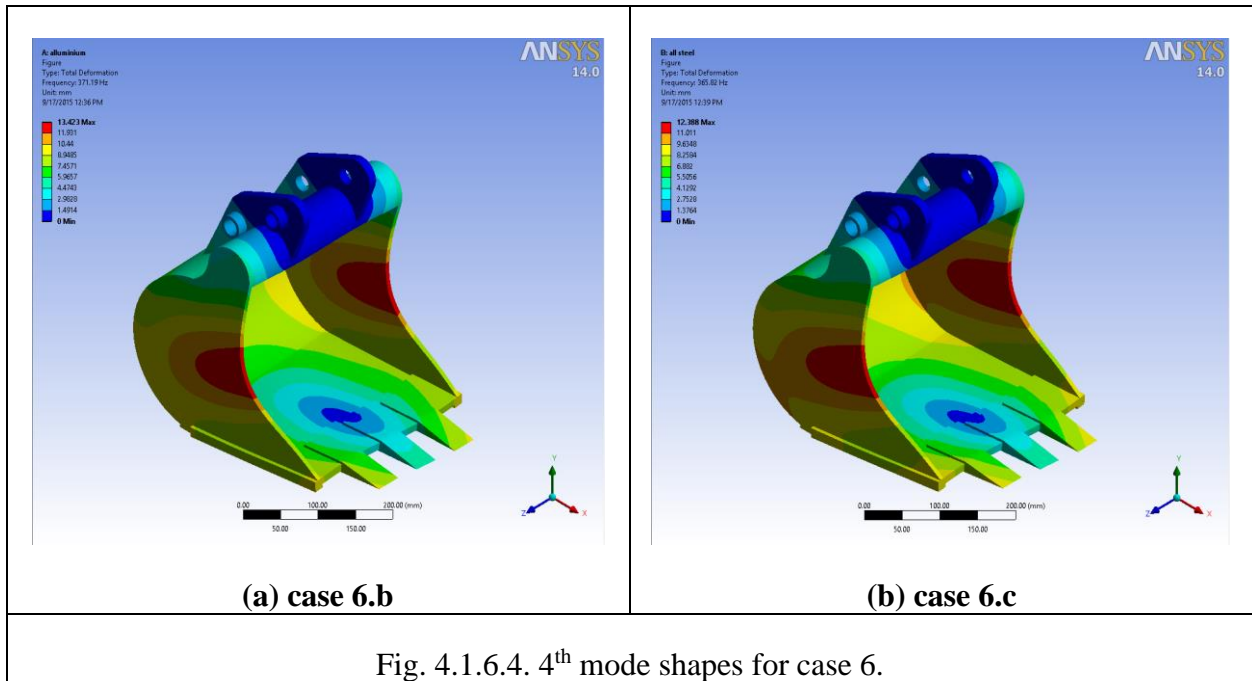
4.1.6.2. 2nd Mode Shapes



4.1.6.3. 3rd Mode Shapes



4.1.6.4. 4th Mode Shapes



4.1.6.5. 5th Mode Shapes

